Studies of Blends Containing Liquid Crystalline Polymers with PET and Related Investigations of Hydroquinone/Biphenol Polysulfone systems

by

Chan Uk Ko

Thesis submitted to the Graduate Faculty of the
Virginia Polytechnic Institute and State University
in partial fulfillment of the requirements for the degree of

MASTER OF SCIENCE
in
Chemical Engineering

APPROVED:

Dr. G.L. Wilkes

Dr. D.G. Baird

Dr. J.E. McGrath

January, 1985
Blacksburg, Virginia

ACKNOWLEDGEMENTS

I would like to express my sincere thanks and gratitute to Dr. Garth L. Wilkes for his constant guidance and suggestions throughout the fulfillment of this degree and the writing of this thesis. I also wish to thank Dr. D.G. Baird and Dr. J.E. McGrath for their valuable suggestions; the 3M Company for their financial support for this project.

I would also like to thank my friends and colleagues-- , , , , , , and for many helpful discussions and all the good times we spent together and for proofreading this thesis.

Finally, this thesis would not have been possible without the support and encouragement of my mother . Also, a deep and sincere thanks goes to my wife , for her company and patience during the final stages of writing this thesis.

TABLE OF CONTENTS

LIST OF FIGURES

LIST OF TABLES

INTRODUCTION

There has been a strong interest in recent years in developing new high strength-low weight materials for commercial applications. One of the reasons for this interest is the fact that liquid crystalline synthetic organic fibers are currently commercially available that have tensile strengths approximately five times as high as that of steel wire, when compared on a weight basis (i.e. specific modulus). Therefore it has been demonstrated that one can in some cases choose a high performance material with reduced weight without sacrificing performance. Table 1 shows some of the tensile properties of high strength-high modulus liquid crystalline aromatic yarns compared with those of glass and steel fibers. The aromatic fibers are about twice as strong and approximately ten to twenty times stiffer than the common high strength nylon and polyester tire yarns.

There have been several investigations of high strength-high modulus polymers (1,2,3). Particularly in recent years the entire concept of fiber modification, physical or chemical, has led to the development of many new materials with useful new applications. The blending of two or more polymers to obtain superior qualities has also been studied extensively in the acrylic, olefin, and polyamide fiber systems (4,5).

TABLE 1 - Tensile properties of high modulus/high strength aromatic polyamide yarns compared with those of glass fibers, steel wire and yarns of nylon and polyester. (3)

	Tensile strength (GPa)	Modulus (GPa)	Elongation (%)
Aromatic polyamide yarn	2.8	124	2.8
E-HTS glass	2.4	69	3-4
S-glass	3.3	88	3-4
Steel wire	3.1	210	2-3
Nylon tire yarn	1.0	6	18
Polyester tire yarn	1.1	14	15

From a molecular standpoint, the basic requirements for high tensile strength are highly oriented and extended polymer chains. There are many ways to achieve these goals. Minimization of chain folding and chain entanglements is one approach. The method chosen for maximizing chain extension and orientation will depend on the chain chemistry since different polymers have inherently different conformational behavior. In the case of symmetric flexible chain systems, the goal is to reduce or prevent the formation of chain folding during crystallization while maximizing molecular orientation. Closely packed parallel extended polymer chains should exhibit the highest achievable specific strength. The characteristics of uniaxially oriented polymers are indeed the basis for the technology of ultrahigh-strength organic polymeric fibers.

Although it was recognized very early that the strength of man-made polymeric fibers is considerably below the theoretical limit, attempts to reach this goal still remain unsuccessful. However, a strength of 100 GPa (for polyethylene in 1979), which was believed to be a limit, was exceeded in laboratory experiments but could not be achieved on a commercial scale. The discovery of very strong polyaramide fibers produced from anisotropic solution along with the realization of the importance of the liquid crystalline state in the preparation of highly ordered extended chain fibers rekindled the research in ultrahigh strength fibers.

The liquid crystal state is one in which some of the molecular order characteristics of a three dimensional crystalline phase is retained in the liquid state because of molecular structure and short range

intermolecular interactions of the Van der Waals forces. Specifically, a certain degree of one or two dimensional order develops when the mesogen is cooled from the isotropic liquid state. The thermal transitions for such a system may be shown schematically as

solid $\rightleftharpoons$ liquid crystal $\rightleftharpoons$ isotropic liquid

In general, there are two means for disrupting the order in the solid state and obtaining the liquid crystalline state: the use of heat and the use of solvent. Systems that show liquid crystallinity by the use of heat (and therefore in the melt) are referred to as thermotropic, while liquid crystallinity present in solution is referred to as lyotropic.

Liquid crystalline order is subcatagorized into three types of mesomorphic arrangements: nematic, smectic and cholesteric. In the case of the nematic phase as shown in Fig. 1(a), the centers of gravity of the molecules are arranged at random but in localized regions and these molecules have the same orientation thereby providing uniaxial order. Thus it is somewhat similar to the ordinary isotropic liquid except that molecules are spontaneously oriented with their long axes approximately parallel. The preferred axis of orientation, referred to as the director and represented by a vector, may vary from point to point in the medium, but a "monodomain" sample of a nematic is optically uniaxial positive and strongly birefringent. For those systems displaying high strength or high modulus, it is generally the nematic morphology that is present.

Figure 1(b) shows the cholesteric mesophase, a second type of ordering for liquid crystalline systems. The cholesteric phase is similar

to the nematic liquid crystal in that it appears to be made up of nematic layers that are systematically rotated with respect to one another in successive planes, each of which lie perpendicular to the cylindrical axis as shown. As a result, the structure acquires a spontaneous twist about an axis perpendicular to the director. The pitch is often of the order of the wavelength of visible light, and thus owing to the periodicity in the structure, the cholesteric gives rise to an intense reflection of light whose wavelength depends on the angle of incidence. However, due to the lack of molecular overlap between the long axis of the molecules arranged between two adjacent layers, it is not likely that these structures would promote high strength or high modulus materials in axis direction in contrast to that of the purely nematic mesophase.

Figure 1(c) schematically shows the third type of liquid crystalline order known as the smectic phase. Here the molecules are arranged side by side in a series of stratified layers and the centers of gravity of these molecules are arranged in equi-distant planes which make up the corresponding layers. Different kinds of molecular arrangement are possible within each stratification due to tilting or periodic inclination of the molecules within the stratified layers (6). The smectic texture does not lead itself to high modulus performance due to the lack of molecular backbone overlap in the orientation direction, however, there may be some exceptions to this.

In 1976, Jackson and Kuhfuss (7) from Tennessee Eastman were the first to demonstrate that thermotropic liquid crystalline behavior existed in copolymers based on poly(ethylene terephthalate) (PET) and parahydroxy benzoic acid (PHB). They also reported that the melt

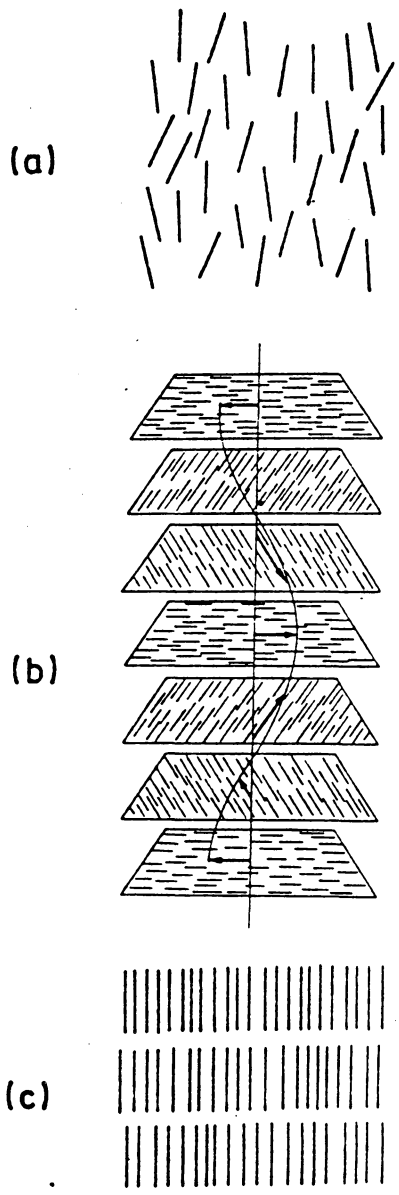

Fig. 1 Schematic representation of the molecular arrangements in (a). nematic, (b). cholesteric, (c). smectic structures. (3)

viscosity at specific shear rate starts to decrease at a PHB value of 30 mole % due to the onset of liquid crystalline order with the lowest viscosity being present at about 60 mole % PHB (Fig. 2). When the basic PHB structure was modified with PET (by transesterification), the ethylene glycol units introduced flexibility into the polymer chain, and the melting point was reduced. The introduction of flexible units into rod-like aromatic polyester structures is one way to reduce the high melting points (about 600°C) so that the final copolymers will be sufficiently mobile yet thermally stable to be melt spun or be injection molded (8,9). Other ways include modification with substituents on the aromatic rings or modification with certain rod-like comonomers.

More recently, Calundann from Celanese (10) reported all-aromatic copolyesters prepared with 2-hydroxyl-6-naphthalene derivatives have lower melting points than those prepared with 1,4- and 1,5- oriented monomers. They exhibit thermotropic liquid crystalline behavior when a high proportion of the polymer chains consisting of the 2,6-oriented naphthalene rings and p-phenylene rings are connected by carboxyl groups. In this case only 20 mole % PHB was required to make the copolyester liquid crystalline, whereas when PET was modified by the transesterification reaction of p-acetoxybenzoic acid with PET, 30 mole % of the PHB component was required to make the copolyester liquid crystalline (7). The difference in the compositions, of course, is the presence of the wider, fused-ring naphthalene structure rather than the single-ring phenylene structure. The study based on a liquid crystalline material (p-hydroxybenzoic acid, 2-hydroxyl-6-naphthoic acid, and hydroquinone) blended with PET will be presented in the first

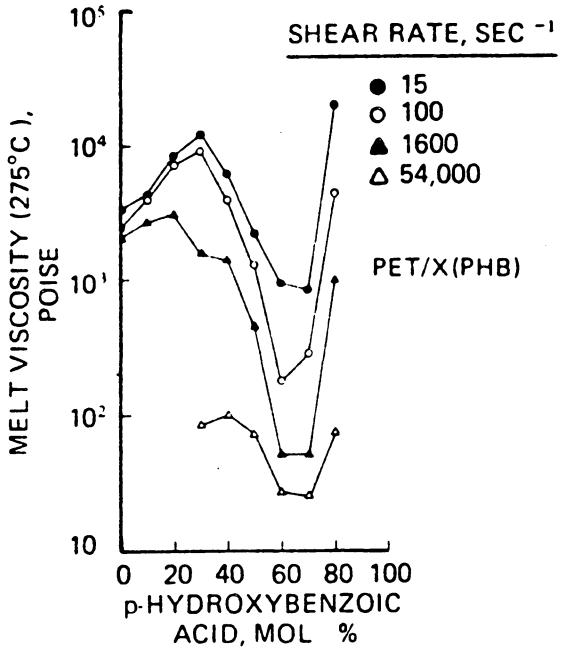

Fig. 2 Melt viscosity of PET modified with p-hydroxybenzoic acid. (7)

chapter of this thesis. The purpose of this study was to potentially develop interesting mechanical behavior of such blends for possible film applications.

In the second chapter of this thesis, the subject of thermotropic liquid crystalline behavior with materials derived from terephthalic acid and either hydroquinone or biphenol copolymerized with varying amounts of "long polysulfone based spacers" is discussed. The objective of this latter investigation was to probe the potential of these copolymers to display signs of liquid crystalline character as well as to note their ability to directly crystallize into three dimensional order and , if so, under what conditions.

Prior to discussing the research carried out by the author, a literature review on the methods used to obtain high modulus-high strength characteristics in polymeric systems will be presented for purposes of assisting later discussions in the thesis.

LITERATURE REVIEW

High modulus-high strength characteristics can be exhibited by polymers that have a flexible chain conformation or a stiff, rod-like conformation. Polymer blends may also exhibit some of these desired properties. The purpose of this section is to provide a brief review of the recent literature that relate to some of the approaches utilized to achieve high modulus-high strength polymeric materials.

(1). High Modulus-High Strength Obtained By Blending A Specific Polymer With Another Component

Blending is often utilized to modify properties, extend the use of expensive engineering resins, reuse off-specification material, or generate unique processable materials.

Industrial applications of dispersed two-phase flow in polymer processing are numerous. Two familiar examples are the processing of rubber-modified polystyrene and acrylonitrile-butadiene-styrene (ABS) plastics. In the high-impact polystyrene and ABS, a rubbery polymer is dispersed in a glassy matrix. This structure can result in a significant increase in impact strength over that of the glassy styrene homopolymer alone without a large decreases in modulus and heat-distortion temperature that would be obtained through ordinary internal or external plasticization. In the melt state, ABS resin has particles of polybutadiene rubber homogeneously dispersed in a styrene-acrylonitrile copolymer, forming a two-phase system. An additive, such

as an impact modifier, which is usually used in small quantities, can also be dispersed in a base polymer, forming a two-phase system (11).

It has been recognized that the properties of blends strongly depend on the matrix morphology (12), size and form of the dispersed phase, and the character of the corresponding interfacial regions. Depending on the processing methodologies, the dispersed phase of these polyblends can be manipulated to provide droplet or rod (fibril) shapes (13).

In recent years the whole concept of polymer modification, physical or chemical, has led to the development of many new materials with useful new applications. To appreciate the special nature of these new blend systems, it is necessary to review in brief the features of some of the more conventional systems in which two or more distinct chemical polymeric entities are involved. Blended fibers, which are special case of blended materials, are used here as examples.

Three two-component fiber systems are illustrated diagrammatically in Fig. 3. The first (Fig. 3a) is the well-known "bi-component fiber" system (14). It consists of two chemically and physically distinct polymeric components which adhere to form a single fiber. When subjected to thermal treatment, the two initially oriented components shrink to different extents and cause a curling or crimping effect which imparts bulking or stretch properties to the fiber or yarn. This system of course does not lead to high modulus behavior yet the tensile strength improvements may be significant. The second two-component fiber system is the skin-core type illustrated in Fig. 3b. This type is frequently found both in natural and synthetic fibers. Wool, for

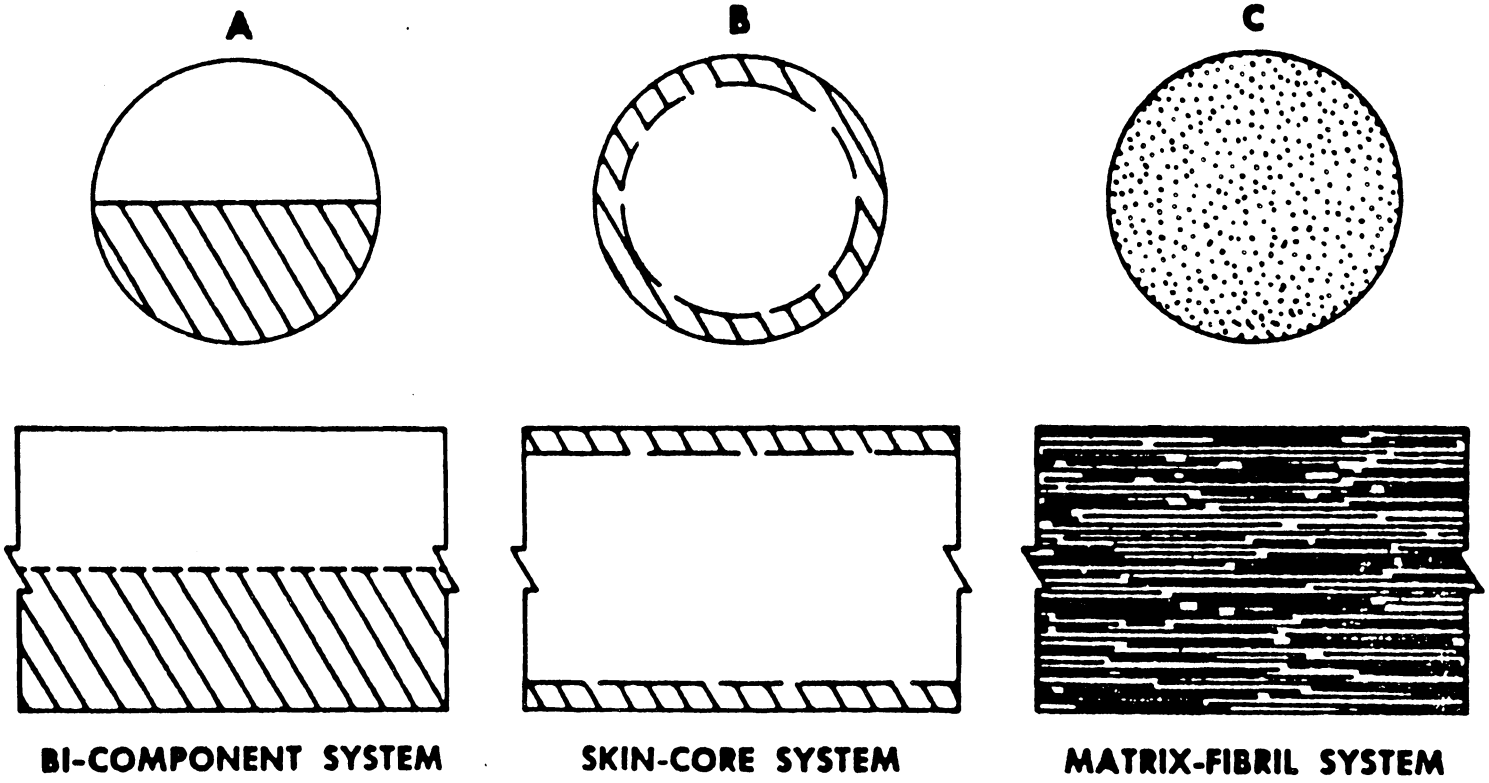

Fig. 3 Two-constituent fiber systems. (14)

example, has a complex inner core with a cellular outer skin which provides some of its characteristic mechanical and chemical properties. In man-made melt-spun fibers, the surface microstructure is often different from the inner structure because of the effect of quenching during spinning. Surface crosslinked cellulosic fiber would also fall in the skin-core category. The two regions in the above two systems will also often exhibit other different properties, e.g. dyeability. The third type, illustrated in Fig. 3c, is the fibril/matrix system (15).

Polyblends are prepared and manufactured in a variety of operations leading, for the same set of components, to diverse morphologies and to potentially different melt rheology behavior as well (16). The outlines for some of these operations are shown in Figs. 4 and 5. It is generally accepted that the basic rheological characteristic in establishing the morphology of a polyblend is that of shear viscosity. Specifically, the ratio of melt viscosities for the polyblend components is decisive in minor phase (droplet, rod) size control (17).

Han & Kim (18) have investigated many processing variables in order to better understand the mechanism of droplet formation. The processing variables were the blending ratio of a mixture, flow rate, and melt temperature. Interestingly, it has been observed that the minimum viscosity occurs at approximately the same blending ratio which gives rise to the maximum elasticity.

When two immiscible fluids are subjected to the shear forces in a given flow field, droplets of one phase are produced within the other. As one may surmise, the question as to which of the two fluids forms droplets depends on, among other factors, the volume ratio of each

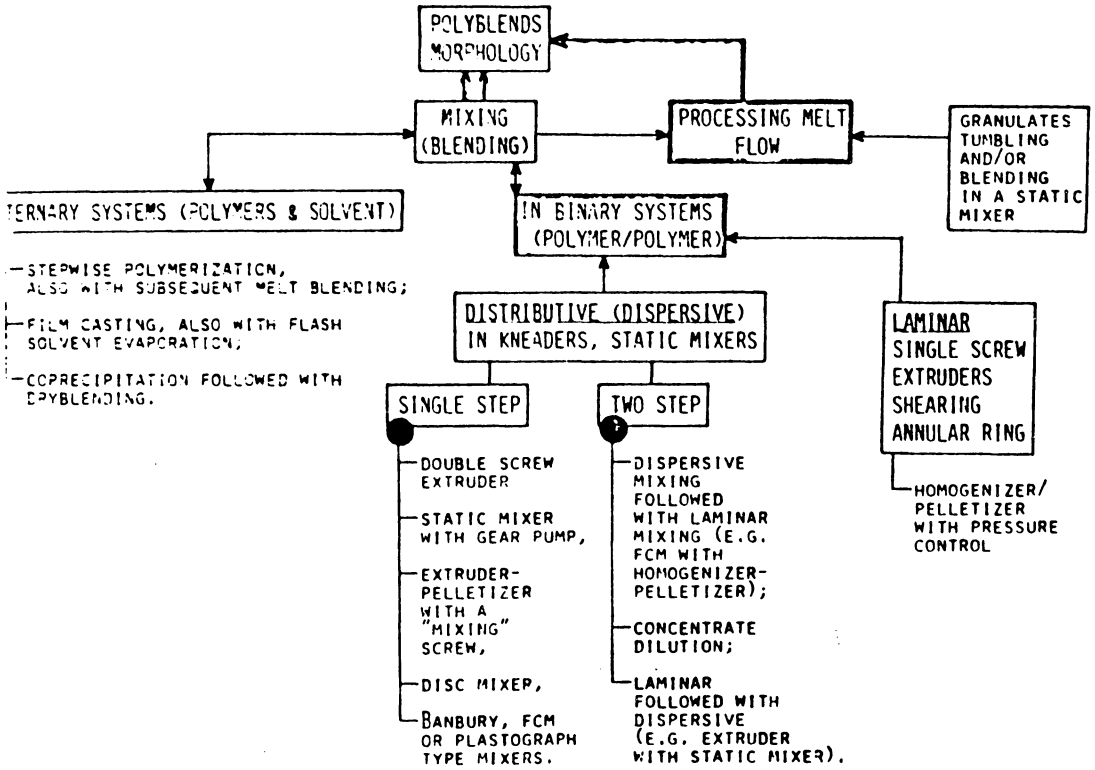

Fig. 4 Polymer mixing and morphology: A classification diagram. (16)

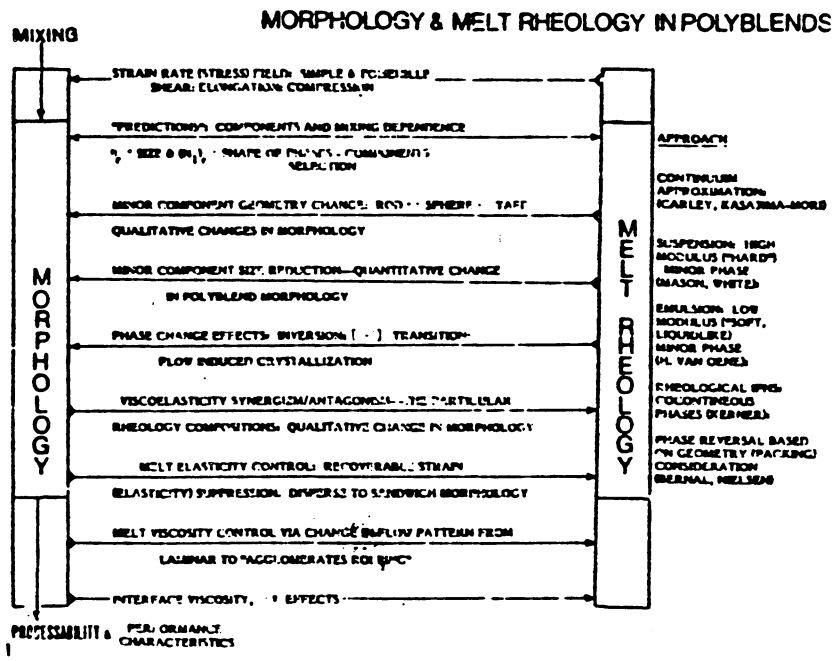

Fig. 5 Binary polymer blends: melt rheology-blend morphology interaction. (16)

component, the viscosity and elasticity ratios of individual components, and the interfacial tension between the two fluids. For instance, depending on the composition ratio, the less viscous fluid may form droplets and be dispersed into the more viscous fluid, or the more viscous fluid may form droplets and be dispersed into the less viscous fluid. In practice, uniform droplets are not obtainable, and the average size of droplets and their size distribution depend very much on the type of mixing equipment that one uses.

A number of other researchers (19,20) have made studies on identifying the variables necessary for describing the morphology and physical properties of polymer blends, and it has been shown that polymer blends usually form two incompatible phases in the molten state due to a phenomenon which often is attributable to the low entropy of mixing of dissimilar polymers, and due to endothermic heat of mixing (21).

Han et al (22) investigated the rheological behavior of an incompatible blend of high density polyethylene (HDPE) and polystyrene (PS) using the capillary rheometer. They concluded that a two-phase fluid which contains deformable droplets will give less resistance to flow, and hence a lower pressure drop (i.e., lower apparent viscosity) and more recoverable elastic energy (i.e., higher apparent elasticity), than a single-phase fluid or a two-phase fluid which contains nondeformable particles. They have further reported, as shown in Fig. 6 that the size of droplets tends to decrease as the melt temperature is increased from 200°C to 240°C. This may be attributed to the fact that an increase in both melt temperature and wall shear stress brings about

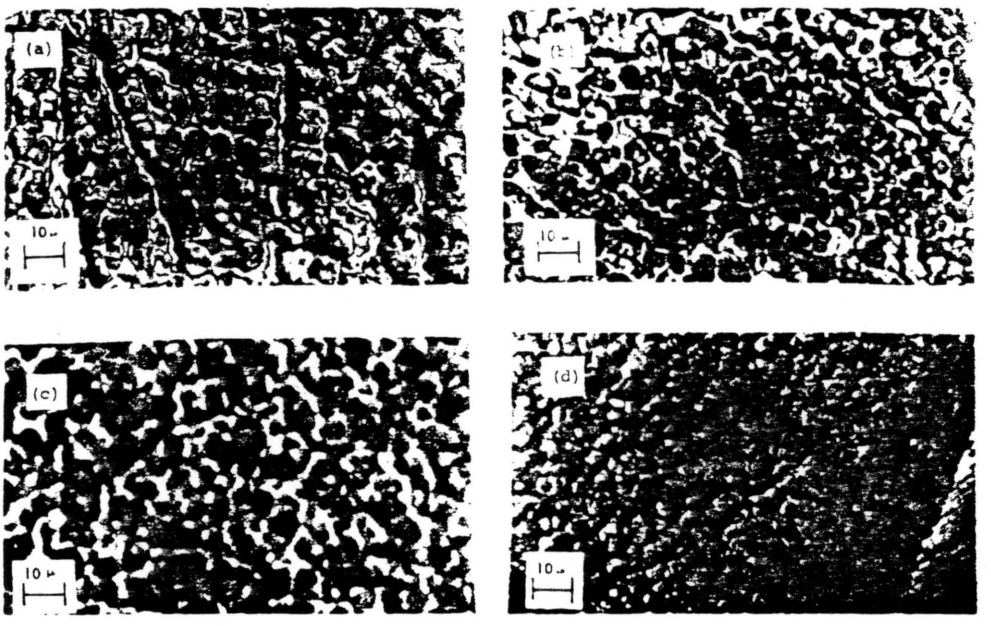

Fig. 6 . Microphotographs of extrudate samples of the blend HDPE/PS = 25/75 (cross-section). Extrusion conditions: (a) T = 200°C, τ_w = 0.603 × 10^6 dynes/cm²; (b) T = 220°C, τ_w = 0.632 × 10^6 dynes/cm²; (c) = 240°C, τ_w = 0.362 × 10^6 dynes/cm²; (d) T = 240°C, τ_w = 0.761 × 10^6 dynes/cm². (22)

a decrease in melt viscosity. The yield strength and the relative elongation varied somewhat depending on the molecular characteristics of the polymers used as well as on the processing employed in making the samples. It was found that the mechanical performance of these blends could be improved by changing operating variables such as temperature and elongation rate. In this way, it was possible to obtain even ultradrawn fibers with sufficiently high modulus and strength (23).

In order to understand the mechanical property behavior in blends, it is important to observe morphological features of the blends. Here some of the morphological studies carried out by Kanori and Geil (24) for polycarbonate(PC)/HDPE system will be presented. Figure 7 shows fractured injection molded sheets of PC/HDPE blends of various compositions. PC/HDPE blends have a domain structure whose morphology is strongly dependent on the fractional content of the dispersed phase; when the dispersed phase fraction is less than 20 % HDPE, the domains are mostly spherical. Above 20 %, agglomeration takes place to form polyethylene domains of rod-like structures. The 50/50 composition is composed of lamellar structures. The size of the spheres increases with increasing PC concentration. Formation of the well defined spherical HDPE domains seems to occur during the molding process; there are still some nonspherically shaped domains in the as-extruded samples of these PC/HDPE blend. As can be seen in Fig. 7, there is no adhesion between the two phases, and the HDPE inclusions are considered to be "loose" in the holes in the matrix. With respect to Young's modulus, when the dispersed phase concentration is lower than

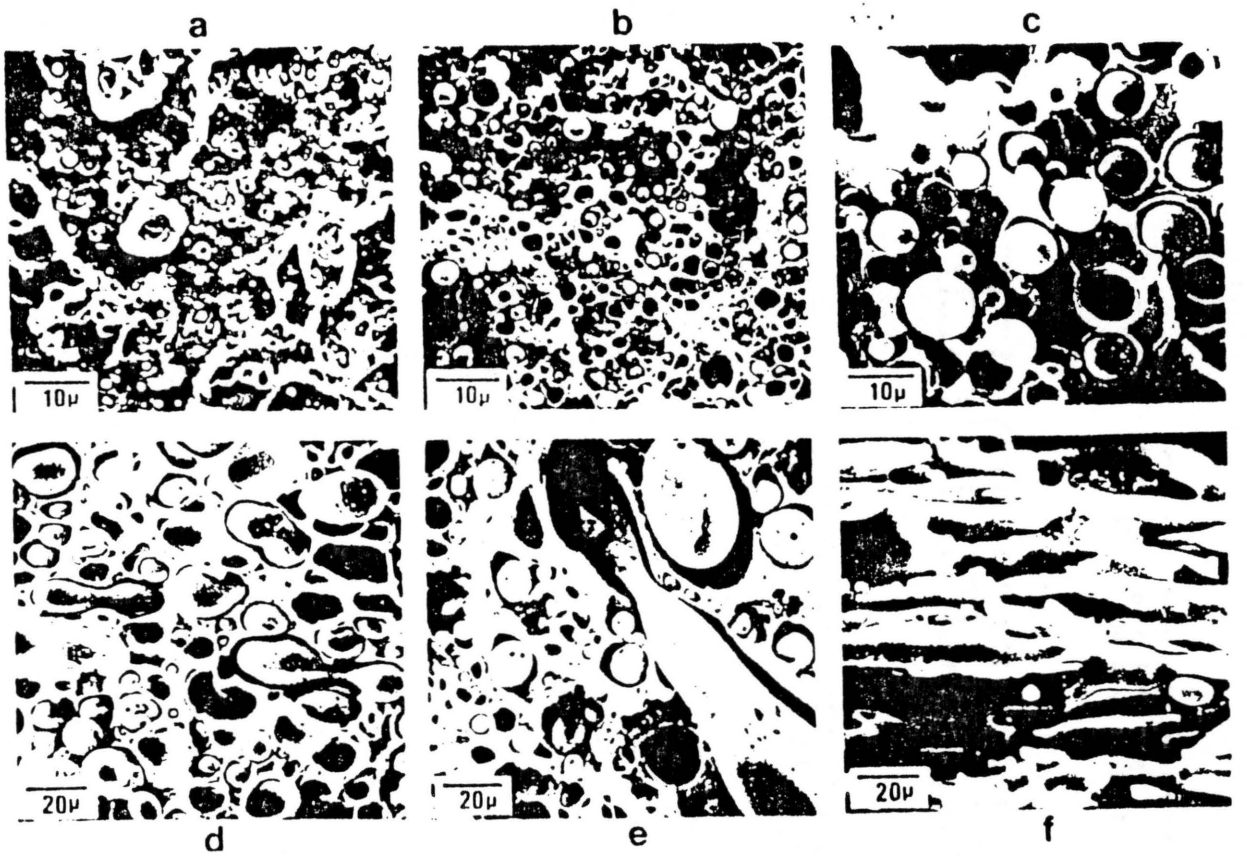

Fig. 7 Scanning electron micrographs obtained from fractured sheets of PC/HDPE blend samples. (a). PC/HDPE=98/2, (b). 95/5, (c). 90/10, (d). 80/20, (e). 70/30, (f). 50/50 (24)

20 %, the PC/HDPE blend is mechanically equivalent to a PC matrix with spherical holes in it, therefore the HDPE does not contribute to the sample's overall Young's modulus. This investigation provides a good example of how poor adhesion of the dispersed phase promotes inferior properties.

Investigations of the effect of temperature and composition on the tensile and impact behavior of various blends, especially when coupled with the evidence gathered from microscopic studies, suggests that the injection-molding process promotes poor dispersion of the dispersed phase. Thus, it is thought that more effective blending, leading to smaller polyethylene domains, should yield improved mechanical properties (25,26).

The above discussion focused on blends of flexible-flexible chain conformation polymers. Blends of flexible and rod-like polymers also can be made. The rod-like comformation often promote liquid crystalline behavior and can sometimes be used to improve the engineering properties when blended with flexible chains. For example, using injection molded samples, Baird and Wilkes (27) investigated the possibility of combining liquid crystal copolyesters made of PET and parahydroxybenzoic acid and PET homopolymer in a sandwich injection molding process. They indicated that the specimens produced by injection molding have lower engineering properties than those observed for fibers spun from the copolymer alone. However, the bending modulus of co-injection molded bars with as little as 35 weight percent liquid crystalline polymer showed a value that was equivalent obtained for the pure liquid crystal polymer. This was due to a skin-core morphology where an oriented liquid crystal skin resulted.

Joseph (28) investigated the blend of flexible chain PET with that of the same PET/PHB liquid crystal copolyester. He studied the polymer blend in which the liquid crystal copolymer served as a reinforcing agent for the PET homopolymer. There were no detailed studies carried out, but he found that among the different PET/PHB materials utilized, the 40 mole % PET/60 mole % PHB material had the most desirable properties in terms of processability and flexural behavior.

(2). Routes To High Modulus-High Strength Polymers Through The Orientation Of Flexible Chain Polymers

In order to obtain maximum high modulus-high strength behavior for a given polymer, a high degree of orientation and chain extension are required. Also minimization of the unoriented amorphous phase improves the modulus, other factors being the same. Due to the often present chain folds in semicrystalline flexible chain polymers, the theoretical modulus is higher than the experimentally determined moduli by an approximate factor of 2-2.5 after orientation. The fact that x-ray diffraction shows a high degree of crystalline orientation for drawn polyethylene fibers demonstrates that not only orientation but chain extension is also important so that high modulus values can be obtained. That is, the orientation determined by x-ray diffraction itself does not distinguish between parallel arrays of chain folded layers and fully chain extended fibrous crystals. This was recognized soon after the discovery of chain folding (29). However, quite high modulus polyethylene having lamellar crystals can be generated provided that

the lamellae are parallel, the lateral extension of the lamellae in all directions is large compared to the lamellar thickness, there is interlocking between lamellae in lateral contact, and a row structure is present. More detailed discussion of this approach can be found elsewhere (30). The procedures to achieve highly extended forms and to obtain high modulus materials involves 1). aligning the chains from the random state and 2). enabling them to crystallize in the extended form. These two approaches are discussed below.

(a). Crystallization Of Molecules In The Extended Form

Higher tenacity fibers have been obtained by increasing the number of tie molecules and decreasing chain folding in the fibrous structure. Some of the techniques are ultra drawing, solid state extrusion, fibrillar crystal growing, gel fiber drawing, annealing at high pressures, and melt flow induced crystallization at high pressures. Ultra-high chain extension of macromolecules also can be accomplished in the presence of elongational flow (31,32). In elongational flow, the velocity gradient is along the flow direction and not normal to it as is the case in simple shear flow.

Chain extended crystalline structures can be produced as has been shown by Pennings (33,34). From solutions, he produced threads of polyethylene, consisting of a core of highly extended chains. His technique was to induce extension of the chain by rotating a cylindrical rotor within a cylindrical stator. Figure 8a shows the crystallization apparatus comprising of a glass vessel, a stator, and a rotor, with the polymer solution being confined between rotor and vessel wall. The effects of simple shear flow and Taylor vortices on crystallization were

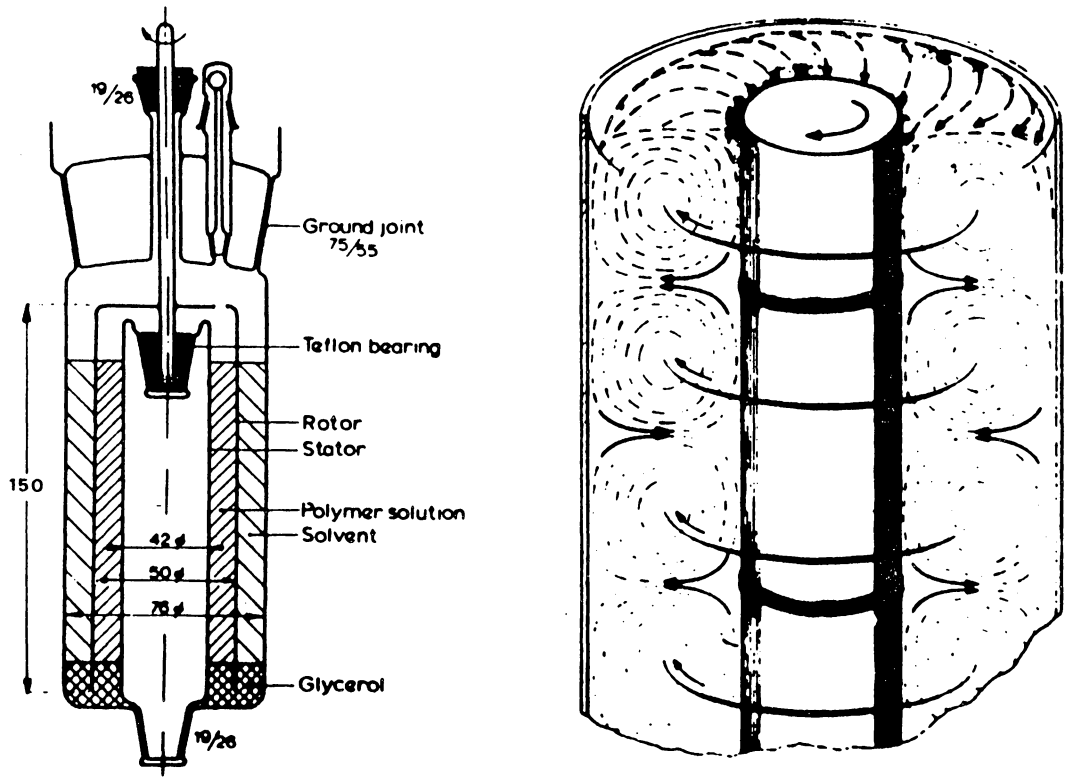

a b

Fig. 8a & b (a). Crystallization apparatus comprising of a glass vessel, a stator, and a rotor, with the polymer solution being confined between rotor and vessel wall. (b). Cutaway view of the coaxial cylinderical apparatus under the conditions of crystallization. The Taylor vortices are shown by dashed lines. (32)

studied. Figure 8b shows a cutaway view of the coaxial cylinderical apparatus under the conditions of crystallization. The Taylor vortices are represented by dashed lines. Fibrous rings revolving around the stirrer in the vortex cores are depicted by the solid lines. Fibrous rings are seen to have wrapped around the stirrer in two positions where the fluid moves towards the vessel wall. This flow pattern promotes the well known Shish-Kebab morphology.

Electron micrographs shown in Fig. 9 revealed that the core (shish) consisted mainly of extended chain crystals while the kebabs were folded chain overgrowth crystals. The extended nature of the crystals is due to the extensional flow field that is present between adjacent Taylor vortices which are generated due to the rotation of the inner cylinder. The higher molecular weight polymer chains become stretched or aligned in the extensional flow field and nucleate and crystallize as extended chain crystals due to the increase in supercooling. Recently, Pennings (35) applied a technique to produce polyethylene fibers with a very high tensile modulus. In this method the thread grows continuously from a 0.4% solution of high-molecular mass polyethylene ($=1.5 \times 10^6$ Kg/Kmol) at 120 C; the fibrous crystal is wound on the rotor at a speed of up to 0.5 cm/s, and has a modulus of up to 50 GN/m^2.

Smith, Lemstra, and Booij (36) reported high molecular weight is required for producing high strength polyethylene. However, as the molecular weight is increased, the material resists deformation due to a greater number of entanglements. They have reported that polyethylene filaments with a drastically improved drawability and 100

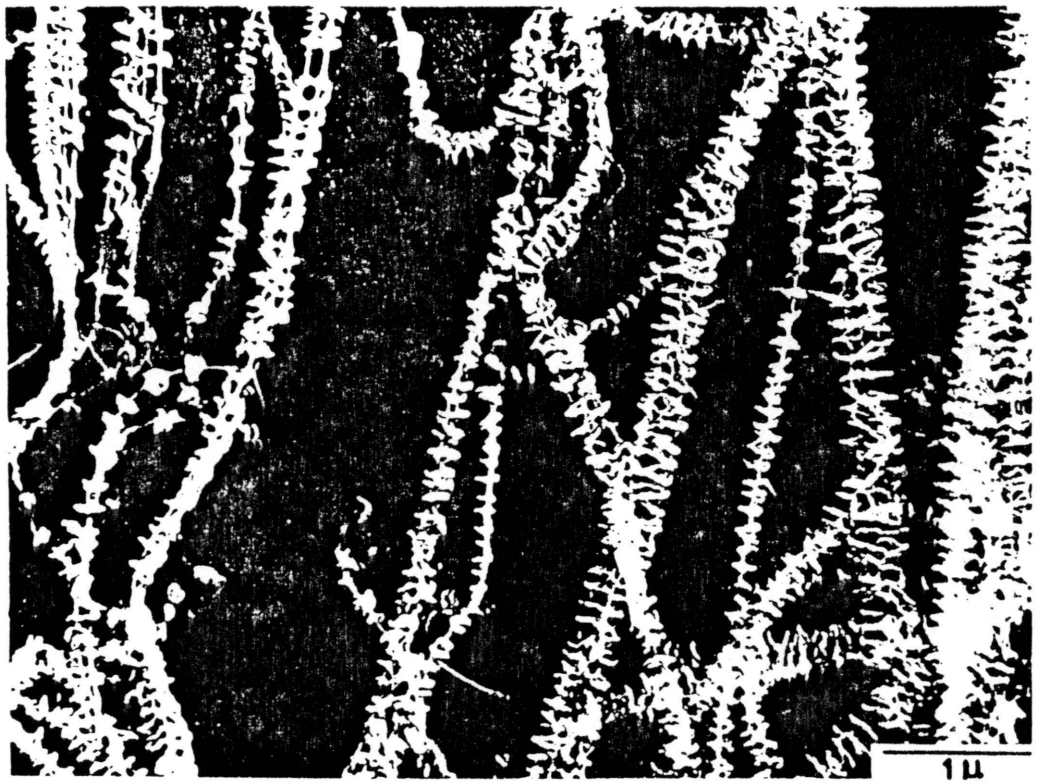

Fig. 9 Scanning electron micrograph of polyethylene Shish kebabs. (32)

GPa modulus and 3 GPa tensile strength values can be obtained by drawing high molecular weight polyethylene cast from a gel. They obtained high modulus and strength values at high draw ratios which depended on the polymer concentration. The reason for the improved drawability was explained in terms of a reduced number of entanglements per macromolecule in the gel.

Polymer melts have also been utilized to form fibers in the presence of elongational flow. Keller et al (37) reported that the same principles apply for both solutions and melts. However, there are certain differences, for example, the higher the number of entanglements, the lower the likelihood of obtaining ultra-high modulus/strength fibers from the melt. Electron microscopy studies on fibers produced in an elongational melt flow field indicate the presence of a morphological structures that are very similar to the shish-kebab morphology. The kebabs are larger and fewer shishs present when produced in the melt, and this is the reason for the relatively lower modulus improvement of melt produced polyethylene (38).

(b) Extension Of Solid Semi-Crystalline Material

Another approach to achieve ultra-high modulus materials from flexible chain polymers is to extend the solid semi-crystalline material in order to stretch out the folded chains. The three types of drawing processes that will be discussed are tensile drawing, solid state extrusion, and die drawing.

By tensile drawing of spun threads, one can enhance the degree of extension of the chains. This drawing should be done near the glass

transition temperature of the polymer. Some polymers, as PET, are spun in a nearly amorphous state or show a low degree of crystallinity. In other polymers, such as nylon 6, the undrawn material is already semi-crystalline. In the latter case, chain unfolding must accompany chain extension. In all cases unoriented material has to be converted into oriented crystalline material. However, in order to obtain high-tenacity yarns, the draw ratio must be high enough to transform a significant fraction of the chains to a more or less extended state.

An interesting model of the possible structure of drawn semi-crystalline yarns is that given by Prevorsek et al (39) and shown in Fig. 10. It consists of fibrils made up of crystallites with a height of about 5 nm and a thickness of the order of 6 nm. Prevorsek indicated that along the fibrils a number of extended tie molecules are present, this number increasing with strength. So at higher draw ratios the fraction of extended tie molecules is increased.

When the drawn PET is annealed under tension, one can further increase the values of the crystallinity and the crystallite sizes. Tension and time influence the growth of crystals to a certain extent but by far the temperature is the most important factor. Generally PET yarns (and yarns with a moderate rate of crystallization in general) show a low crystallinity which is built up of many small crystallites if the yarns are annealed at low temperatures. If annealed at a high temperature, the yarns contain fewer but larger crystallites. So the overall crystallinity increases.

In drawing above the natural draw ratio which is called superdrawing, further lamellar unfolding takes place. Such a process

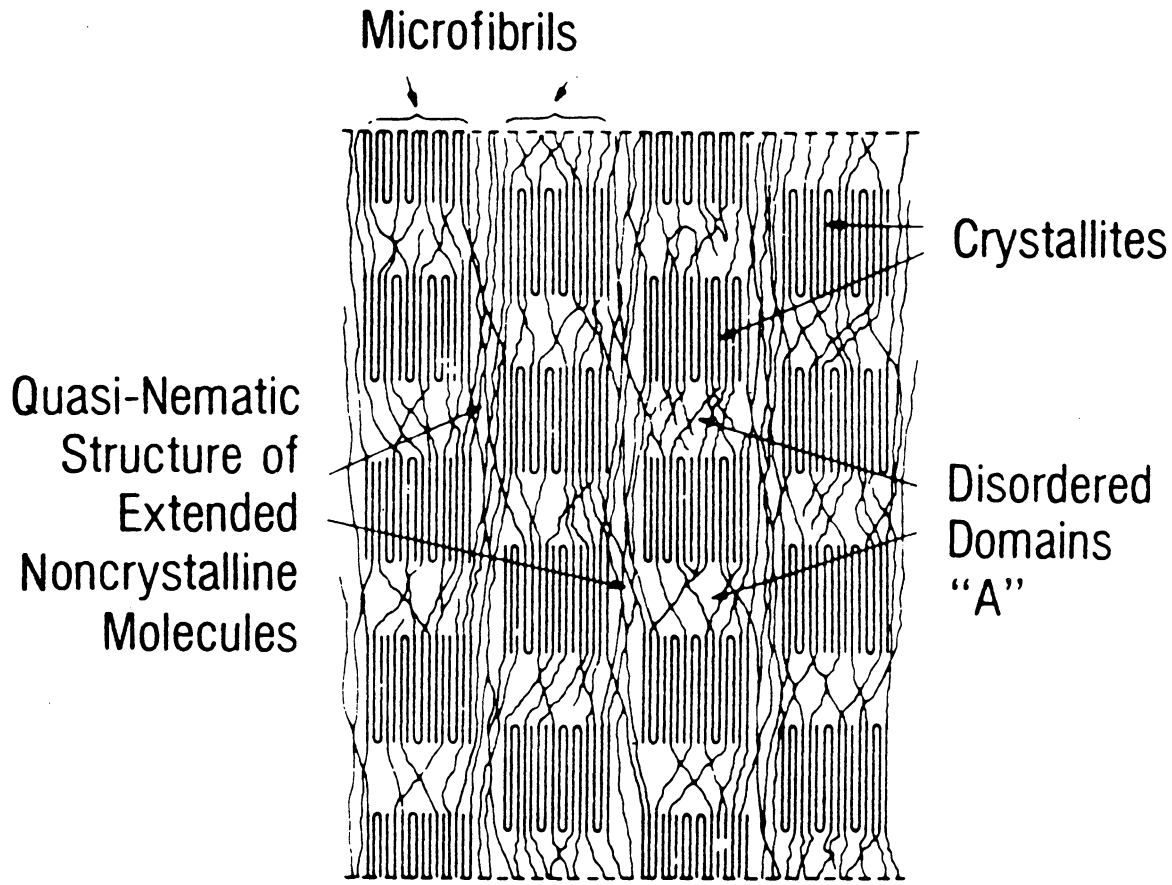

Fig. 10 Model representing the structure of melt-spun fibers of flexible polymers such as PET, aliphatic polyamides, and polyethylene. (39)

at very high draw ratios must be conducted with the utmost care since critical concentrations of stress on the folded chain surface of the crystal blocks must be avoided because they may lead to chain scission. The superdrawing can be carried out in one or two stage operations. The two stage superdrawing consists of a normal fast drawing process as a first stage, followed by a second slower drawing process to very high draw ratios. Excellent results have been obtained with two-stage drawing of polyoxymethylene by Clark and Scott (40). The polymer is drawn to the natural draw ratio of about 7 in the first stage. The second stage takes place at a very low rate (50% elongation per minute) up to a draw ratio of about 20. The optimum temperature for the second step is about 30°C below the melting point. A modulus of 35 GN/m^2, about 70% of the theoretical value, has been obtained this way. Drawn materials of this type no longer show folded chain periodicity as generally noted by small angle x-ray scattering.

Very high draw ratios can also be obtained by extremely careful one-stage drawing. Using polyethylene, Capaccio and Ward in 1974 (41) obtained draw ratios up to 30 and moduli up to 70 GN/m^2 by compression molding sheets of polyethylene at 160°C and either quenching directly into water at room temperature or slow cooling at a rate of 7-9 C/min to 110°C and then quenching into water at room temperature. Differences in mechanical properties for these two types of materials were due to their different morphological textures. The quenched sample showed typical banded spherulitic structure and the slow cooled sample showed a much coarser structure (42).

Sheehan and Cole (43) have drawn polypropylene at a speed of 2 cm/sec in a glycerol bath at 135°C and obtained draw ratios up to 50 and a modulus of about 15 GN/m^2.

Therefore, tensile drawing studies on polyethylene and related flexible chain polymers show that high modulus characteristics can be achieved by varying the draw temperature, draw tension, and the resulting polymer morphology.

Utilization of solid state and die drawing have been studied for the production of high modulus flexible chain polymers (44,45). When solid state extrusion is used, the extrusion rate is relatively slow. Continuous samples, however, are difficult to produce. These limitations have been overcome by a new technique called solid state co-extrusion in which high extrusion draw ratios can be produced at fast extrusion rates. Details on these two techniques are found in the literature (3,44,45).

(3). High Modulus-High Strength Characteristics Using Liquid Crystalline Polymers

Molecules that display liquid crystalline properties were discovered nearly a century ago, and a large volume of literature, including many notable books, has evolved concerning these compounds (46,47,48). But only in the past decade have polymeric liquid crystals based on rod-like or rigid chain structures been studied in some detail (49,50,51). In the present review some of the features of liquid crystal polymers based on the structures that have mesogenic component in the backbone will be discussed.

The liquid crystal state, which has been called by some the fourth state of matter, exists between the boundaries of the solid crystalline phase and the conventional isotropic liquid phase. Thus, the liquid crystal state is one in which some of the molecular order characteristic of a crystalline solid phase is retained in the liquid state because of molecular structure and short-range intermolecular interaction of the van der Waals type. A certain degree of order returns when the mesogen (i.e., liquid crystal substance) is cooled from the isotropic liquid state.

Flory (52) has developed a theory which predict that rod-like molecules having an axial ratio of less than 6.4 are capable of undergoing a transition in the melt from the nematic liquid crystalline state to the isotropic liquid state. The compounds with larger axial ratios, melt at too high a temperature to obtain the liquid crystal state and proceed directly to the isotropic state.

The basic mesogenic promoting structures in many of these liquid crystal polyesters are benzene rings attached at the para position often through ester groups. For example, they can be derived from terephthalic acid plus hydroquinone or from p-hydroxybenzoic acid (53). As in the monomeric systems, these rigid rod-like polymers will often align in the melt or solution to give a highly ordered structure. The processing of such a polymer into a fiber, film, or molded article from this state results in structures that are highly ordered and exhibit higher modulus and strength along the flow direction than conventional folded chain polymers processed in similar ways.

In order to prepare a thermotropic polymer, careful attention must be given to chain composition. A highly rigid and symmetric polymer, such as that obtained from terephthalic acid and hydroquinone, is much too intractable for melt processing. Other monomers must be introduced that would increase tractability so that melt processing is possible. This can be accomplished through slight disruption of molecular order. Three approaches to lower the melting temperature can be used: 1) incorporation of some flexible linkages e.g. (-CH_2-CH_2-); 2) the use of an asymmetric substituted benzene ring (such as chlorohydroquinone); or 3) a molecule that would provide a kink in the chain (such as a naphthalene moiety). These approaches will be discussed below.

It was Jackson and Kuhfuss (7) who first utilized Hamb's (54) method of synthesis for the modification of PET with p-hydroxybenzoic acid (PHB). They determined the range of composition that yield turbid melts which are characteristic of liquid crystalline behavior, and found that copolyesters containing 40 mol % or higher concentration of p-hydroxybenzoic acid exhibit liquid crystalline structure. Later, McFarlane et al (55) studied the synthesis of various copolyesters exhibiting liquid crystalline behavior. For instance, they obtained liquid crystalline copolyesters by modifying PET with p-acetoxybenzoic acid and both p-hydroquinone diacetate and terephthalic acid.

Aguilera and Ringsdorf (56) have prepared and characterized polyesters with substituted hydroquinone and a highly flexible dimethylsiloxane spacers to attain a better understanding of the effect of the flexible oligosiloxane spacers and mesogenic groups on the thermotropic properties of this polyester as shown below.

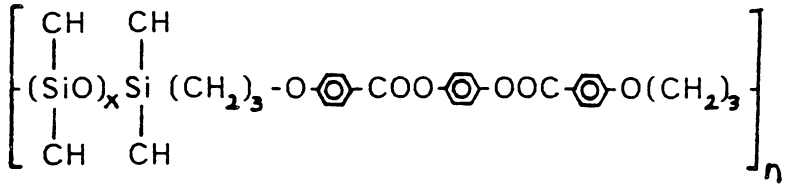

They found that the substitution on the hydroquinone units for these polyesters have a remarkable influence on the thermal phase width (liquid crystal transition to glass transition temperature) and on the clearing temperature when compared with those without substitution. By increasing the spacer length, it decreases both the glass and clearing transition. Another interesting observation was that for short siloxane units, when x=2 or 3, the polyesters containing chloro-substituted hydroquinone have greater "phase width" than those polyesters with methyl substituents. Therefore, by having a longer spacer length in the polyester, the greater phase widths dissapears.

Jo, Jin, and Lenz (57) studied properties of new liquid crystal polyesters with structure denoted below where Ar was either phenylhydroquinone or 4,4'-biphenol.

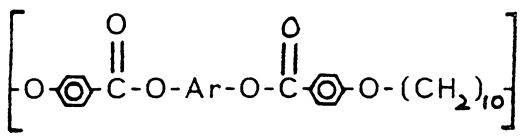

They found the transition temperatures, Tm and Ti (liquid crystal to isotropic transition temperature), for the biphenol polymer were higher than those observed for the hydroquinone polymer. In particular, the clearing temperature of the former was much higher than that of the latter. The longer, more rigid mesogenic groups in the biphenol polymer must be responsible for the much enhanced thermal stability of the mesophase and thus the increased Ti.

Lenz and Jin (58) demonstrated that the thermotropic liquid crystalline properties of the aromatic polyesters derived from terephthalic acid and either methylhydroquinone or chlorohydroquinone copolymerized with varying amounts of different bisphenols were greatly dependent upon both the structure and the amount of the nonlinear comonomer units or spacers. The nonlinear bisphenol spacers containing large or bulky central substituents between the two phenolic rings were found to be more effective in destroying the liquid crystal properties of the resulting copolyesters than those with smaller substituents. Hence, it was concluded that the geometric and steric effects imparted to the polymer chain backbone by the comonomers were the most important controlling factors affecting the liquid crystallinity of the aromatic copolyesters.

Once a liquid crystal polymer is formed, orientation can be developed to enhance modulus and strength in the direction of orientation. This is discussed below.

Ide and Ophir (59) studied the orientation development in thermotropic liquid crystal polymers containing 60 mole % p-acetoxy benzoic acid, 20 mole % 2,6-naphthalene diacetate and 20 mole % terephthalic acid. This material was extruded and drawn down in the melt. They report that a sample with virtually no draw down does not show any molecular orientation in spite of having been extruded at a high shear rate. With increasing draw down ratio the modulus and the orientation increase. It was found that high molecular orientation is readily obtained by elongational flow but not so with shear flow. Ide and Ophir (60) later studied the injection molding of this same liquid

crystal polymer. Figure 11 is the cross section of one of their tensile bars that was extruded at 340°C and injected into a 100°C mold at high speed. The structures shown are a light skin layer (A) (the edges of the bars are marked on the picture) and a dark layer (B). WAXS patterns of layers A and B are shown in Fig. 12. The x-ray photographs were taken with the incident beam normal to the flow direction of the samples. It is apparent that the skin layer is highly oriented in the flow direction while the sub-skin layer is almost unoriented. The highly oriented skin layer originates from the 'fountain flow' (this can give rise to uniaxial or biaxial orientation depending upon flow cross section) at the melt front and deposited on the wall with the flow direction orientation. The elongational flow field can induce high molecular orientation, and the orientation is immediately frozen in upon contact with the mold's surface. The sub-skin layer B experienced mainly spreading radial flow and had more time to relax, therefore, its orientation is minimal.

In summary, liquid crystalline aromatic polyesters can form fibers or other forms of high strength and stiffness by melt spinning or injection molding in the liquid crystal state. However, one of the simplest aromatic polyesters of this type, those derived from terephthalic acid and hydroquinone or from p-hydroxybenzoic acid, melt well above 600°C, and the processing of these polymers by conventional methods is impossible. Several methods to obtain liquid crystal polymers with considerably lower melting points have been discussed.

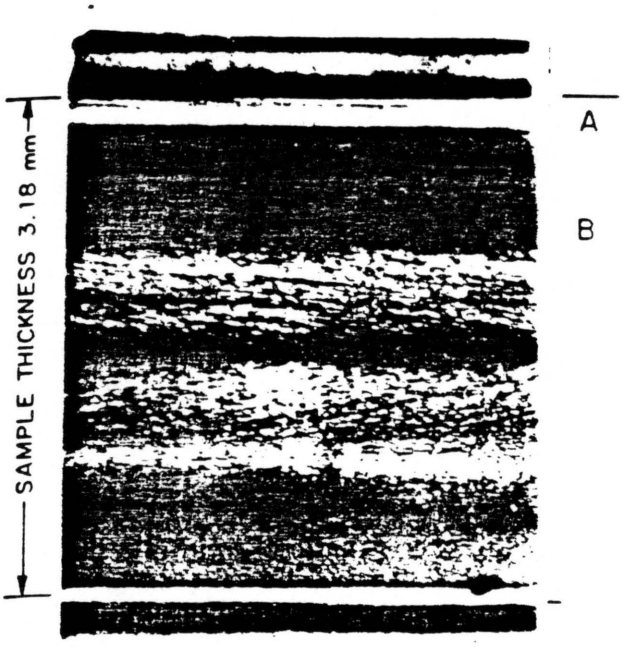

Fig. 11 View of the cross-section of a tensile bar (sample was taken from the center of the bar, arrow indicates flow direction). (60)

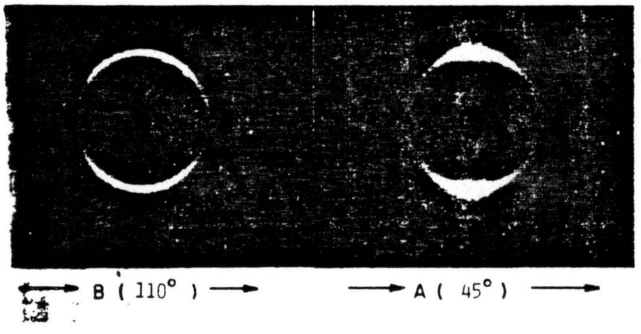

Fig. 12 Wide angle x-ray scattering patterns of the skin layer A, and sub-skin layer B and their orientation angles, respectively. (60)

CHAPTER 1

The first part of this chapter concerns the investigation of structure-property behavior of extruded cast films prepared from blends of thermotropic liquid crystalline copolyesters with polyethylene terephthalate (PET). Orientation effects were clearly observed in these materials. Data were obtained which showed not only the temperature dependence of the moduli and stress-strain behavior but also the orientation effects that must be prevalent in order to explain the differences between the moduli measured parallel and perpendicular to the extrusion direction. Only at high liquid crystal polymer (LCP) compositions is the modulus particularly increased. If indeed phase inversion occured, as might have been expected around at 40-60 % LCP, the modulus should have risen much faster than was observed. Various morphological features of the fracture surfaces were examined as will be discussed.

The second part of this chapter concerns modulus enhancement with lower LCP content and utilization of process variables. One major drawback to this approach is that while the modulus was increased greatly in the extrusion direction, very poor properties are observed in the transverse direction due to the fact that there was little continuity of the LCP component in this direction. The extruder gear pump speed did not enhance Young's modulus at the same LCP content as extensively as did the effect of extruder screw speed. In the blown films, it was seen that take-up speed did not as affect the texture of

the LCP component as strongly as did the blow-up ratio for these samples.

MATERIALS

The principal liquid crystalline polymer for this work was obtained from Celanese company and is based on p-hydroxybenzoic acid, 2-hydroxyl-6-naphthoic acid and hydroquinone. Utilizing the Celanese nomenclature, this system will be denoted as LCP 2000. Details on the synthesis of LCP 2000 appear in the literature (61) and hence only a brief summary will be given below for one of the batch processes.

A three-neck, round bottom flask was equipped with a stirrer, nitrogen inlet tube, and a heating tape wrapped around the distillation head which is connected to a condenser is used. The following are added to the reactor:

a) 0.3 mole of p-acetoxybenzoic acid

b) 0.15 mole of 2,6-naphthalene diacetate

c) 0.15 mole of hydroquinone

This mixture is then brought to a temperature of 250°C. At 250°C most of the terephthalic acid is suspended as a finely divided solid in a molten solution of p-acetoxybenzoic acid and 2,6-naphthalene diacetate. The contents of the flask are stirred rapidly at 250°C under a slow steam of dry nitrogen for about 2 hours while acetic acid is distilled from the polymerization vessel. The polymerization suspension is then raised to a temperature of 280°C and is stirred at this temperature for 1 hour under a nitrogen flow while additional acetic acid is evolved. About 40 ml of acetic acid is collected during these stages. The polymerization temperature is next increased to 320°C. The viscous polymer melt is held for 15 minutes at 320°C under a nitrogen flow and

then subjected to a series of reduced pressure stages. During these stages, the polymer melt continues to increase in viscosity and is stirred more slowly while the remaining acetic acid is removed from the reaction vessel. The polymer melt is next allowed to cool to ambient temperature (i.e., about 25°C). Figure 13 shows the general chemical structure of the resulting LCP 2000 polymer system.

A polymer designated as LCP 4060 was also utilized as a blending agent for PET. This latter polymer also obtained from Celanese, is a copolyester-amide involving terephthalic acid, p-aminophenol and 2-hydroxyl-6-naphthoic acid. No further details on the synthesis of LCP 4060 were available.

Sample Preparation

(a). Dry Blended and Extruded Films

The LCP 2000 polymer was first dry blended with PET in pellet form, dried in vacuum oven at 120°C overnight, and then mixed within an extruder in the process of producing quenched cast film (2-4 mil) on a pilot scale production line. Extrusion was done in a Wayne 1 inch extruder. The screw has a 3:1 compression ratio and a Maddock mixing section was used for better mixing. Extruder barrel temperature was at 295°C. The blend was extruded through a slit die at 280-288 C and quenched onto a chilled roll at ambient temperature. The screw speed was kept constant at 20 rpm. The extruded film was removed from the quench roll and characterized. Also, the samples were prepared with different levels of LCP content, that is 20, 40, 60, and 80 % LCP 2000 polymer blended with PET. The content of LCP in the blend will be in wt. % throughout this chapter unless otherwise noted.

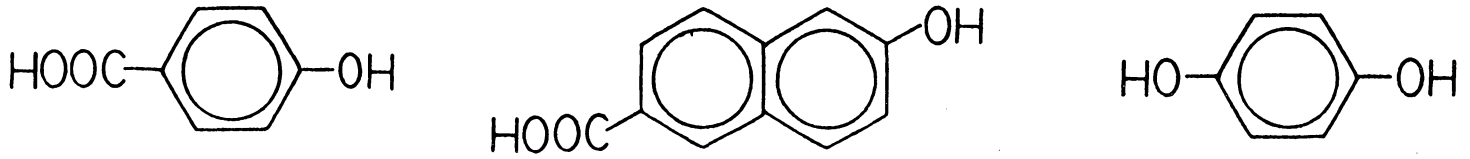

CHEMICAL STRUCTURE OF LCP 2000

Fig. 13 The general chemical structure of the LCP 2000 polymer. It contains p-hydroxybenzoic acid, 2-hydroxyl-6-naphthoic acid, and hydroquinone.

(b). Films Produced By Systematic Variation Of The Process Conditions

Specific process parameters that were varied to produce the films were extruder screw speed and gear pump speed.

For the samples that were prepared by systematic variation in the screw speed, the samples were first dry blended in pellet form, and then dried at 150°C in a hot air oven for 48 hours. Extrusion was done with a Wayne extruder where the screw speed was controlled from 10 to 70 rpm. The extrudate was quenched onto a chilled roll immediately. (There was no gear pump to regulate speed, therefore, residence time in the extruder can be viewed as inversely proportional to screw speed).

For the samples that were prepared by systematic variation in the gear pump speed variable, extrusion was done in a small 3/4 inch laboratory extruder equipped with a gear pump to regulate extrusion rate. The screw speed was kept constant at low rates, but the screw speed had to be increased with the gear pump speed at high rates. The extrudate was quenched onto a quench roll and taken up with little or no stretching. The nomenclature for different screw speed and gear pump speed samples are given in Table 2.

TABLE 2 - Nomenclature of the various process variable and different liquid crystal polymer samples

LCP 2000-30-SS 30 % LCP 2000, 70 % PET
SS = SCREW SPEED IN RPM
LCP 2000-30-SS-10
LCP 2000-30-SS-20
LCP 2000-30-SS-30
LCP 2000-30-SS-50
LCP 2000-30-SS-70

LCP 2000-30-GPS 30 % LCP 2000, 70 % PET
GPS = GEAR PUMP SPEED IN RPM

SAMPLE	VOLUME RATE (cc/min)
LCP 2000-30-GPS-5	2.5
LCP 2000-30-GPS-8	4
LCP 2000-30-GPS-17	8.5
LCP 2000-30-GPS-27	13.5
LCP 2000-30-GPS-52	26
LCP 2000-30-GPS-78	39
LCP 2000-30-GPS-105	52.5

LCP 2000-40-GPS 40 % LCP 2000, 60 % PET
GPS = GEAR PUMP SPEED IN RPM

SAMPLE	VOLUME RATE (cc/min)
LCP 2000-40-GPS-10	5
LCP 2000-40-GPS-17	8.5
LCP 2000-40-GPS-27	13.5
LCP 2000-40-GPS-52	26
LCP 2000-40-GPS-78	39
LCP 2000-40-GPS-105	52.5

LCP 4060-30-GPS 30 % LCP 4060, 70 % PET
GPS = GEAR PUMP SPEED IN RPM

SAMPLE	VOLUME RATE (cc/min)
LCP 4060-30-GPS-5	2.5
LCP 4060-30-GPS-10	5
LCP 4060-30-GPS-17	8.5
LCP 4060-30-GPS-27	13.5
LCP 4060-30-GPS-52	26
LCP 4060-30-GPS-78	39
LCP 4060-30-GPS-105	52.5

EXPERIMENTAL METHODS

The techniques of contact chemical etching, direct solvation and cold fracture will be discussed. The techniques used for characterization of these liquid crystalline copolyester films are also presented.

Chemical Etching: The technique of chemical etching relies on the use of a suitable chemical reagent which preferentially attacks a specific component of a material. In the case of a two component polymer blend, the ideal reagent would etch one component while leaving the other structure undisturbed. This non etched structure of the sample could then be analyzed by scanning electron microscopy (SEM).

N-propylamine was utilized initially for purposes of etching away the PET phase and revealing information regarding the structure of the LCP component. N-propylamine will readily attack PET causing its degradation to ethylene glycol and n-propylterephthalamide. This technique involves placing a sample between two glass slides, and this glass slide sandwich is placed inside a Petri dish containing n-propylamine. A more detailed description of this method can be found elsewhere (62). However, while this method was useful in revealing morphological texture, the method stated below was more successful for this study.

Direct Solvation and Extraction of the PET Component by Trifluoroacetic Acid (TFA):

This method was utilized in the majority of this work since it clearly provided the most direct means of highlighting the morphological features of the blends. Specifically, TFA solvates PET readily whereas it does not solvate the LCP 2000 or 4060 polymer utilized in this study. Samples of LCP 2000 placed in TFA for 36 hours showed no signs of dissolution. The PET phase could thus be preferentially removed and followed by direct SEM investigation of the remaining LCP solid phase.

Figure 14 schematically shows the apparatus used for preferential solvation and extraction of the films. In this experiment, a fine screen (100 mesh) was used for two purposes: 1) to keep the non-solvated liquid crystal polymer component in one place in the solution and 2) to prevent the sample from being oriented when the sample is being removed from the solution after extraction. Due to the toxicity of the volatile TFA, the experiment was always carried out in a well-ventilated hood.

Below is a step by step description of the procedure.

1. Place a sample between two fine screens.
2. Place the screens with sample in a glass Petri dish.
3. Pour enough dissolving reagent (TFA) into the petri dish so that screens with samples are completely immersed in the liquid reagent, and then cover the petri dish.
4. Allow dissolution to be carried out at room temperature for the desired period of time. (Desired period depends on the sample thickness. In general, it was found that the optimum time of extraction for the samples of 10-20 microns thickness was

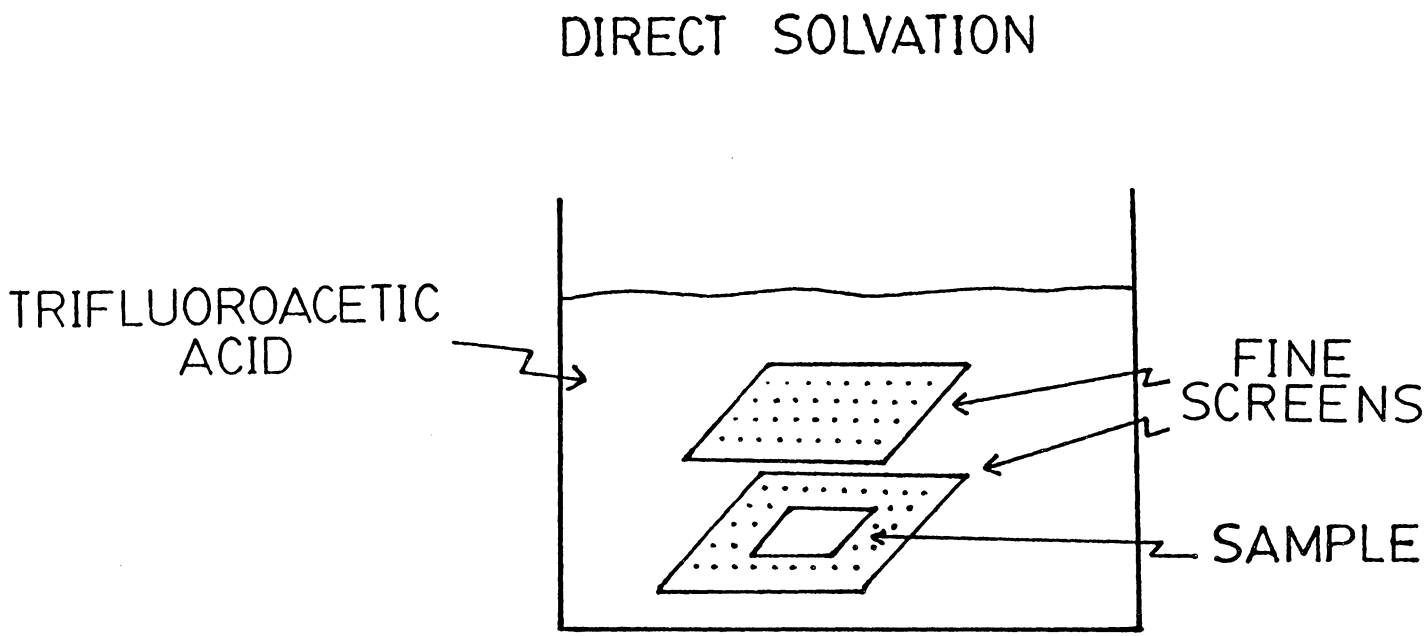

Fig. 14 Schematic diagram of apparatus used for direct solvation.

6-8 hours).

5. After the desired period for dissolution of the PET, carefully remove the screens (with sample) with a tweezer from the Petri dish and carefully remove the remaining sample from the screens and let it dry under a hood.

Direct Fracture of the Materials Following their Immersion in Liquid Nitrogen (cold snaps): This method proved useful since it revealed the general two phase morphology of the blend due to the different mechanical properties of the two components at the time of fracture. That is, the boundary of the dispersed phase in the matrix of the other component was directly observable. The sample was immersed in liquid nitrogen for 10 minutes and was fractured while submerged with a pair of tweezers which were also kept at liquid nitrogen temperature.

Morphological Characterization Techniques

(a). Scanning Electron Microscopy (SEM)

The SEM technique is an useful tool to study the morphological structure of polymers. It is widely used in polymer science, and some of the reasons for its popularity are the easy procedure by which the samples can be prepared for viewing and the high resolution and depth of focus that it offers.

In the present studies an ISI super III-A scanning electron microscope along with a SPI sputter coater, T.M. model 13131 (for coating the sample with a layer of gold) were used.

(b). Wide Angle X-ray Scattering (WAXS)

X-ray diffraction is induced by periodic fluctuations in electron density that occur over small distances (approximately up to 20 Å). Wide angle x-ray scattering from crystals as well as from semi-crystalline polymers can be utilized to determine the degree of crystallinity and obtain information regarding size, perfection and orientation of the crystals. Detailed reviews of wide angle x-ray scattering and its application to polymers can be found elsewhere (63,64). WAXS studies were performed during the course of this study in order to qualitatively obtain the level of crystallinity and relative degree of orientation.

A typical WAXS pattern of an amorphous PET film shows a diffuse halo. When x-ray diffraction is performed on a unoriented polycrystalline sample, a scattering pattern consisting of sharp rings will be obtained. The multiple rings are caused by scattering from different planes in the unit cell. The sharpness of these rings is related to the crystalline perfection, size, and amount of the crystalline phase. If the crystallites are not oriented at random but rather have their crystal axes oriented in a preferred direction, the WAXS pattern will take the form of arcs. A more detailed review of WAXS and its application to oriented polymers can be found in the literature (65).

A Phillips PW 1720 table top x-ray generator equipped with Warhus cameras was utilized for all studies. The general operating conditions for the x-ray generator were a 40 kV voltage and a beam current of 20 mA. Sample thickness for the WAXS specimens ranged from 4 mils to 15 mils while the x-ray exposure time varied from 8-15 hours. A sample to film distance utilized was 7.8 cm. in all cases.

(c). Mechanical Testing.

Mechanical properties were investigated by use of a Model 1122 Instron which is a standard instrument in determining such properties. Detailed reviews on mechanical properties of polymers can be found elsewhere (66).

Stress-strain behavior was obtained by stretching dog bone samples (10 mm long) at a constant crosshead speed of 10 mm /minute. In order to observe stress/strain behavior at high temperatures, a "home built" thermal chamber with proportional controller was utilized for maintaining the environment temperature in the range of 80 °C-240 C. The environment temperature was controlled within +/- 2 °C.

RESULTS AND DISCUSSION.

EXTRUDER BLENDS OF PET AND LCP 2000

In this section, mechanical studies will be discussed followed by the results of the SEM studies of various fracture surfaces. WAXS studies are also included.

Mechanical Studies

In Figs. 15A through 15D, the general stress-strain behavior of the blends of LCP 2000 with PET are shown as determined at 80 and 120 C, respectively. At each temperature, the curves are shown for measurements that have been made parallel and perpendicular to the extrusion direction. It should be emphasized that no post extrusion draw was utilized in preparing these films. As might be expected, the general stress-strain behavior differs for the two different draw temperatures in that at the lower temperature, a higher stress is observed at an equal elongation and blend content. The PET in the blend remained amorphous during these stress-strain experiment even at 120°C, which is above its Tg (80°C). If the PET component had been semicrystalline this would have helped to rigidify the PET phase and raised the modulus. Indeed, it was noted that in the extrusion and quench roll process, the PET component did not crystallize. Therefore, the PET component should be viewed as being amorphous in these mechanical studies as per Fig. 15. Wide angle x-ray diffraction (WAXS) later confirmed this.

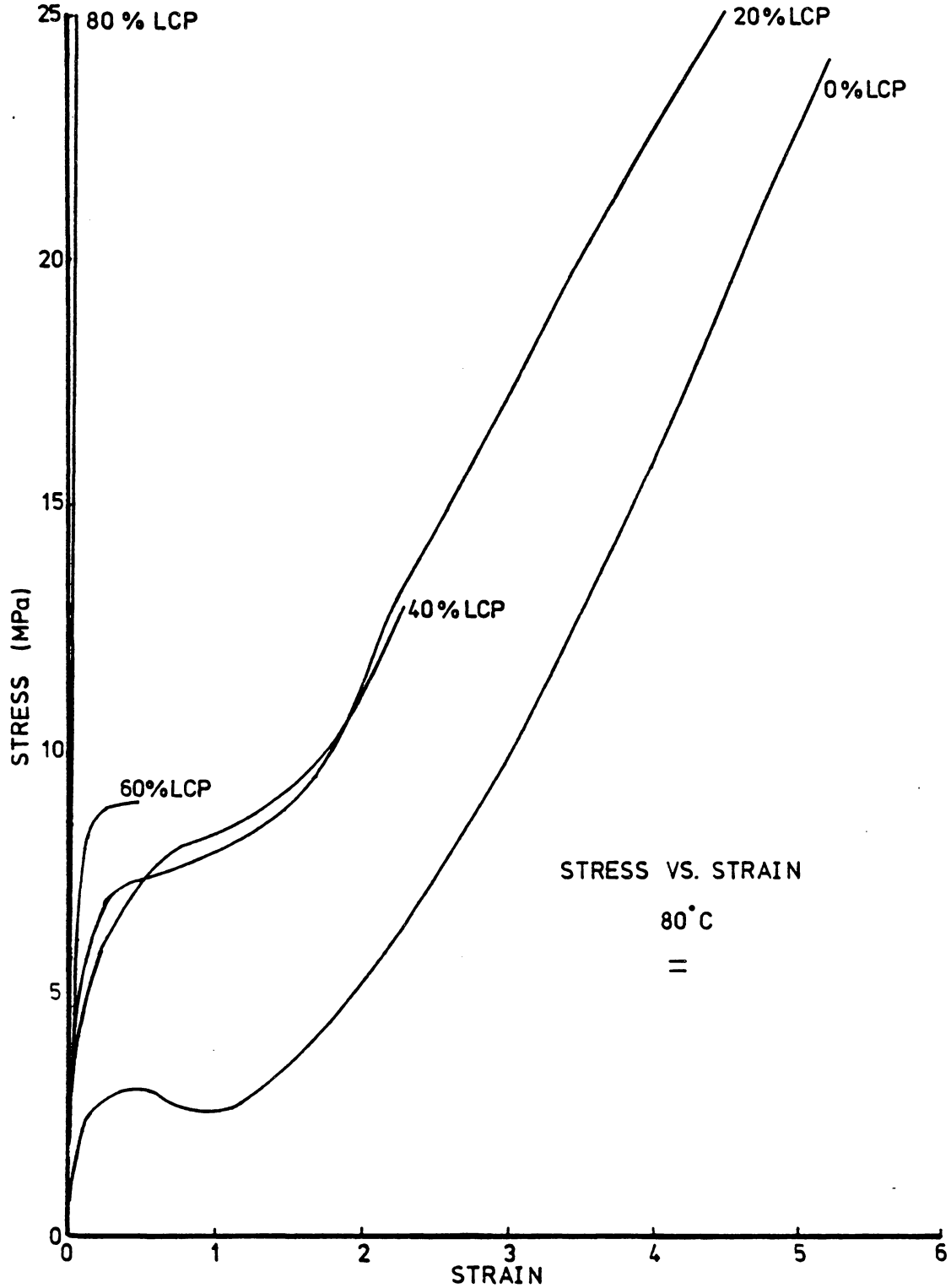

Fig. 15A Stress-strain curves of various LCP 2000 compositions determined at 80 C. The draw direction is parallel to the film flow direction.

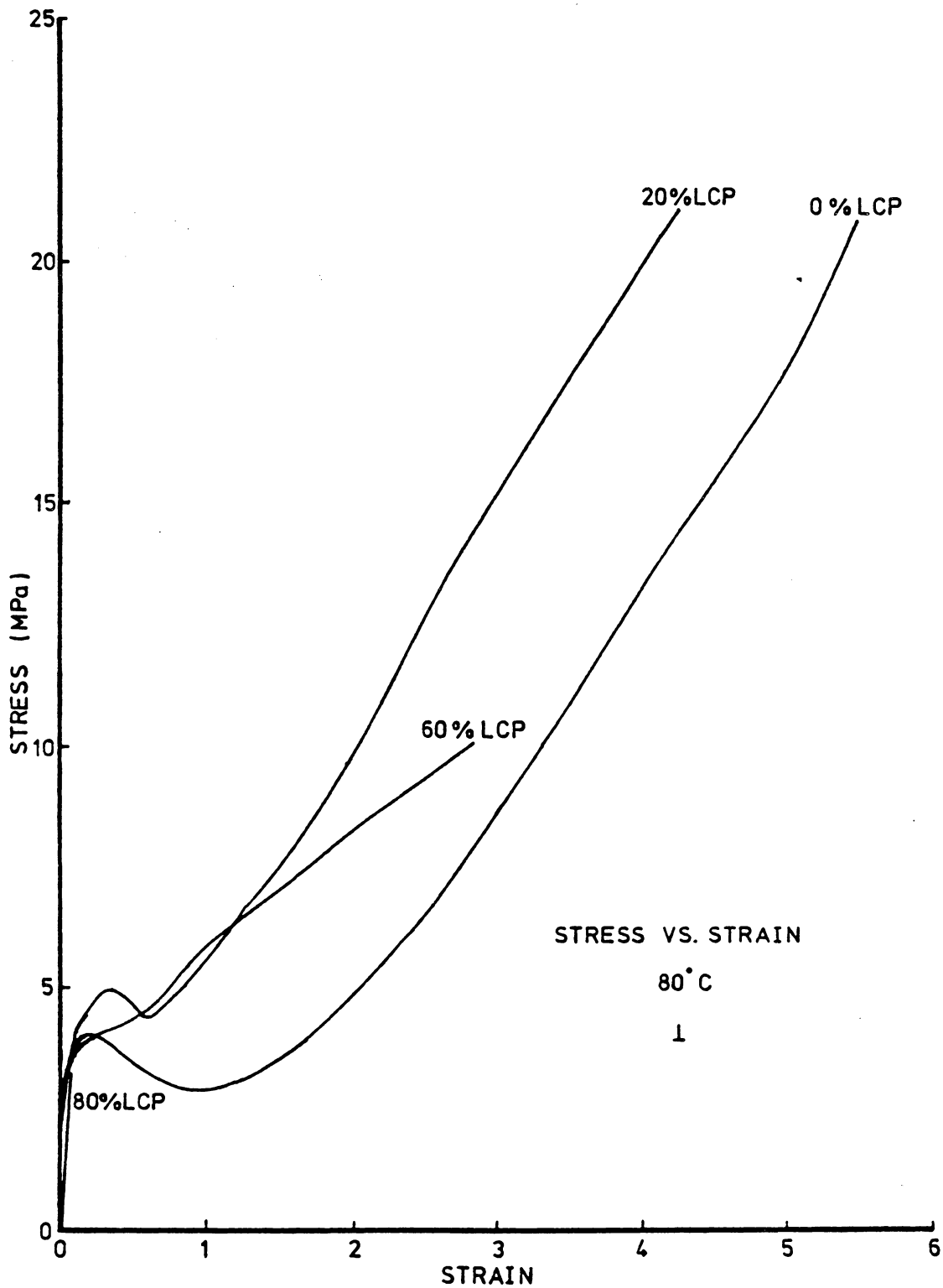

Fig. 15B Stress-strain curves of various LCP 2000 compositions determined at 80 C. The draw direction is perpendicular to the film flow direction.

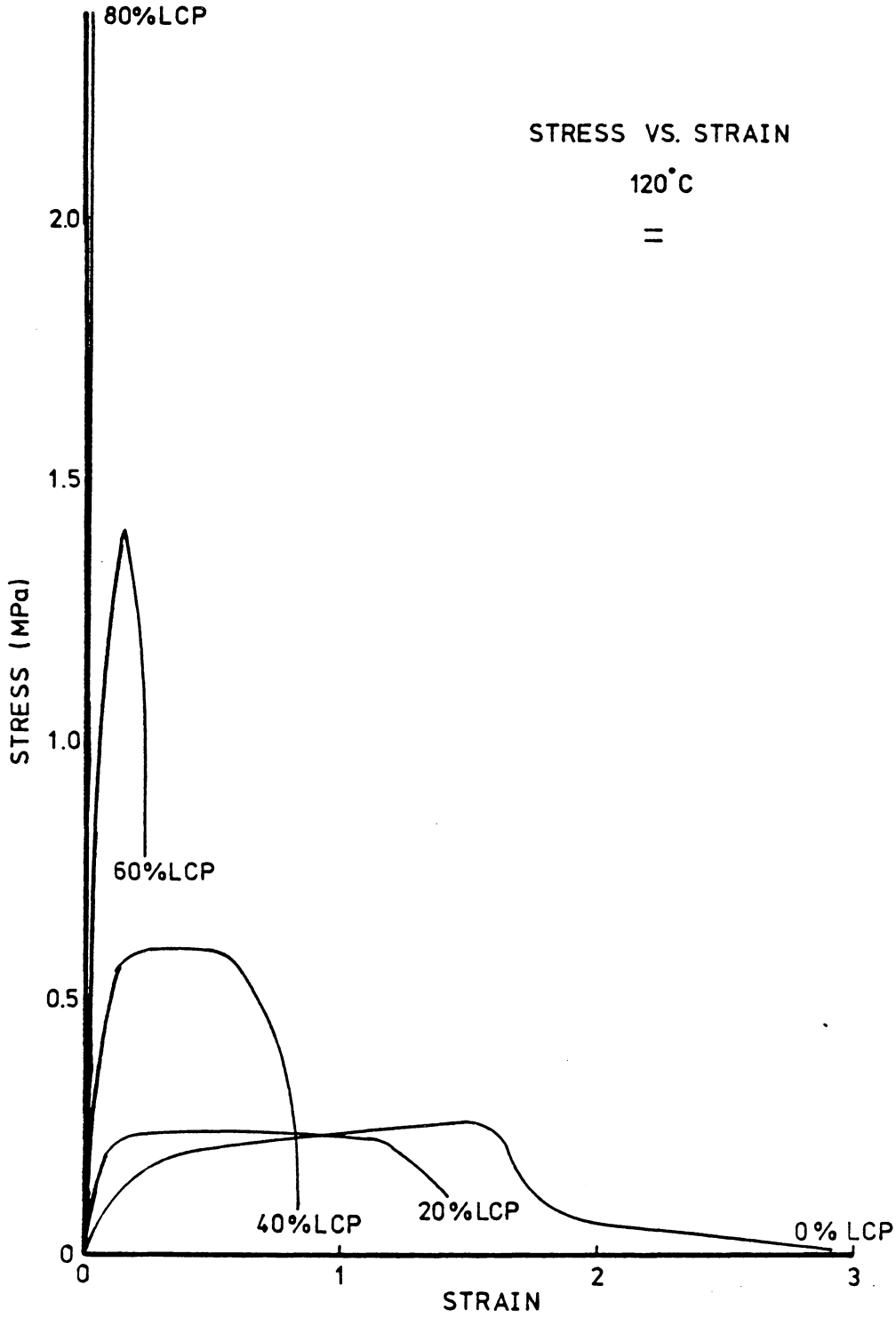

Fig. 15C Stress-strain curves of various LCP 2000 compositions determined at 120 C. The draw direction is parallel to the film flow direction.

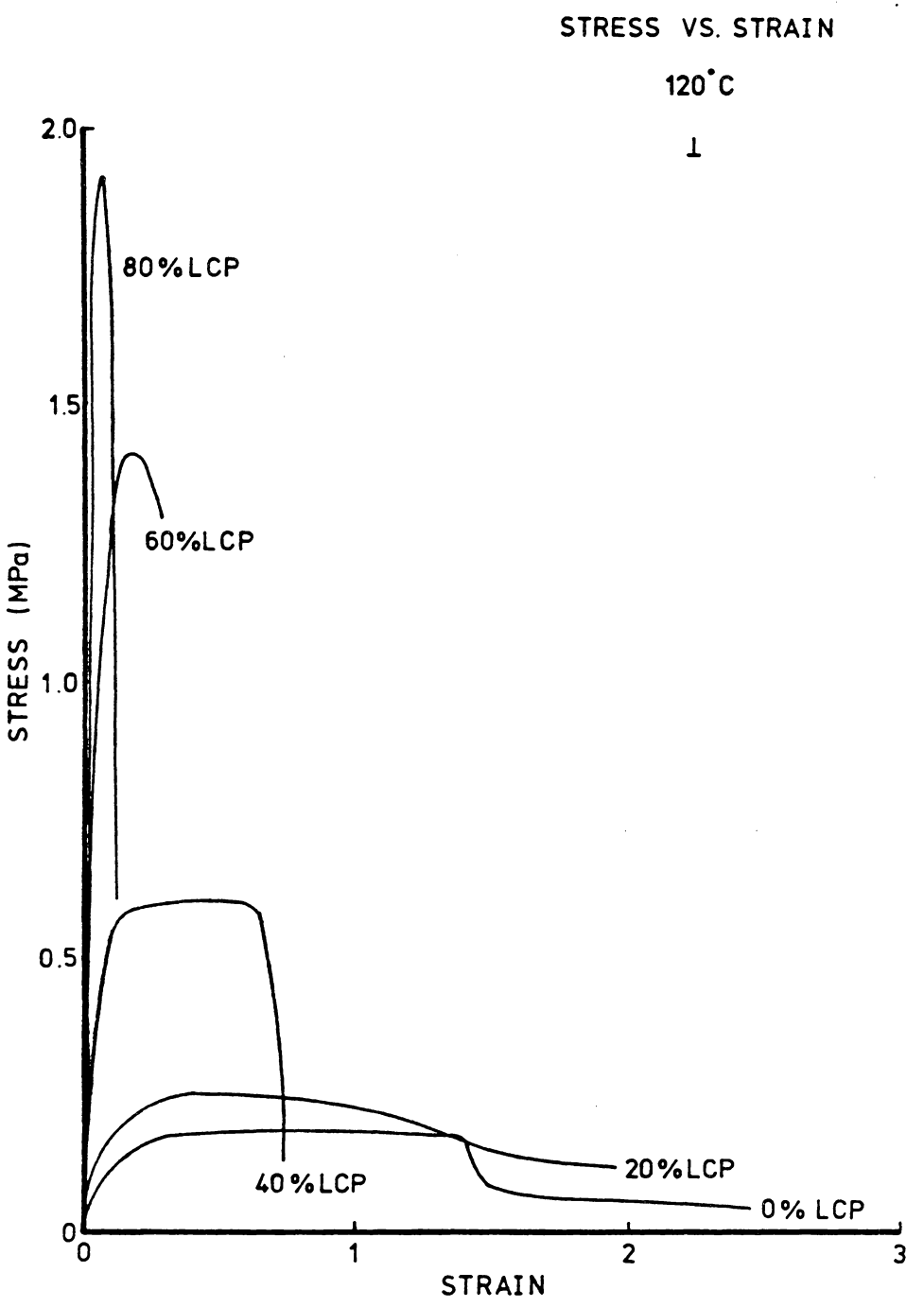

Fig. 15D Stress-strain curves of various LCP 2000 compositions determined at 120 C. The draw direction is perpendicular to the film flow direction.

Differences in molecular orientation is suggested by the differences between the parallel and perpendicular stress-strain behaviors and was verified by work to be discussed later. This orientation is due to the fact that the film was extruded through a die, and orientation was developed in the extrusion direction. As expected, lower stresses were obtained on the perpendicularly drawn film samples in which the testing direction is perpendicular to the initial extrusion axis. Later discussion of the morphological texture will further explain why the observed mechanical properties are as found.

It is interesting to note from the overall data that the general yield characteristics as well as the strain at break are clearly affected by the LCP component. In particular, as the LCP content increases, the extension to break decreases while yield stress either becomes higher or is not apparent at all in the stress-strain behavior. It was particularly surprising that even with 60% LCP content, some degree of drawability still existed, e.g., see Fig. 15A. This was initially unexpected since it was anticipated that above the order of 40 to 50% LCP content, the LCP component would likely form a continuous phase. Since it is a nonductile material at 80°C, ultimate strains above a very few percent were not expected.

Utilizing this stress/strain data, the modulus of elasticity, i.e., Young's modulus, was extracted from the initial slopes of the curves and these values have been plotted in Fig. 16 as a function of the LCP composition. These data again clearly show not only the temperature dependence of the behavior but also the orientation effects of the LCP 2000 phase that clearly must play a role in the differences between the

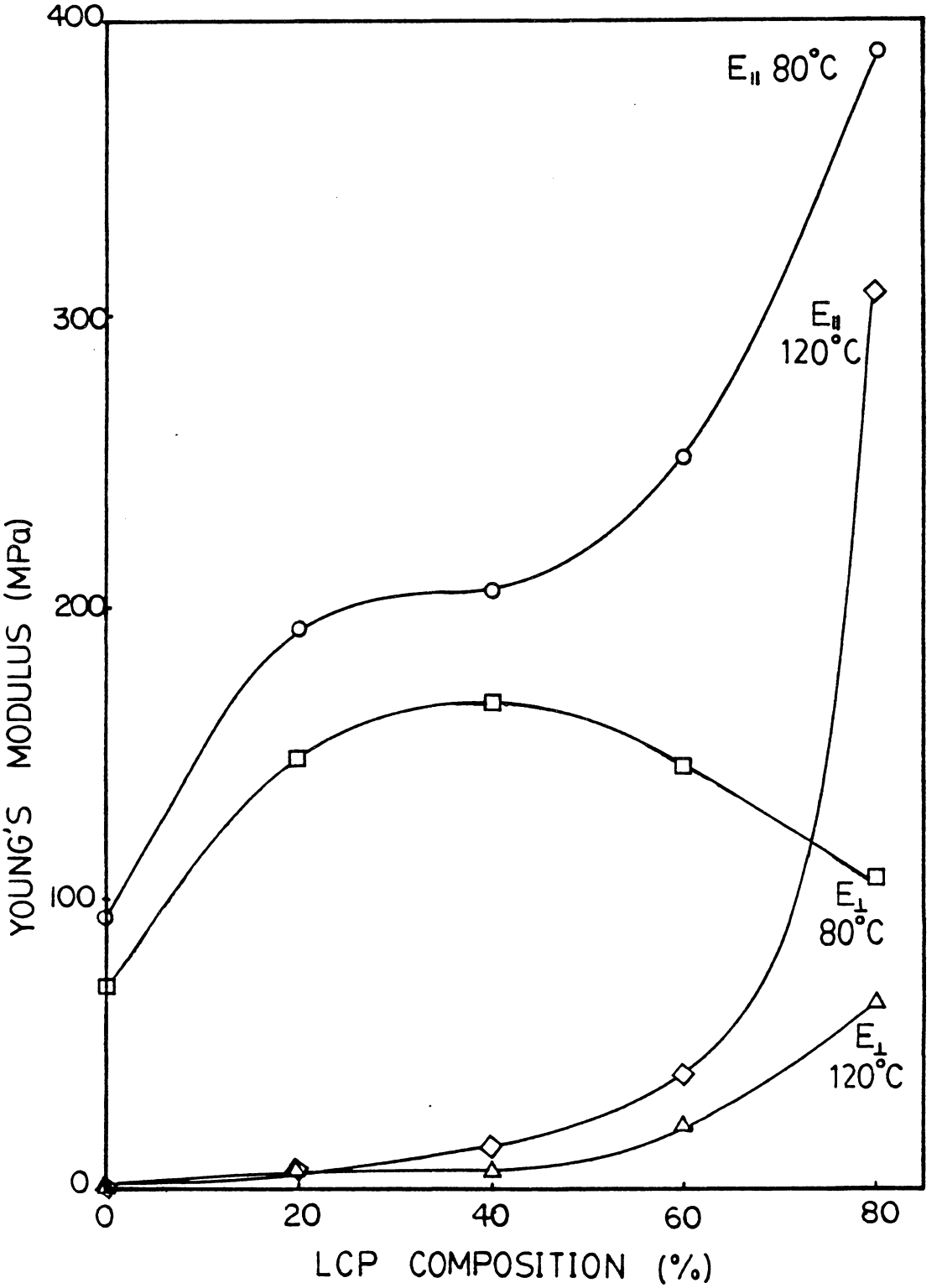

Fig. 16 Young's modulus of various LCP 2000 compositions. Measurements were made perpendicular to the film flow direction.

moduli measured with the draw axis parallel to the extrusion direction ($E_{\parallel}$) and those determined perpendicular to the extrusion axis ($E_{\perp}$). These data again reflect the fact that only at high LCP composition (greater than 60 % LCP) is the modulus particularly enhanced. If indeed phase inversion occurred, as might have been expected in the range of 40 to 60% LCP, the modulus would be expected to rise much faster than is shown in Fig. 16.

Due to the fact that the PET component was later determined to be amorphous in the initial stress-strain behavior, samples of the same blends were annealed in an unstrained state for one hour at 160°C under vacuum for purposes of promoting the crystallization of the PET component. Samples were then removed, and the stress-strain behavior was determined at 120°C. From these data, the value of Young's modulus was determined as shown in Fig. 17. Here it is clear that the values are considerably higher and show little dependence on LCP composition up to 80% where the modulus then rises strongly, suggesting some continuity of the LCP phase. When these data are compared with those in Fig. 16 obtained at the same draw temperature, it is seen that there is a difference of a factor of five which results from PET crystallinity.

SEM Studies Of Fracture Surfaces

The morphological features of the fracture surfaces prepared by cold snaps are presented in Figs. 18A-18E. Each of these figures presents a "parallel" as well as a "perpendicular" fracture with respect to the extrusion axis. More specifically, the micrographs on the left

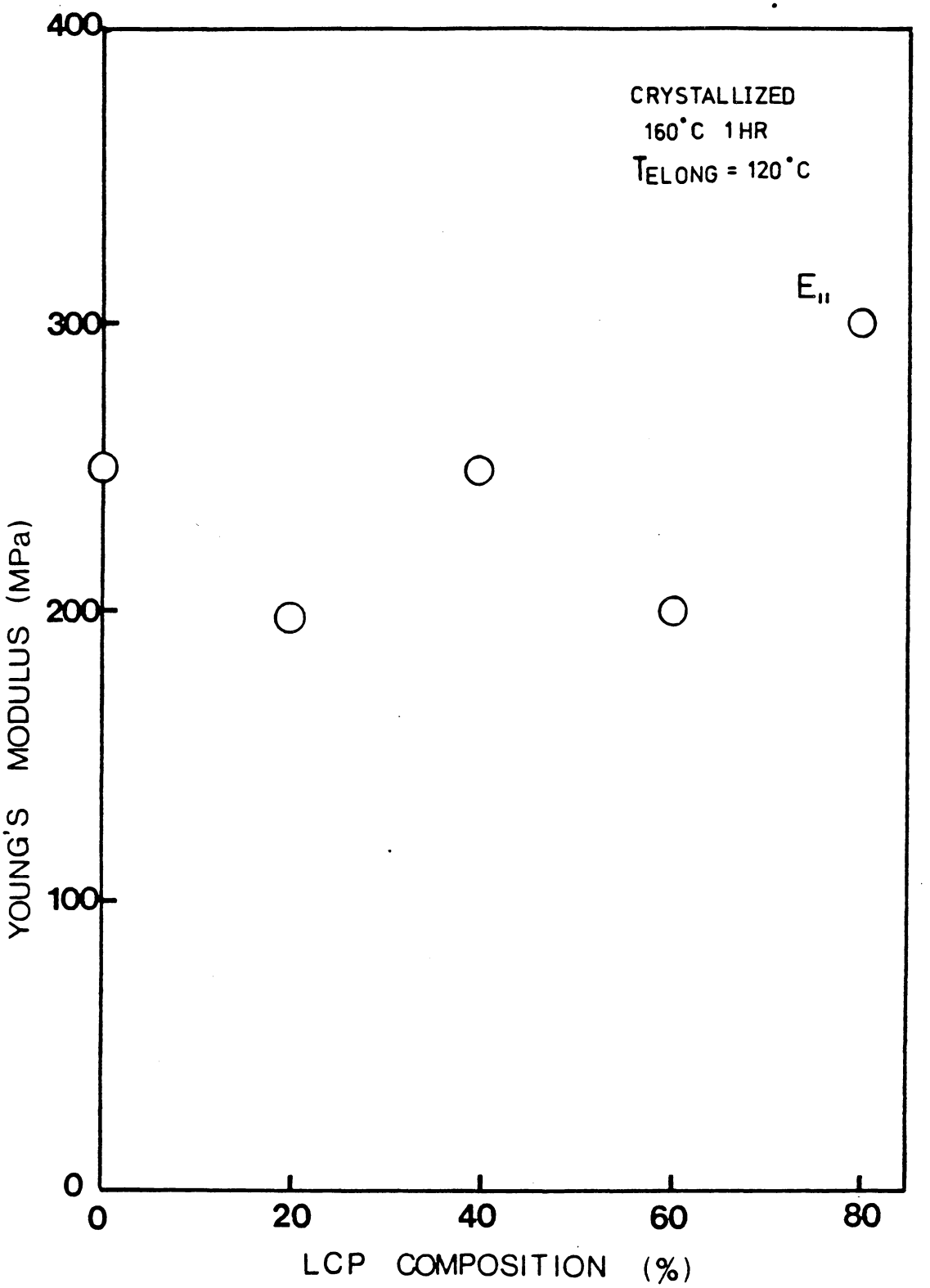

Fig. 17 Modulus of various LCP 2000 compositions that were first annealed at 160 C for 1 hr. Samples were drawn at 120 C parallel to the film flow direction.

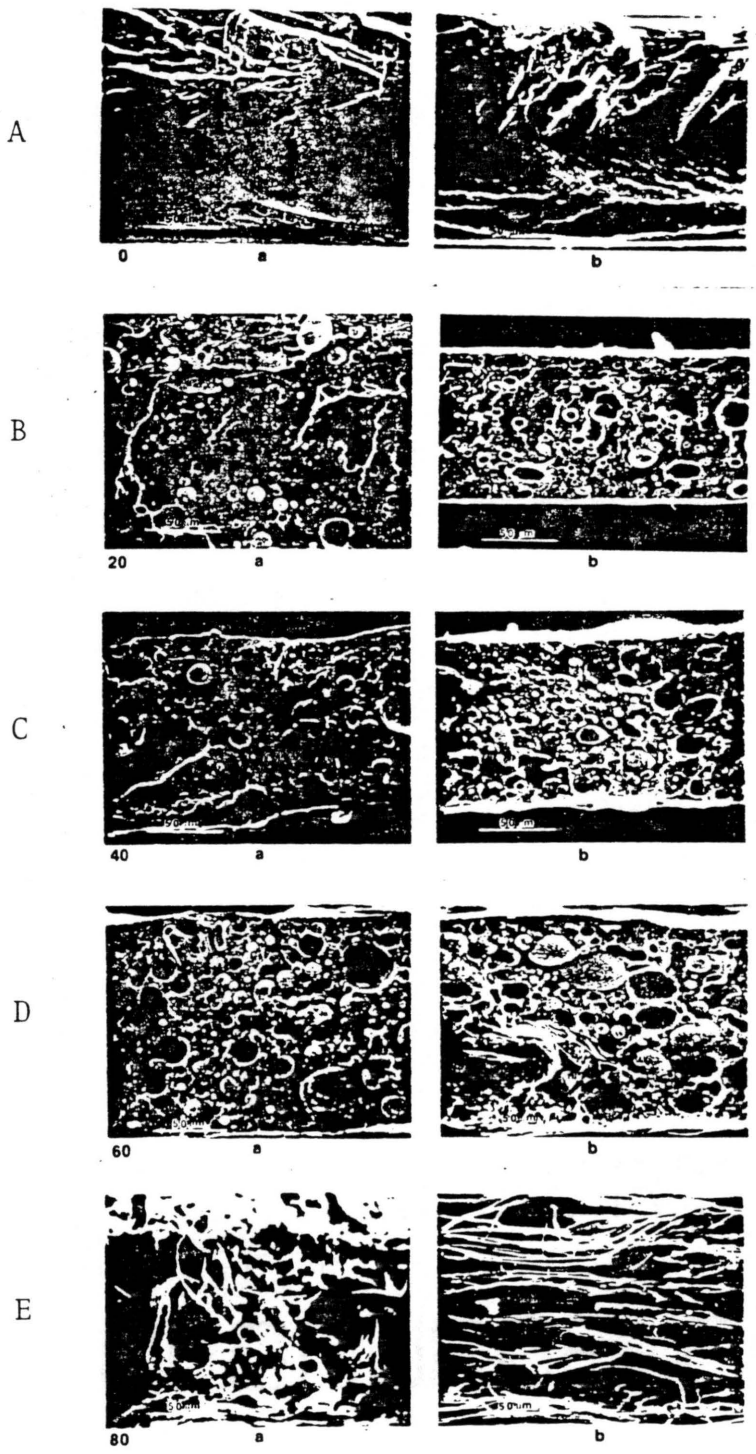

Fig. 18A-E Fracture surfaces of 0%, 20%, 40%, 60% and 80% LCP 2000 film samples. "a" denotes samples fractured perpendicular to the film flow direction and "b" denotes samples fractured parallel to the film flow direction.

show the fracture surface perpendicular to the extrusion axis while those on the right represents a cold snap surface parallel to the extrusion axis.

Figure 18A shows the pure PET material to be homogeneous as expected while Figs. 18B through 18E clearly display a two-phase morphological texture where the dispersed phase in Figs. 18B, 18C and 18D represents the LCP component. The matrix is that of PET as was later confirmed by preferential solvation. It is noted in Figs. 18B-18D that the relative size of the dispersed phase, i.e., the LCP component, tends to increase in size with increasing LCP content in the blend from 20 to 60 percent. Furthermore, while there is a distinct two phase morphology and discrete fracture of the matrix around the particles, there is also the observation that the dispersed LCP component shows a somewhat "fuzzy" surface implying that there had been reasonably good adhesion of the LCP with the matrix polymer. This, of course, is important from the point of view of stress transfer between phases and the relative effects on mechanical behavior. (Recall the earlier discussion in the literature review on the blends of PC and HDPE). Another observation is that in observing the parallel and perpendicular fracture surfaces, it is clear that the micrograph which depicts the fracture parallel to the extrusion axes shows signs of an oriented dispersed phase. This is in contrast to what is observed when the fracture is perpendicular to the extrusion axis. In the first case, the LCP component is in the form of elliptically shaped dispersed particles whereas in the fracture surface perpendicular to the extrusion axis, an "end-on" view of these ellipsoidal particles is displayed. Observation of

only the latter photos could have led one to erroneously interpret that these were spherical particles and hence not oriented.

Interestingly, once an 80% LCP content is achieved, the nature of the morphological texture becomes considerably different, as shown in Fig. 18E. Here the fracture surface perpendicular to the extrusion axis tends to display more continuity for the LCP component which takes on distinct fibril-like structure. This is clearly confirmed from the fracture surface parallel to the extrusion axis where one can easily view the LCP component now showing continuity and a fibrous-like texture. These textures clearly show how the moduli values and corresponding stress-strain behavior begin to be dominated by the LCP component at the 80% LCP content. The fact that this particular component does not display continuity until high weight percent content is likely the result of the difference in the melt viscosity of the two blend components. In the case of two-phase viscoelastic polymer melts, the total entrance pressure drop comes from both phases. The extent of deformation which occurs in the two fluids at the entrance region would depend on, among other factors, incoming droplet size and distribution, interfacial tension, and differences in the viscoelastic properties of the two fluids. The melt viscosity ratio of the two polymers used in the present study is about 2.0. The ratios of viscosity and elasticity of the components determine the size and shape, respectively, of these phases. A complete investigation of viscosity versus composition of LCP 2000 in the blend would help explain this behavior. It is reasonable to assume from the preceding study that below 80 weight percent LCP 2000, the LCP is dispersed as a droplet in molten PET.

To help further demonstrate the continuity of the LCP component in the 80% blends, TFA was utilized to preferentially extract the PET component. As is shown in Fig. 19B, the surface that is remaining is clearly that of the continuous LCP component; The "trenches" represent areas that had been rich in PET which was removed by the TFA. Contrast is directly made with the untreated surface which is shown in Fig. 19A. The vertical direction is the extrusion axis.

Wide Angle X-ray Scattering Studies

Noting the strong support of the morphological features lead to the observed mechanical behavior, one additional technique was utilized for purposes of giving further support to the above analysis. Specifically, WAXS patterns of the extruded films were taken with the x-ray beam normal to the plane of the film and the extrusion axis oriented vertically. These WAXS patterns are shown in Figs. 20A-20E for the corresponding 0, 20, 40, 60 and 80% LCP/PET blends. No sign of PET crystallinity nor significant orientation of the LCP component is displayed in the first four WAXS patterns although there is some variability due to the differences in the amorphous scattering behavior of the two components. However, in the final WAXS pattern, i.e., the 80% LCP blend, very distinct orientation of the LCP phase occurs, and this helps to account particularly for the much greater modulus observed from the stress-strain behavior. This is directly in agreement with the observed fracture surfaces treated or untreated with TFA (Fig. 19). To illustrate the effect of the 160°C annealing treatment on the initial films to produce a semicrystalline PET phase, Figs. 21A-21D

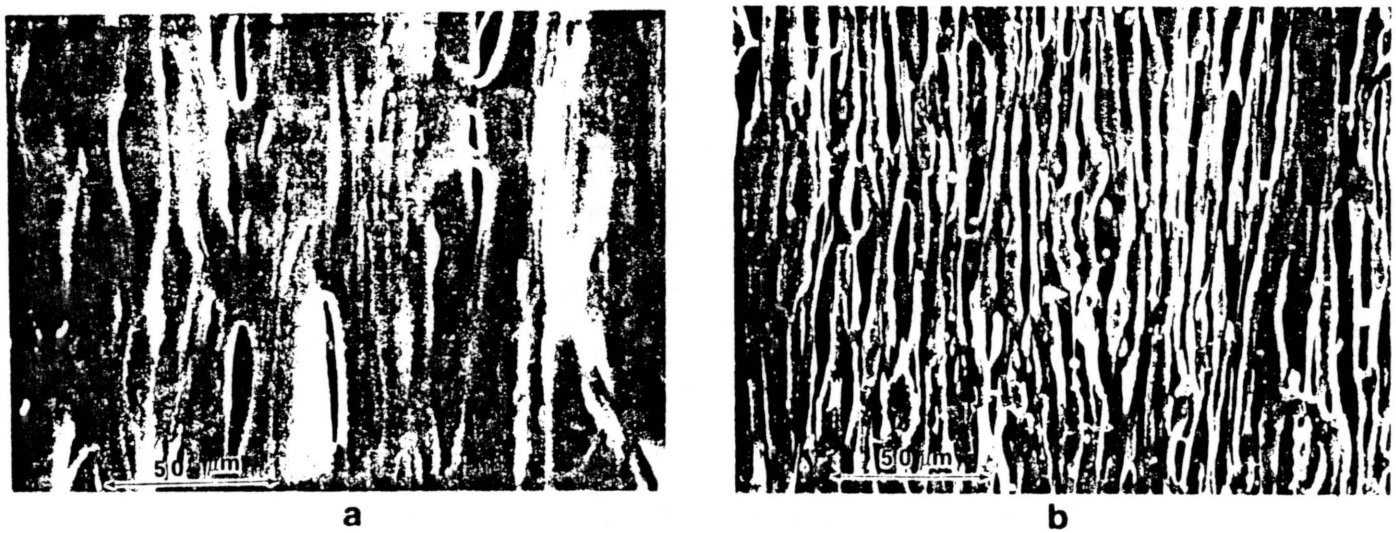

Fig. 19 80% LCP 2000 film samples. (a). No dissolution. (b). Dissolved in trifluoroacetic acid for 36 hrs. The vertical direction is the extrusion axis.

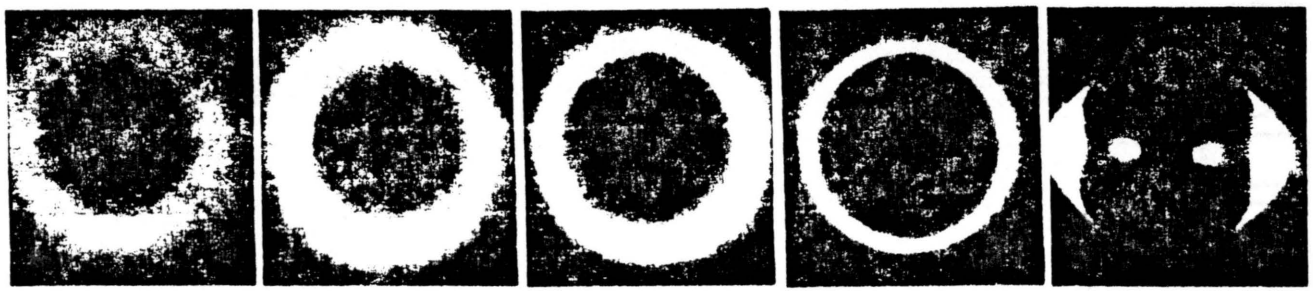

Fig. 20A-E WAXS patterns of 0%, 20%, 40%, 60% and 80% LCP 2000 film samples.

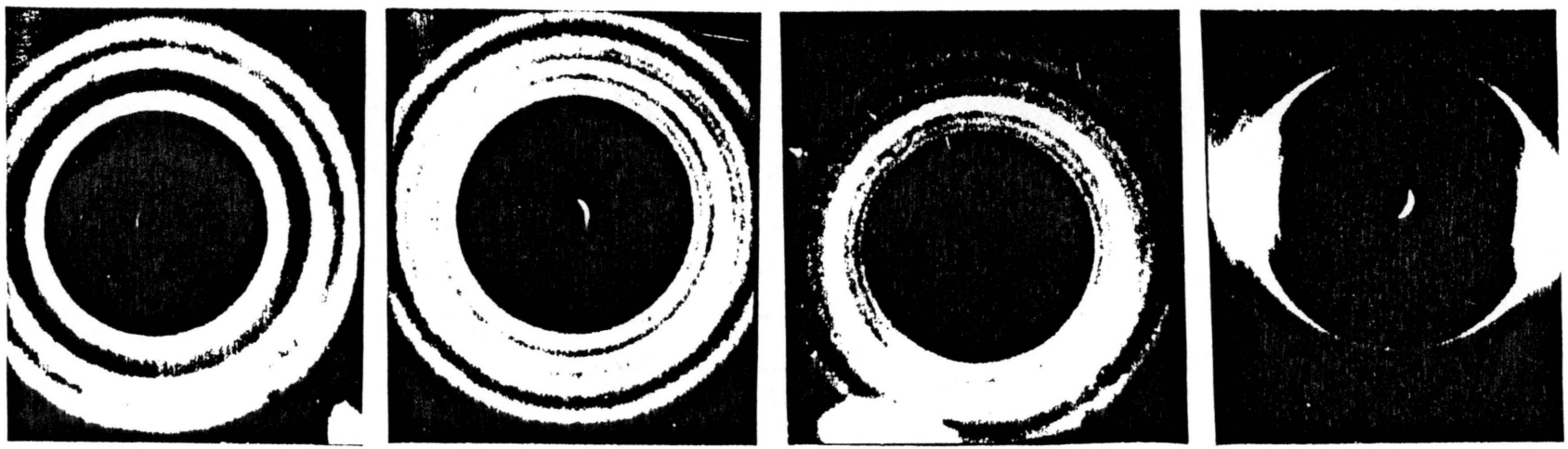

0% LCP A | 40% LCP B | 60% LCP C | 80% LCP D

Fig. 21A-D WAXS patterns of 0%, 40%, 60% and 80% LCP 2000 film samples which were annealed at 160 C for 1 hr.

present WAXS patterns for four of these materials showing that a one-hour annealing converts the PET phase to a semicrystalline phase. This is very clear from the WAXS patterns, and it also demonstrates that in those systems which show significant signs of orientation of the LCP component, the effect of annealing does not strongly alter this orientation.

In summary of this particular portion of the study, there is a very strong correlation between the observed properties of the materials in terms of their mechanical behavior and their structure as denoted by both SEM and wide angle x-ray scattering.

THE EFFECT OF PROCESS VARIABLES ON THE MORPHOLOGICAL TEXTURES. BLENDS OF PET WITH THERMOTROPIC LIQUID CRYSTALLINE COPOLYESTERS-LCP 2000

Based on the observations that direct dry blending and extrusion under conventional conditions did not produce signs of a continuous LCP phase in low content LCP blends, some investigations were made as to the effect of two particular process variables on the relative dispersability of the LCP component. The specific aim was to influence the morphology of the blend and improve the film's mechanical properties. Some range of composition was also investigated. The two process variables that were utilized for this study were the speed of the extruder screw, which will be simply referred to as screw speed (SS), and gear pump speed (GPS). For these studies, dry blends of the materials were made of PET with LCP 2000. A second thermotropic liquid crystalline copolyester denoted as LCP 4060 was also blended with PET. The principal thrust of the investigation was then to investigate the morphological features of the films that had been produced by a systematic variation in the SS as well as the GPS of blends based on these two thermotropic liquid crystalline polymers blended with PET.

(a) Effect Of Extruder Screw Speed (SS)

The variable of screw speed will be discussed in this section. The results of the SEM studies are presented first and followed by mechanical property investigations and wide angle x-ray scattering studies.

SEM Studies Following Preferential Dissolution of PET

SEM micrographs of blends of 30 % LCP 2000 with PET, are given in Figs. 22A-22E. The effect of variable screw speed is clearly indicated. These figures display dual magnification micrographs, i.e., two different magnifications for a sample processed at each screw speed. The samples have been prepared by first solvating and extracting the PET component with TFA thereby leaving the LCP phase. This method has worked out extremely well and therefore fracture surfaces are not shown but only the micrographs of extracted films are provided. As is clear from all of the micrographs shown in Figs. 22A-22E, it is obvious that increasing the value of SS has a very pronounced effect on the general texture of the LCP component and its dispersability as seen by the progression from a distinct particulate to a continuous strand-like fibrous network. For example, in sample LCP 2000-30-SS-10, the screw speed 10 RPM is the lowest and while there are some strand-like LCP phases, there are many globular or distinct particulate components as well. However, at the highest screw speed represented by sample LCP 2000-30-SS-70, there is a very highly pronounced fibrous texture which also is highly aligned following the extrusion process. Clearly the effect of screw speed plays a very important role on the general dispersability of these systems all of which have 30% of the LCP 2000 component. This suggests that this variable is important for this blend. Recall the earlier statement that the morphology in a molten polyblend is a result of the components' viscosity ratio (size) and elasticity ratio (shape), which are obviously

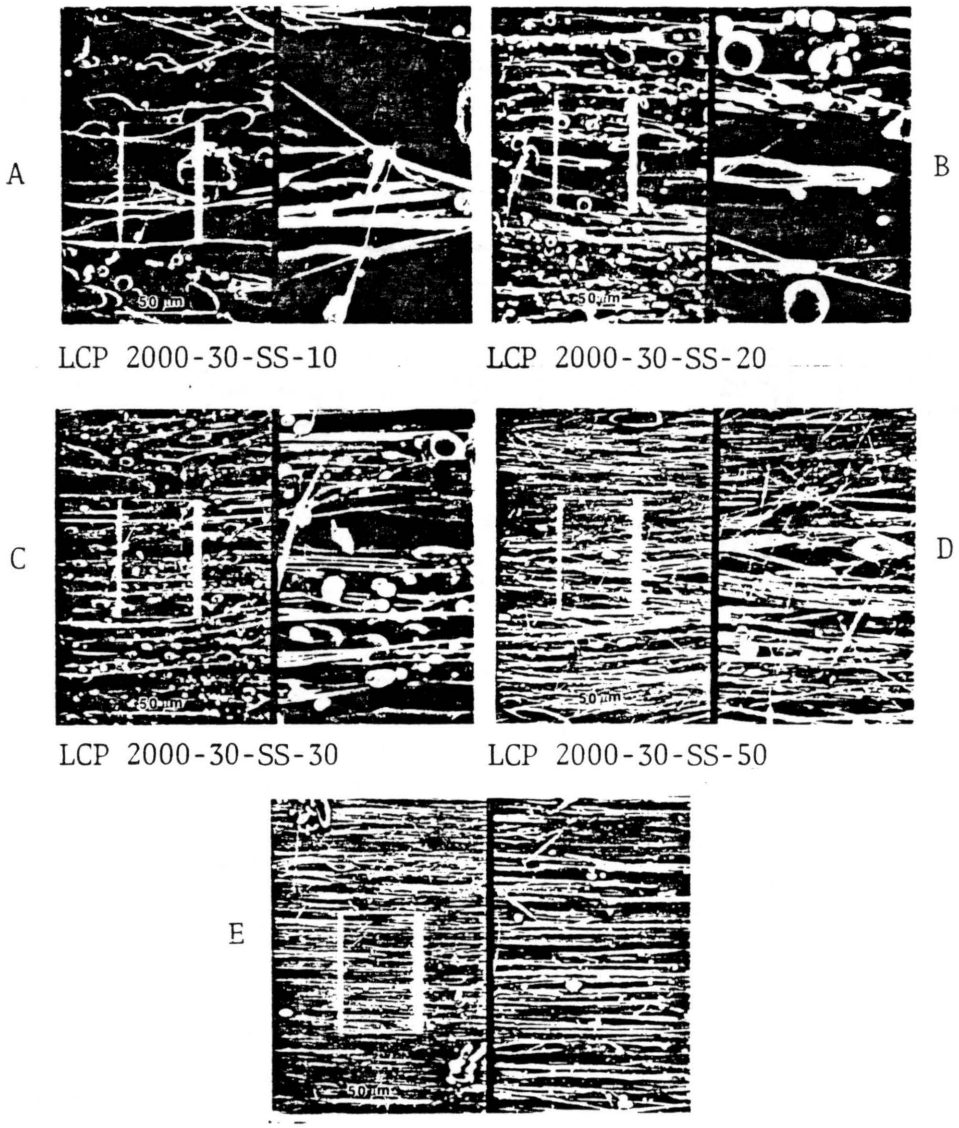

Fig. 22A-E SEM micrographs of trifluoroacetic acid treated 30% LCP 2000 blends. The highest extruder screw speed being 70 rpm.

dependent on the level shear stress or shear rate level as well as on the initial size of the components. Specifically, the ratio of melt viscosities determined at a specific shear rate and temperature for the polyblend components influences the phase grain size (droplet, rod) control as mentioned before.

Mechanical Studies

Figure 23A shows the values of Young's modulus determined for the films produced after utilizing different screw speeds. The moduli values shown are those that were determined at 80°C. While there is some scatter in the data, it is clear that producing a more continuous or fibrous-like network structure in the LCP component has promoted a much higher modulus (800 MPa) than was observed in comparable LCP-containing films (200 MPa) produced through "conventional" extrusion conditions as discussed earlier. The basic point is therefore that a much more enhanced modulus can be obtained with lower LCP content by utilizing the appropriate process variables to alter the dispersability of the LCP component for purposes of promoting a continuous phase. One major drawback, to this approach, however, is that while the modulus can be increased greatly in the extrusion direction, the same films displayed very poor properties in the transverse direction due to the fact that there was little continuity of the LCP component in this direction. Recall that a transverse modulus of only 120 MPa was obtained for the 80 % LCP 2000 blend in the earlier study.

Figure 23B provides the more complete stress/strain behavior for the LCP 2000-30-SS-X samples as determined at 80°C. Besides denoting

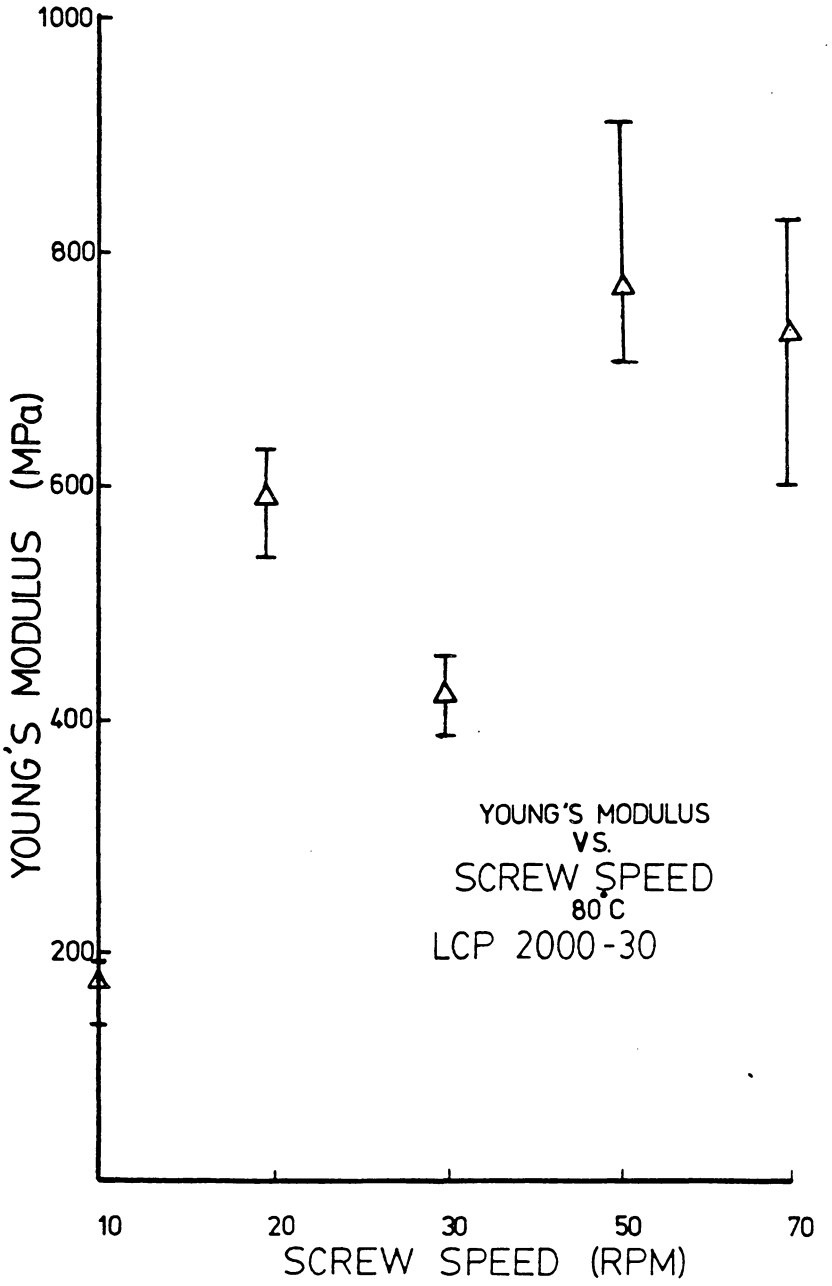

Fig. 23A Modulus of 30% LCP 2000 blends with increasing extruder screw speed from left to right.

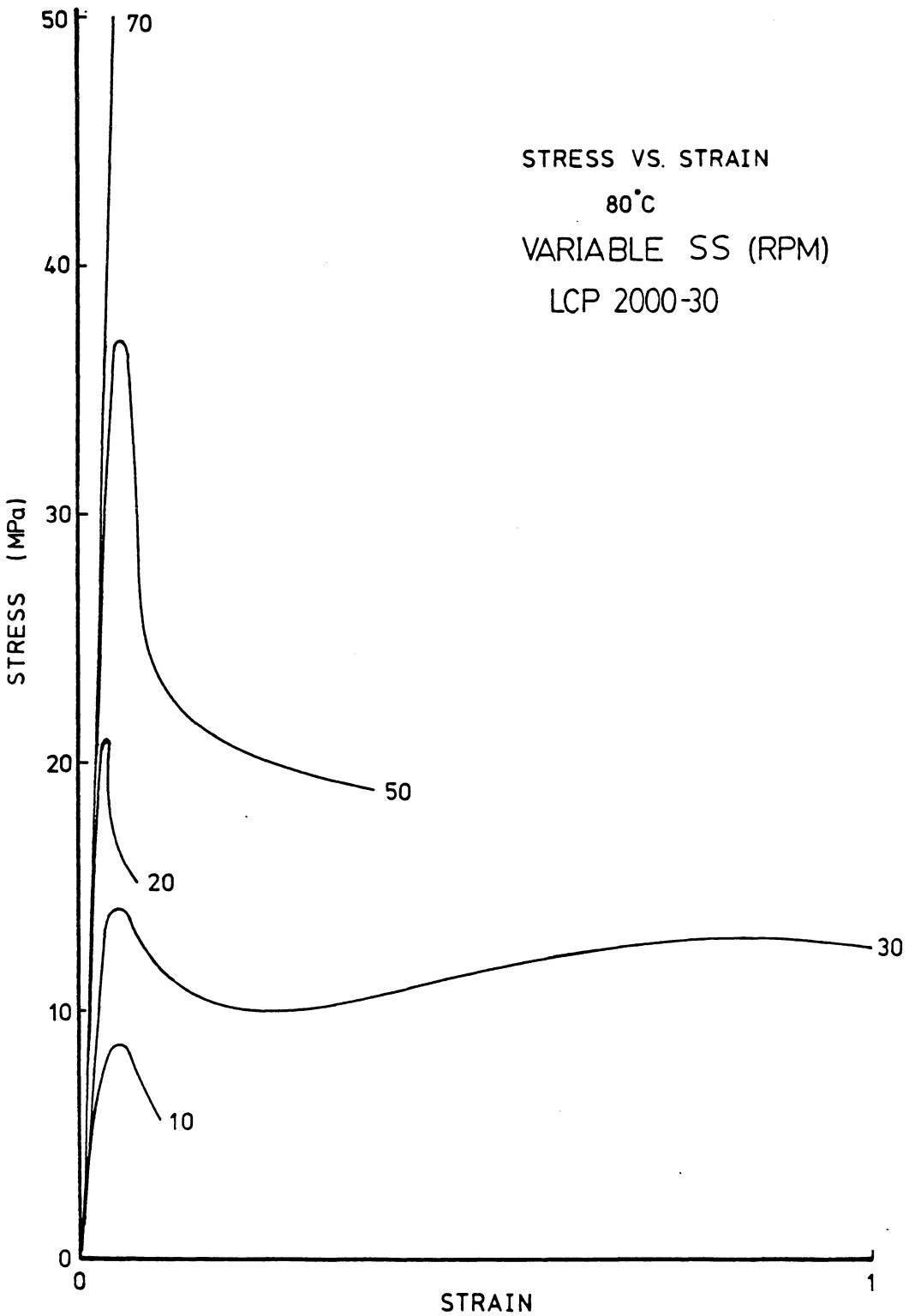

Fig. 23B Stress-strain curves of 30% LCP 2000 blend samples with different extruder screw speeds. 70 is the highest screw speed.

a much higher modulus as was quantified in Fig. 23A, the general strain to break has decreased considerably from what was observed from the earlier stress-strain curves measured at 80°C for the conventionally extruded LCP/PET blends. Once again, the effects of the SS are clear in terms of its effect on the morphological features. These results are in turn directly related to the observed properties. Similar mechanical data determined at 120°C led to similar conclusions as might be expected and is shown in Figs. 23C and 23D.

Wide Angle X-ray Scattering Studies

As is seen in Figs. 24A-24E, increasing screw speed promotes the orientation of the LCP phase in all cases. There are differences in the general character of the WAXS patterns and the general observation is that at the higher screw speeds, more distinct orientation of the LCP component is produced. The general amorphous character that still remains for the PET phase is also clear since there are no signs whatsoever of PET crystallinity in the WAXS patterns.

In summary, one can enhance the modulus in the extrusion direction considerably by varying the SS even with low content (30%) of LCP 2000 polymer in the blend. However, the modulus in the transverse direction did not improve. Also, the strain to break was about 15 MPa and maximum elongation was about 30 %.

(b) Effect Of Extruder Gear Pump Speed (GPS)

In this section, the results of SEM studies after preferential dissolution are discussed and followed by mechanical studies and wide

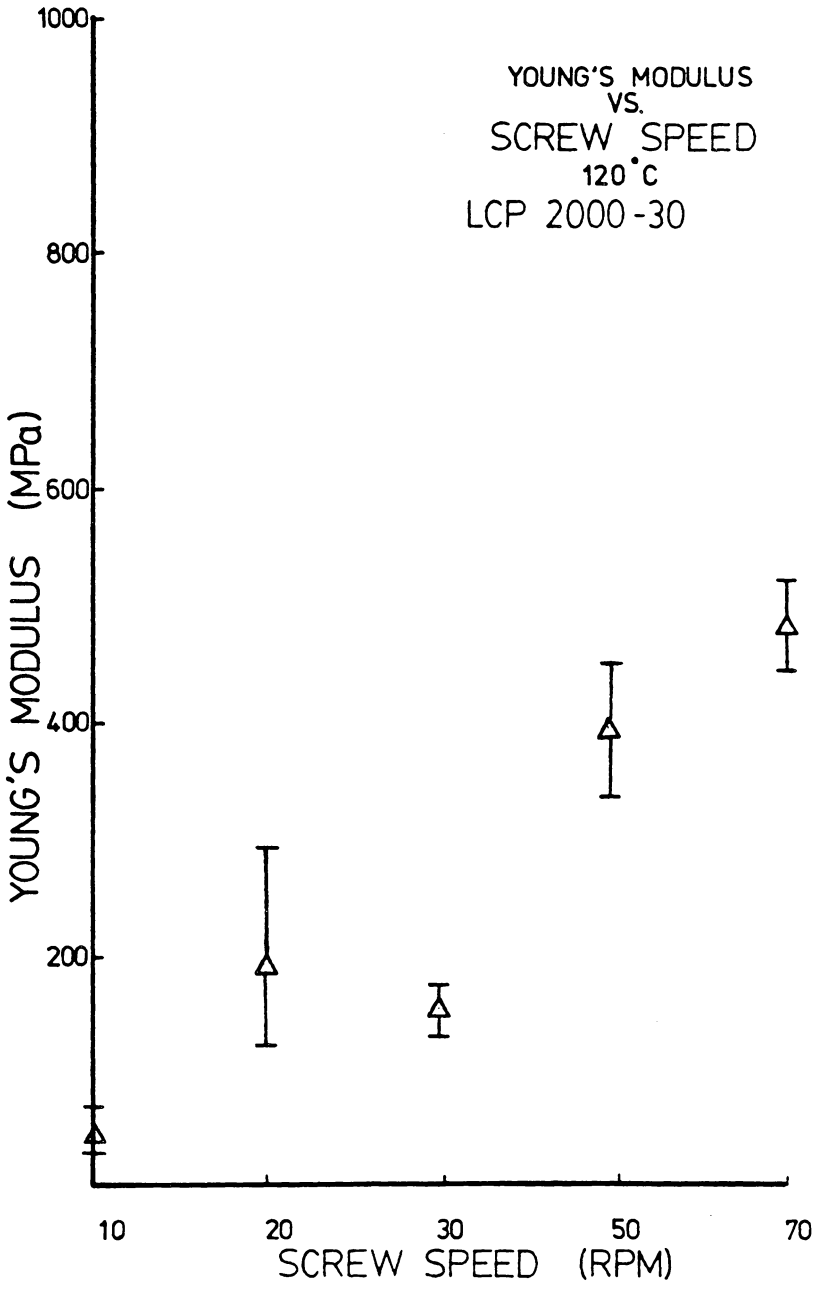

Fig. 23C Modulus of 30% LCP 2000 blends at 120 C with increasing extruder screw speed from left to right.

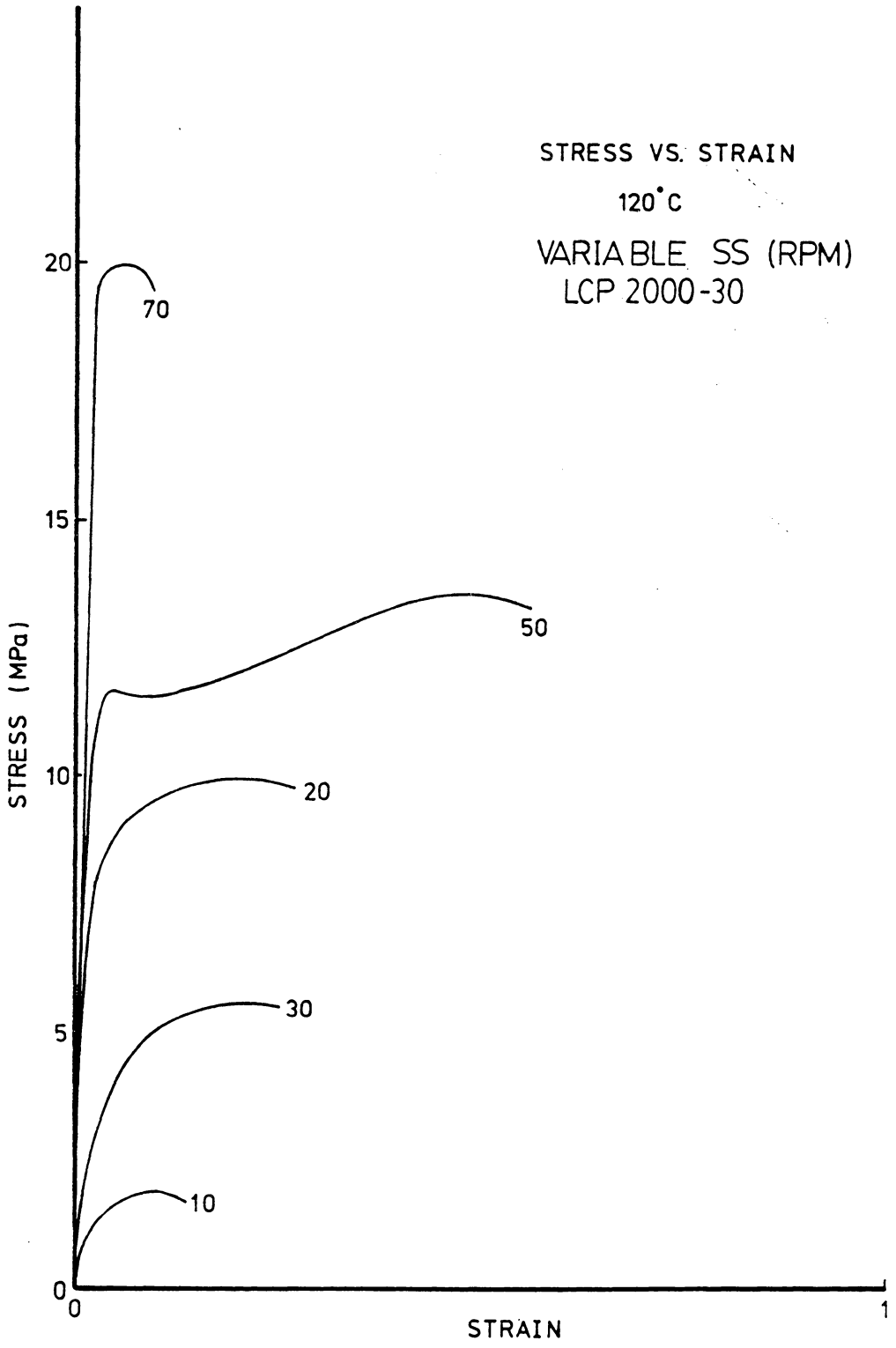

Fig. 23D Stress-strain curves of 30% LCP 2000 blend samples at 120 C with different extruder screw speeds. 70 is the highest screw speed.

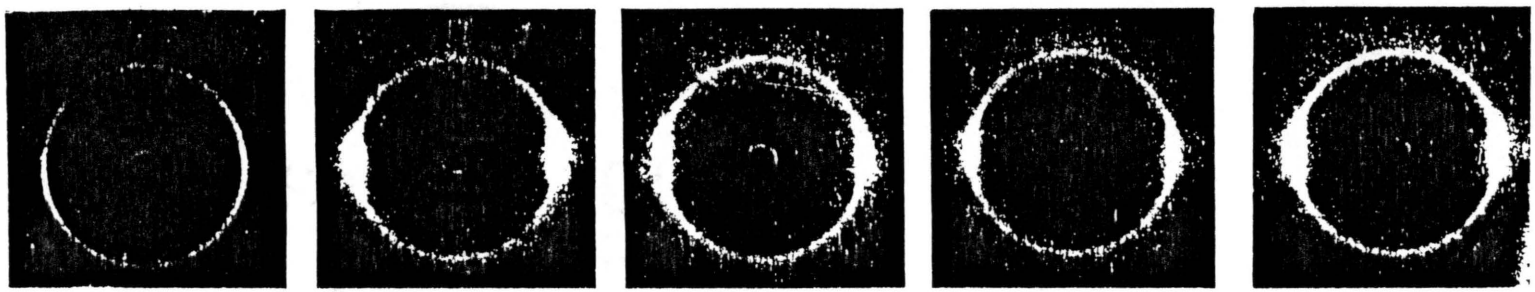

Fig. 24A-E WAXS patterns of 30% LCP 2000 blends. The extruder screw speed increases from left to right.

angle x-ray scattering studies. The results of this GPS study will be compared to the SS results.

SEM Studies Following Preferential Dissolution of PET

Figures 25A-25G illustrate the effect of gear pump speed on the structure-property behavior of the LCP 2000/PET blends. These are based on the morphological features observed following TFA extraction of the PET component. In particular, Figs. 25A-25D show a particulate texture which results from the fact that the PET component was the continuous phase. Therefore following extraction with TFA, only the particulate LCP 2000 remained on the surface. This LCP material in general shows little sign of orientation except for sample LCP 2000-30-GPS-5, which is from an intermediate gear pump speed. However, at higher gear pump speeds, some strand or fiber-like formation of the LCP component is clearly produced. (See Figs. 25E and 25F). Here indeed, there is a strong dependence on the process variable of gear pump speed, especially at higher gear pump speeds.

To note the effect of LCP composition, a 40% blend of LCP 2000 was also investigated for the effects of gear pump speed. The results are shown in Figs. 26A-26F which again illustrate a very similar behavior as was shown in the last series of micrographs. Specifically as gear pump speed goes from lower to higher values, the LCP phase is transformed from a particulate to a partially oriented particulate phase to that of continuous fibrous-like structures. It was once more found that a higher GPS encourages the strand or fibrous-like textures.

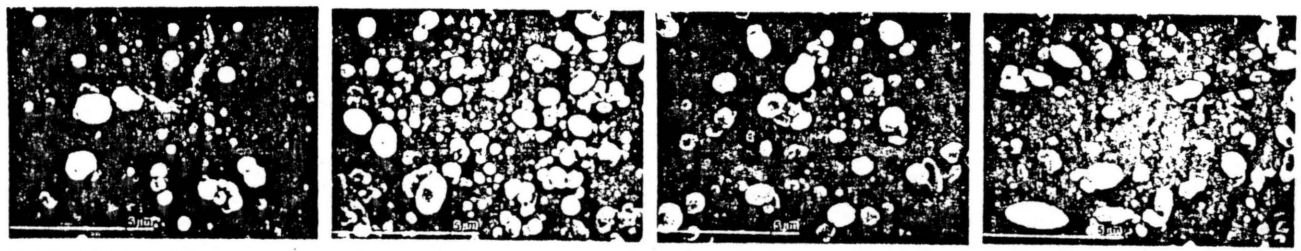

LCP 2000-30-GPS-5 A

LCP 2000-30-GPS-8 B

LCP 2000-30-GPS-17 C

LCP 2000-30-GPS-27 D

LCP 2000-30-GPS-52 E

LCP 2000-30-GPS-78 F

LCP 2000-30-GPS-105 G

Fig. 25A-G SEM micrographs of trifluoroacetic acid treated 30% LCP 2000 blends. The gear pump speed increases in the order of 5,8,17,27,52,78, and 105. The highest gear pump speed being 105 rpm.

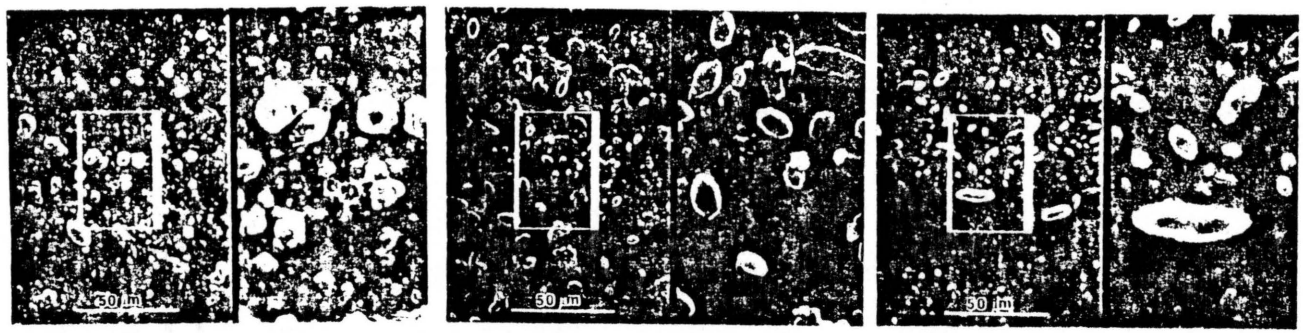

LCP 2000-40-GPS-10
A

LCP 2000-40-GPS-17
B

LCP 2000-40-GPS-27
C

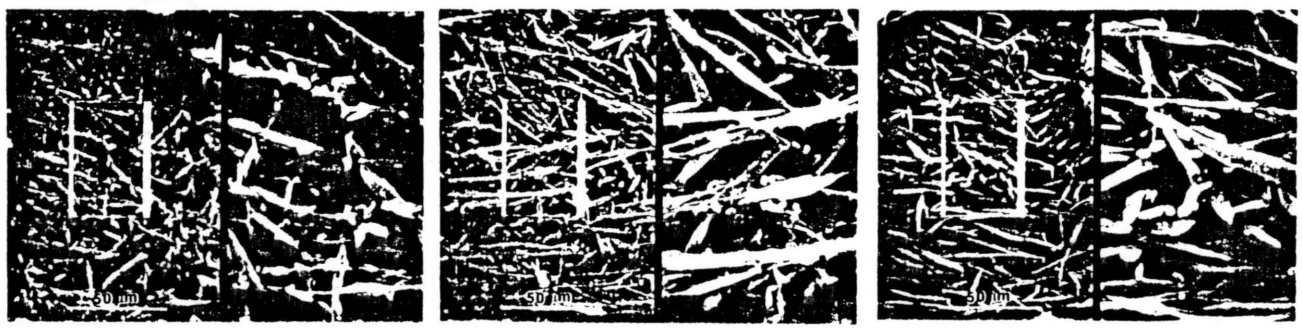

LCP 2000-40-GPS-52
D

LCP 2000-40-GPS-78
E

LCP 2000-40-105
F

Fig. 26A-F SEM micrographs of trifluoroacetic acid treated 40% LCP 2000 blends. The gear pump speed increases in the order of 10,17,27,52,78, and 105. The highest gear pump speed being 105 rpm.

Mechanical Studies.

The general trend was that the effect of gear pump speed did not strongly enhance Young's modulus in the extrusion direction at the same LCP content as extensively as did the effect of screw speed. Although the morphological textures just reviewed show the formation of LCP 2000 strands at high GPS, the formation of LCP 2000 strands by the GPS process did not improve the mechanical properties in the extrusion direction -- see Figs. 27 A and 27 B for 80 and 120 °C measurements, respectively.

Wide Angle X-ray Scattering Studies.

Interestingly, when the blends of LCP 2000/PET are investigated by WAXS following film production with varied gear pump speed, there is relatively little sign of orientation in most cases. This is shown more explicitly in Figs. 28A-28D where three of the four patterns show relatively little or no orientation of the LCP phase although one of these (LCP 2000-30-GPS-105) does clearly indicate LCP orientation to some extent.

In summary, the GPS does not enhance the mechanical properties as well as SS with the same composition of LCP 2000 in the blend. From a morphological point of view, the SS had more effect in terms of producing strand like fibers than the GPS. Also, by increasing the LCP 2000 content to 40 % in the blend, GPS alone does not enhance the mechanical properties.

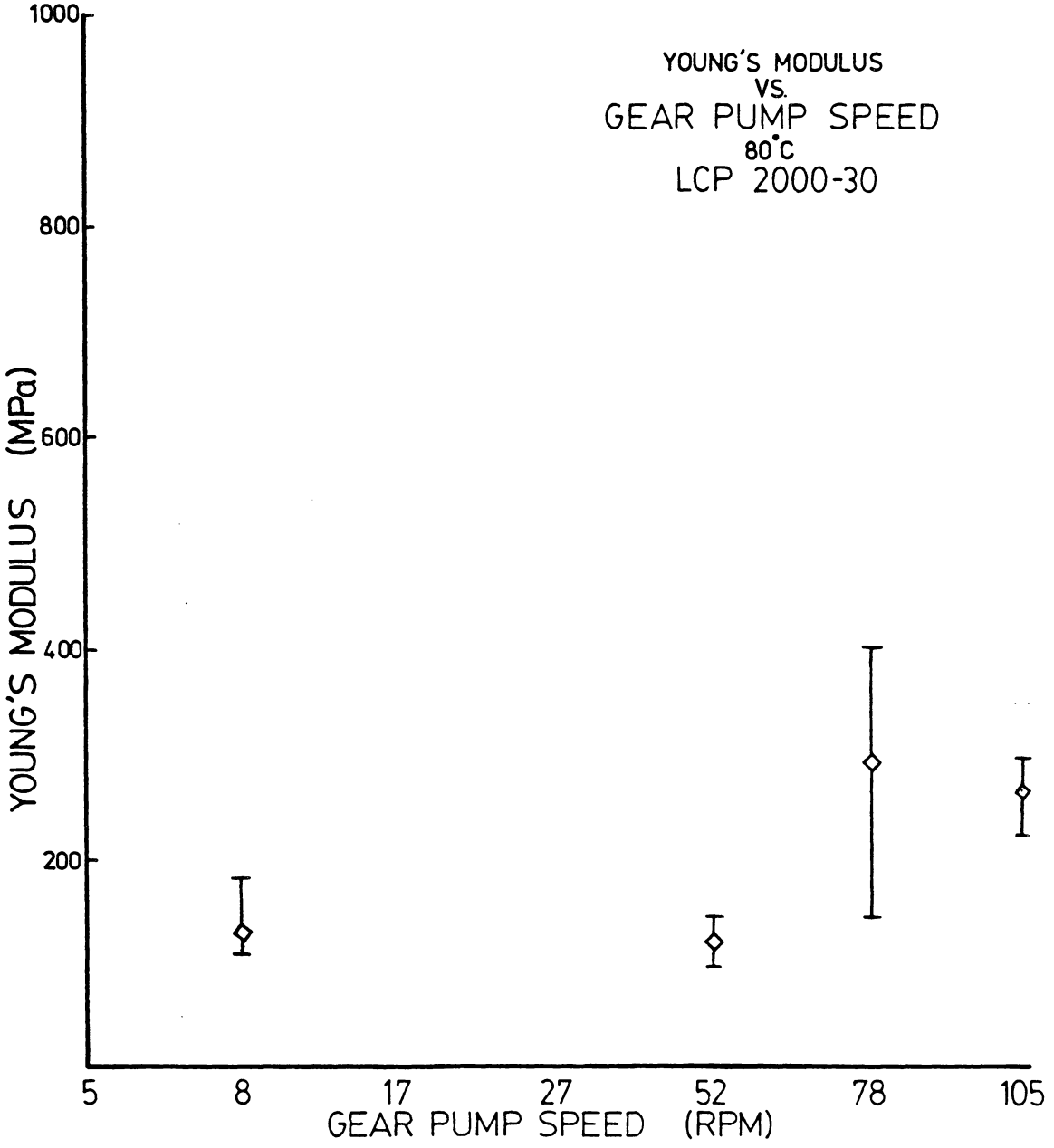

Fig. 27A Modulus of 30% LCP 2000 blends at 80 C with increasing gear pump speed from left to right.

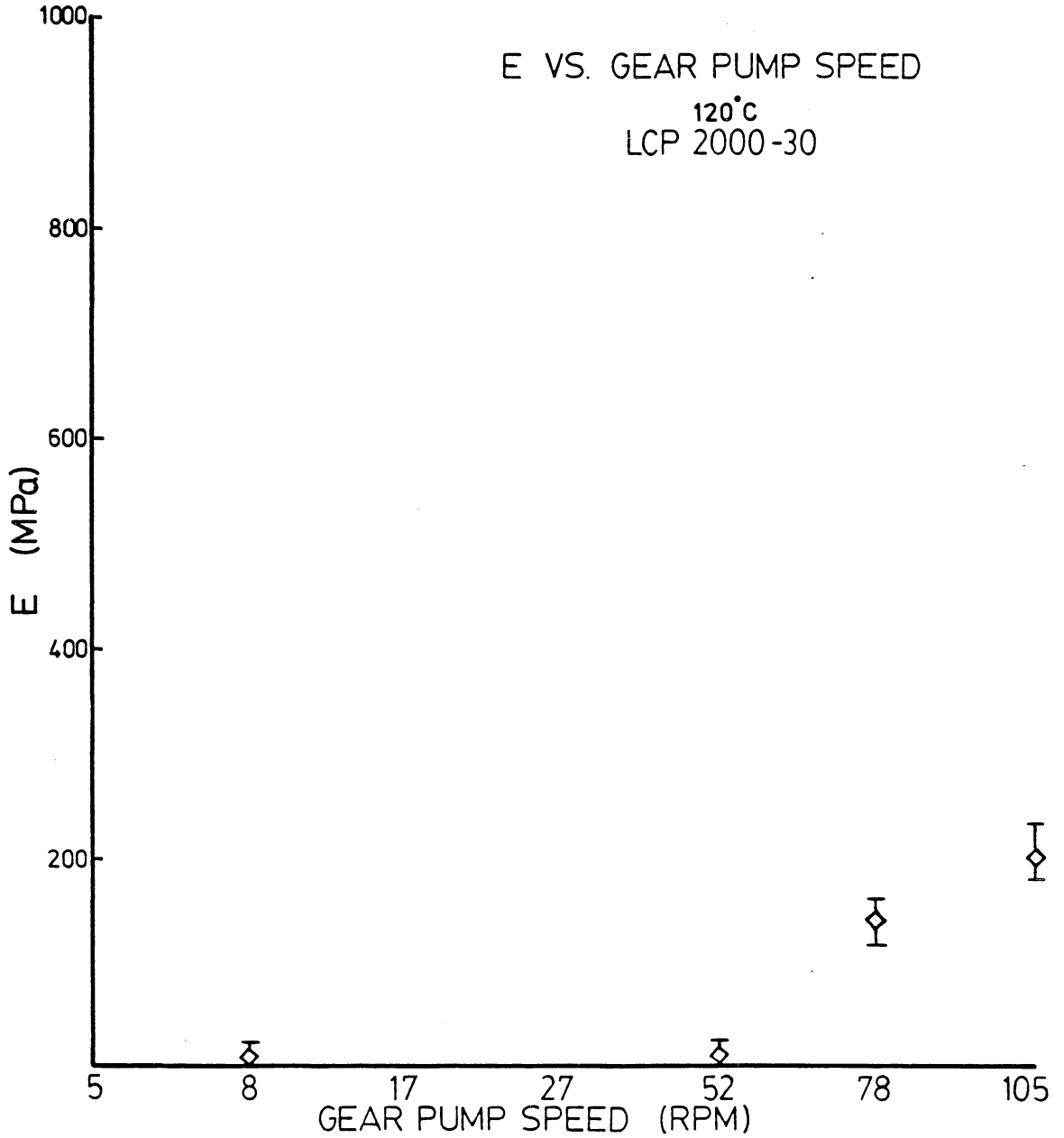

Fig. 27B Modulus of 30% LCP 2000 blends at 120 C with increasing gear pump speed from left to right.

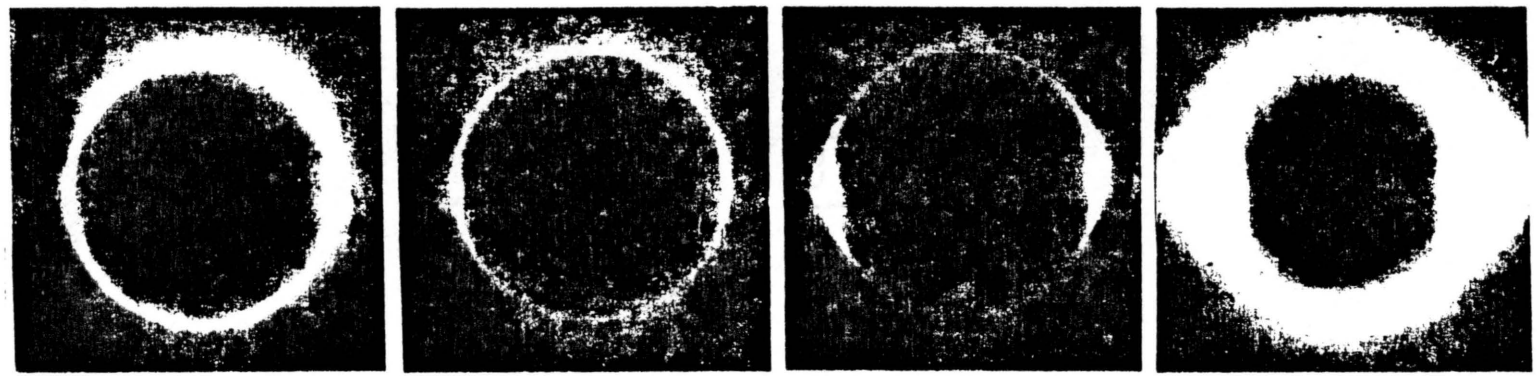

8 rpm | 52 | 78 | 105

A | B | C | D

Fig. 28A-D WAXS patterns of 30% LCP 2000 blends. The gear pump speed increases from left to right.

STRUCTURE-PROPERTY STUDIES UTILIZING THE SECOND LCP POLYMER-LCP 4060

SEM Studies Following PET Extraction

In Figs. 29A-29G are presented the corresponding TFA extracted textures of the blends based on 30% of the liquid crystalline polymer LCP 4060. As mentioned before, the LCP 4060 is a copolyester-amide involving terephthalic acid, p-aminophenol, and 2-hydroxyl-6-naphthoic acid. In Fig. 29, it is denoted that the effect of gear pump speed shows much less development of fibrous morphological features than was observed for the LCP 2000 series discussed previously and shown in Fig. 25. Identical gear pump speeds and extrusion conditions were utilized for both studies. The origin of this difference in behavior between the two liquid crystalline polymers is speculated to be due to the difference in the melt rheological behavior of these components. That is, the melt viscosity measured at 285°C, with shear rate of 10/sec for LCP 2000 is 2000 poise, whereas that for LCP 4060 is 4200 poise under the same temperature and shear rate. In summary, the LCP 4060 system did not in general provide as strong a dependence on the process variables as did the LCP 2000 component, which suggests that the melt viscosity difference between LCP 4060 and PET is too great to allow the formation of fibrious LCP 4060.

Wide Angle X-ray Scattering Studies

To contrast the general behavior of the LCP 4060 with that of LCP 2000, three WAXS patterns of the 30% containing LCP 4060 blend are

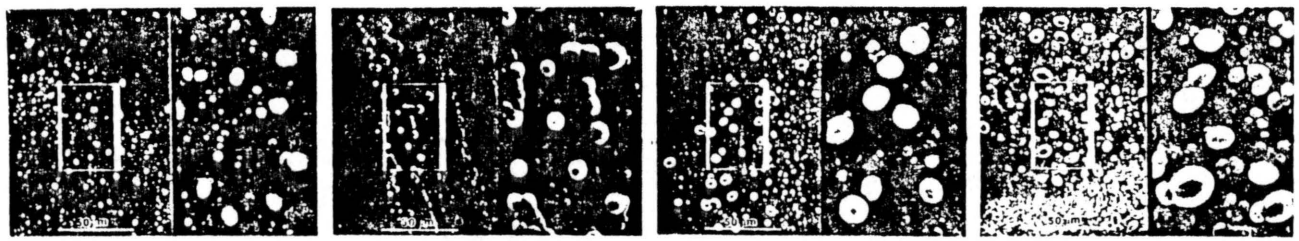

LCP 4060-30-GPS-5 LCP 4060-30-GPS-10 LCP 4060-30-GPS-17 LCP 4060-30-GPS-27

A B C D

LCP 4060-30-GPS-52 LCP 4060-30-GPS-78 LCP 4060-30-GPS-105

E F G

Fig. 29A-G SEM micrographs of trifluoroacetic acid treated 30% LCP 4060 blends. The gear pump speed increases in the order of 5,10,17,27,52,78, and 105. The highest gear pump speed being 105 rpm.

shown in Figs. 30A-30C. It is clear that there are no strong signs of crystal texture in these patterns. However, an azimuthal dependence of the scattered intensity is clear which is in line with the general orientation of the LCP phase.

In summary, under comparable conditions, LCP 4060 polymer does not generate fiber-like structure as well as LCP 2000 polymer when blended with PET.

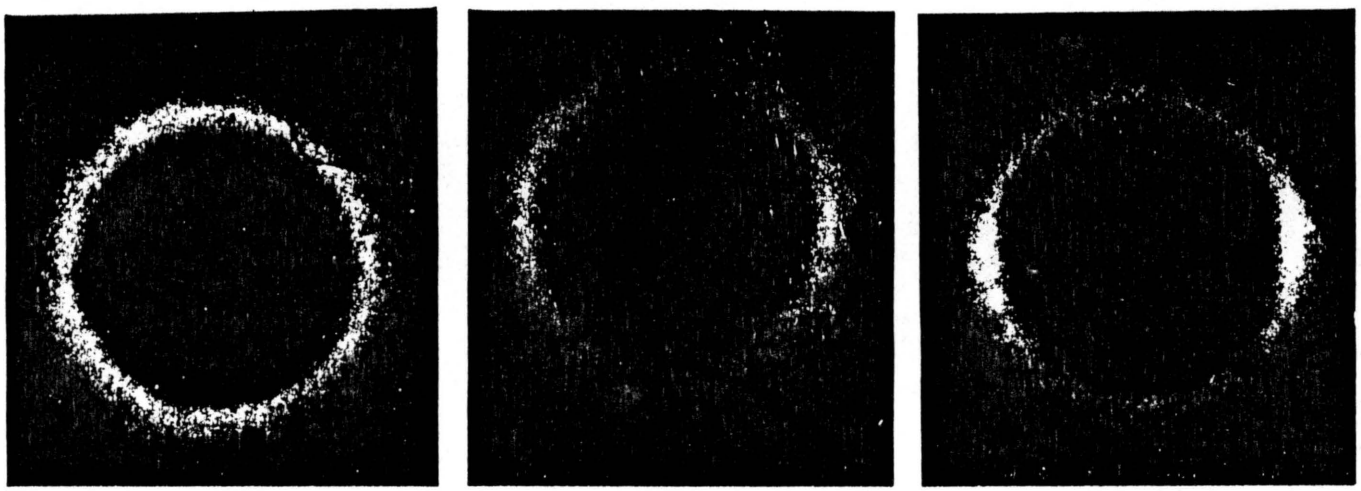

10 rpm | 52 | 105

A | B | C

Fig. 30A-C WAXS patterns of 30% LCP 4060 blends. The gear pump speed increases from left to right.

BLOWN FILMS OF LCP 2000/PET BLEND

The blown film process is a continuous on-line process which produces tubular films. Biaxial orientation is usually introduced during the blowing operations. Only very preliminary investigations have been carried out here on blown films and hence only a few remarks will be made below. These relate to SEM studies after preferential solvation as well as some WAXS studies.

Basically, the principal objective of this part of the study was to briefly investigate the morphological features of blown film that had been produced by variations in the blow-up ratio as well as film "take-up" speed during processing. The blended blown film materials were made of PET with 30% LCP 2000 component with the goal of producing a film which is oriented by the blown film process.

SEM Studies Following PET Extraction

Micrographs given in Figs. 31A-31C show the effect of blow-up ratio as well as take-up speed on the blown film produced. These micrographs display a dual magnification for each blow-up ratio. The samples have been prepared by extracting the PET component with TFA, thereby leaving the LCP phase. As can be seen in micrographs, all three of the films indicate a strong uniaxially oriented LCP phase.

As shown in micrographs in Figs. 31A and 31B, increasing the blow up ratio has some effect on the general texture of the LCP component in terms of smoothness of the strand-like fibrous network. The less smooth strand-like fibrous network at high blow-up ratio (see

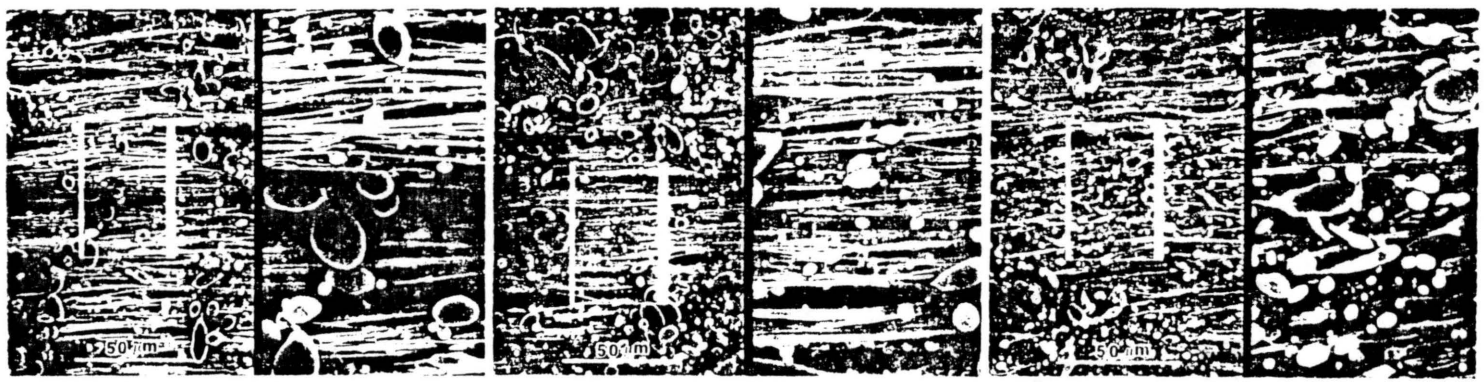

A B C

Fig. 31A-C SEM micrographs of trifluoroacetic acid treated 30% LCP 2000 blown film.
(A). The blow up ratio (BUR) is 2.0 and take up speed (TUS) is 19 ft/min.
(B). The BUR is 2.3 and TUS is 28 ft/min.
(C). The BUR is 2.9 and TUS is 28 ft/min.

Fig. 31B) is probably due to the higher speed in film forming at the higher blow-up ratio. The effect of take-up speed is illustrated in Figs. 31A and 31C for samples which have similar blow-up ratios of 2.3 and 2.0. If one concludes that the effects of the two blow-up ratios are about the same, then the only significant variable is the take-up speed. The take-up speed for the samples in Figs. 31A and 31C are 28 ft/min and 19 ft/min, respectively.

Wide Angle X-ray Scattering Studies.

To give further support to the morphological features just discussed, wide angle x-ray scattering studies were performed on the blown film samples to investigate the orientation effect of LCP 2000 phase in the blend when the sample films were produced by the blowing process.

As is seen in Figs. 32A and 32B, increasing take-up speed on these films promotes orientation of the LCP phase. However, increasing take-up speed from 19 ft/min to 28 ft/min did not increase orientation very much as observed by WAXS. The WAXS patterns for the blow-up ratio effects (not shown) displays basically the same behavior as those corresponding to different take-up speeds. Therefore the WAXS patterns indicate that both take-up speed and blow-up ratio utilized in this study promote uniaxial orientation in this material.

In summary, the observation is that take-up speed did not as affect the texture of the LCP component in terms of smoothness of the strand-like fibrous network as strongly as did the blow-up ratio for these samples.

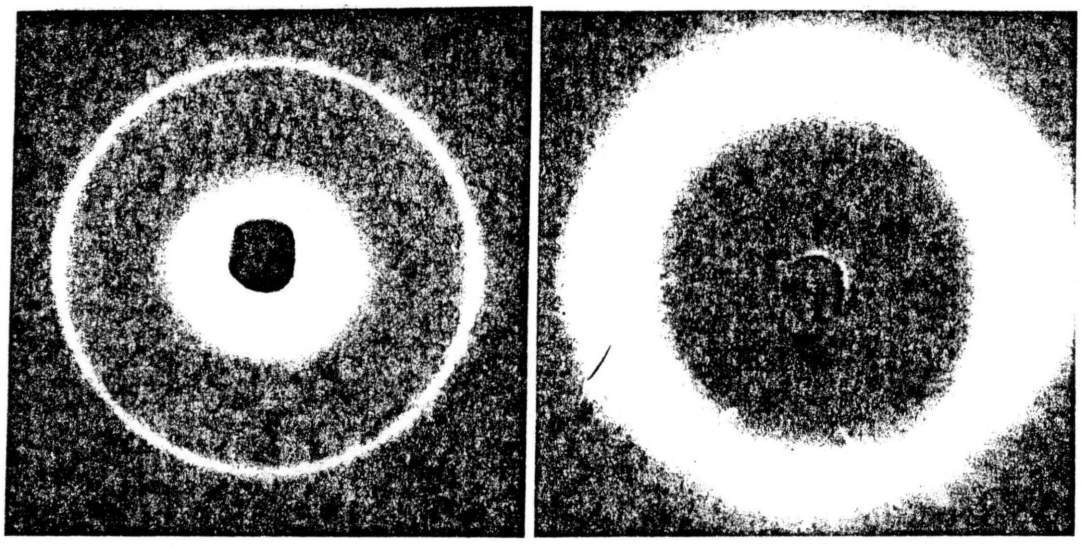

A B

Fig. 32 A-B WAXS patterns for blown films of different take up speed (TUS).
(A). The TUS is 19 ft/min.
(B). The TUS is 28 ft/min.

CONCLUSIONS

The goal of this study was to correlate observed mechanical properties, as measured at high temperatures, to the morphological features of blends of PET and LCP. From this study, the following highlights were denoted.

1. The technique of selective chemical dissolving is very useful for studying the morphological textures of blends of PET and LCP 2000 polymer. Specifically, using trifluoroacetic acid, PET rich regions can be selectively dissolved away.

2. Preferential dissolution on these blended samples show that at low LCP 2000 levels, PET is the continuous phase. The PET rich phase remains the continuous phase until the LCP 2000 content reaches 80 wt. % in the blend. In the 80 % LCP 2000, however, it is the LCP 2000 rich phase that is the continuous phase, and PET is the dispersed phase. At this higher content of the liquid crystal polymer, LCP 2000 provides high strength through orientation. These studies indicate that the thermotropic copolyester system does not reach continuous fiber like structure until 80 % LCP 2000. This is due to the melt viscosity difference between the LCP 2000 component and PET component and also the ratio of the melt viscosities of these two components.

3. Scanning electron microscopy studies on the 20, 40, and 60 % LCP 2000 fracture surface shows the presence of LCP 2000 ball shapes which are in the 5-25 micron size range. The balls, however, are deformed forming "football" shapes in the extrusion direction. At 80 % LCP 2000, the morphological texture appears to be more fiber-like.

4. The fibril-like structures which were obtained by incorporating 80 % of LCP 2000 into the blend with PET with conventional extrusion can also be obtained at lower content of LCP 2000 (30 % LCP 2000) by varying the screw speed and gear pump speed. These effects were studied using a blend of 30 % LCP 2000 and 70 % PET. Specifically, for the sample LCP 2000-30-SS-70, the modulus in the extrusion direction at 80°C is 800 MPa versus for the sample with 80 % LCP 2000 in the blend with PET, which the modulus is 400 MPa determined under same conditions.

5. The modulus in the extrusion direction can be enhanced considerably at the low content of LCP 2000 polymer (30 %) in the blend by increasing screw speed from 10 RPM to 70 RPM. However, the gear pump speed does not enhance the mechanical properties in the extrusion direction as well as screw speed at the same composition of LCP 2000. Even at higher (40 %) LCP 2000 content, varying gear pump speed alone does not improve mechanical properties in the extrusion direction.

6. Blending LCP 4060 into PET did not generate the same fiber like structure as LCP 2000 blends at the same gear pump speed. This morphological difference in the blends is due to the difference in the melt viscosity of two components and viscosity ratio of these two components.

7. For the limited blown film samples studied, it was found that the take-up speed did not as strongly affect the texture of the LCP component in terms of relative size of the strand-like fibrous network as did the blow-up ratio for these samples.

RECOMMENDATIONS FOR FUTURE STUDIES

1. It was anticipated that above the order of 40 to 50 % LCP 2000 content, the LCP component would likely form a continuous phase, however, continuity did not form until 80 % LCP 2000 content in the blend. In order to explain the continuity of LCP 2000 phase at 80 % LCP 2000 content rather than 40-50 % LCP 2000 content in the blend, a study of viscosity versus composition at different shear rates is recommended.

2. When a blend of PET homopolymer and the liquid crystal polymer is injection molded, it is expected that the liquid crystal polymer would form a skin layer due to its lower viscosity. Studies can be performed to measure the thickness of this skin layer by varying the injection speed. The effect of this expected skin layer on mechanical properties could also be investigated.

3. To complement the study of the effects of screw speed and gear pump speed, the mechanical properties of the films in the transverse direction should be studied to compare with the study done in the extrusion direction. This should be accompanied by morphological investigations.

4. In the process of developing potentially interesting mechanical behavior of such blends for possible film applications, only the uniaxial orientation was observed in the extrusion direction in these investigations. However, for balanced properties in both directions of the film, techniques to orient these blend film samples biaxially should be studied.

5. The modulus in the extrusion direction can be increased by increasing screw speed from 10 to 70 RPM. However, varying the gear pump speed did not enhance the mechanical properties in the extrusion direction for LCP 2000 contents of either 30 or 40 %. Therefore, it is recommended to study the effects of composition while varying the screw speed (as opposed to gear pump speed).

CHAPTER II

The purpose of this study was to synthesize and characterize new segmented copolymers that could produce unusual film properties. The approach involved the synthesis of high Tg (220°C) isotropic poly(aryl ether sulfone) oligomers of varying molecular weights. The oligomers were designed to possess terminal aromatic hydroxyl groups which are capable of subsequent copolymerization reactions. Suitable synthetic techniques were developed for preparing hydroxyl terminated poly(aryl ether sulfones) of 2000 to 8000 segment oligomer molecular weight. The hydroxyl terminated oligomers were then converted to copolymers by reaction with terephthaloyl chloride. M. Lambert, a graduate student in the Chemistry Department at Virginia Tech, carried out the polymer synthesis.

The thermal and mechanical studies of the copolymers have been completed by the author. The principal objectives of the initial characterization investigations have been to probe the potential of these copolymers for signs of liquid crystalline character and to note their ability to thermally crystallize as well as to crystallize by solvent or strain inducement. Along these lines, thermal analysis, polarizing hot-stage microscopy, wide angle x-ray scattering and mechanical testing were utilized in this investigation and are discussed in this chapter.

MATERIALS

The monomers used in the preparation of hydroquinone/biphenol polysulfone copolymer systems denoted as HQ/BP PSF are as follows. The 4,4'-dichlorodiphenyl sulfone (DCDPS) was obtained from the Union Carbide Corporation. Hydroquinone was purchased from the Tennessee Eastman Company. The 4,4'-biphenol was obtained from the Buffalo Color Company. The potassium carbonate and toluene were obtained from various sources while the terephthaloyl chloride was purchased from Aldrich Company.

Scheme 1 shows the important steps of the polymer synthesis. Detailed procedures of the synthesis are given in Appendix A rather than the main body of this thesis due to the fact that author did not carry out the polymer synthesis but was carried out by M. Lambert in Chemistry.

Sulfone oligomers were formed by reaction between dichloro diphenol sulfone and biphenol (BP) and/or hydroquinone (HQ). A system containing all BP will be denoted as BP-PSF. Likewise, a system containing all HQ will be denoted as HQ-PSF. If BP and HQ mole percent are both 50 %, the designation is HQ/BP PSF. Oligomers were also copolymerized with terephthaloyl chloride and, in some cases, terephthaloyl chloride along with BP. This latter use of BP, as distinct from oligomer synthesis, will be referred as "excess BP". Excess BP was added to increase the likelihood of liquid crystalline behavior in the HQ/BP PSF samples.

Scheme 1

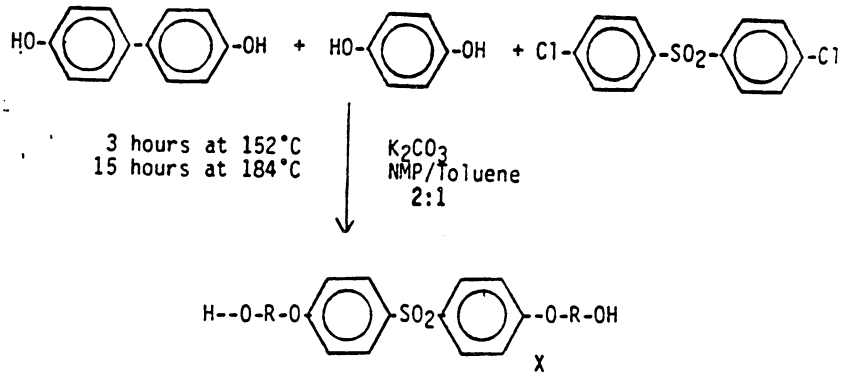

Hydroxyl Terminated Poly(arylene ether sulfone) oligomer

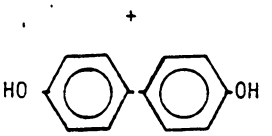

4,4'-Biphenol

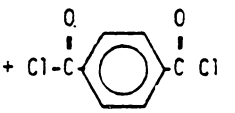

Terephthaloyl Chloride

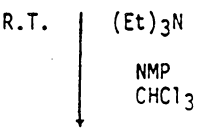

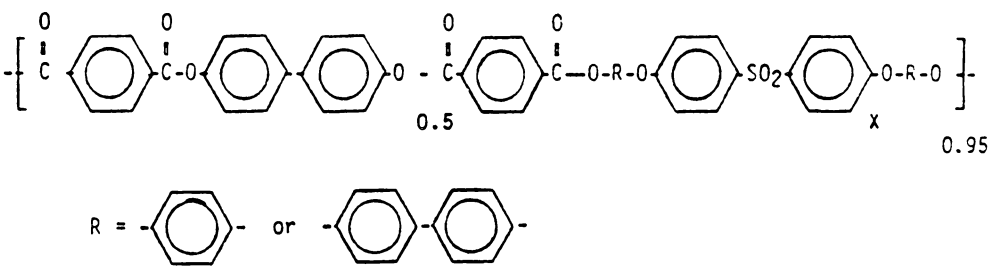

Segmented Poly(arylene ether sulfone) - Biphenol Terephthalate Terpolymers

Sample preparation

(a). Solution cast films

The hydroquinone/biphenol polysulfone polymers were cast into film form by one of the following methods. One gram of the copolymer was dissolved in 10 ml of chloroform. Chloroform was chosen over methylene chloride because of its slower evaporation rate. However, some samples were cast in methylene chloride to study solvent induced crystallization. The dissolved polymer solution was first filtered through a disposable pipet packed with glass wool to remove any dust or insoluble material in the solution. The filtered solution was then poured into a 9 cm diameter Petri dish and a large beaker was used to cover the solution to exclude dust and to limit the rate of solvent evaporation. The film was allowed to air dry for 4-6 hours and then the Petri dish (with sample) was placed in a vacuum oven with no heat for 12-15 hours. Finally, the vacuum oven was heated to 150°C for 24 hours to remove any last traces of solvent. After being allowed to cool, the film was removed from the Petri dish. The films produced in this manner were 2-4 mils thick.

(b). Thermally pressed films

In order to minimize hydrolysis by moisture absorption, all samples were heated in a vacuum oven at 100°C for approximately 48 hours prior to being compression molded into thin films using a Pasadena Hydraulics model 520 press. The HQ/BP PSF systems of different molecular weights were molded at 285°C. The films were quenched in an ice-water bath upon removal from the press. The thickness of the films ranged from 5 to 10 mils.

EXPERIMENTAL METHODS

For characterization purposes, many of the polymers and copolymers synthesized were solvent cast or thermally pressed into films. The polymer films were studied with respect to optical clarity, mechanical properties, thermal properties, and signs of liquid crystallinity. The appropriate characterization techniques will be discussed below.

Characterization Techniques

(a). Optical Microscopy

Optical microscopy was performed on a Zeiss RP polarizing-microscope. For hot stage microscopy studies, the sample was sandwiched between glass slides and placed inside a Mettler FP2 microscope hot stage. The hot stage was positioned within a linearly polarized light beam and the sample was heated (10°C/min) from ambient temperature to 290°C. During heating, the sample was observed for physical changes, specifically, signs of liquid crystallinity induced in the HQ/BP PSF system. In general, fluctuations in light intensity are brought about by a depolarization effect. On a molecular scale, changes in optical anisotropy can be coupled to melting and changes in orientation induced by heating as well as liquid crystal transition phenomena if present. At selected times, images were recorded on Polaroid film at different temperatures.

(b). Differential Scanning Calorimetry (DSC)

Differential scanning calorimetry is a technique that is widely used to study the thermal properties of polymer systems, and detailed reviews are presented elsewhere (67,68). A typical DSC scan of a semi-crystalline polymer appears in Fig. 33 and the glass transition temperature (Tg), crystallization temperature (Tc), and melting temperature (Tm) are shown. The area under the crystallization and melting peaks represent enthalpies of crystallization and melting respectively.

(c). Dynamic Mechanical Testing

A Rheovibron viscoelastometer was utilized to measure the dynamic mechanical properties of the HQ/BP PSF systems. The temperature dependence of the dynamic storage modulus (E'), dynamic loss modulus (E"), and dynamic loss tangent (tan δ) were studied at a frequency of 110 Hz for these samples. A sinusoidal tensile strain is applied at one end of the sample and the sinusoidal tensile stress response is measured at the other end. The tangent of the phase angle (tan δ) between stress and strain in the sample is measured directly while E' and E" can be calculated.

(d). Potentiometric titration

The absolute number average molecular weight of these hydroxyl terminated polymers was determined by potentiometric titration of the end groups in a non-aqueous medium using tetrabutylammonium hydroxide as titrant. The method is discussed in more detail in the Appendix B. Viscosity average molecular weight was measured using an Ubbelohde viscometer as discussed in Appendix B. Both these methods were utilized by M. Lambert as part of this study and hence are indirectly relevant.

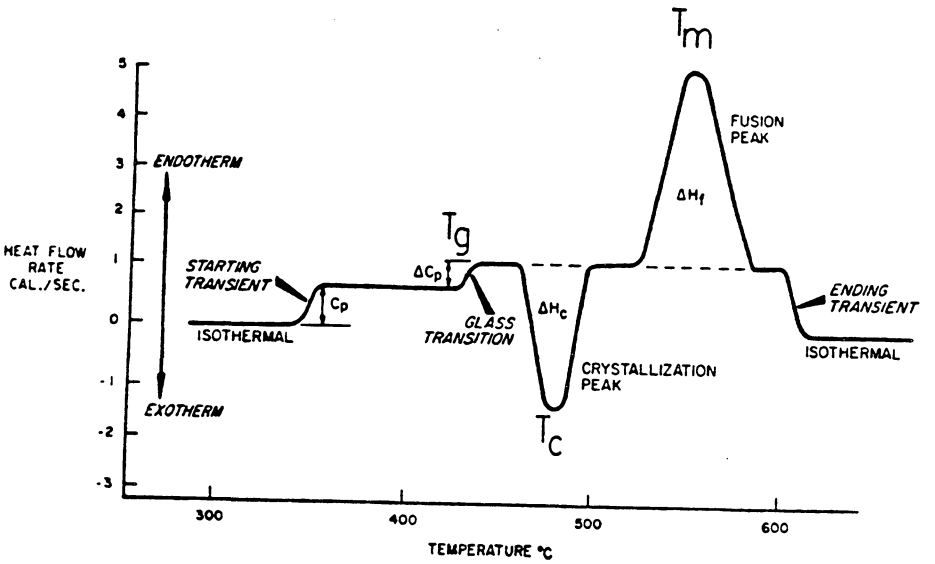

Fig. 33 Representative DSC scan of a semi-crystalline polymer showing parameters of Tg - Glass transition temperature, Tc - Crystallization temperature, and Tm - Melting temperature. (68)

(e). Wide Angle X-ray Scattering and Mechanical Testing

Wide angle x-ray scattering utilizing a Phillips PW 1720 table top x-ray generator with Warhus camera and mechanical testing using a Instron model 1122 is described in Chapter I within the *Experimental Methods* section.

RESULTS AND DISCUSSION

The oligomer synthesis, their characterization, and subsequent polymerization into polymers of interest is given in Appendix C. Details of the copolymerization incorporating terephthaloyl chloride into the oligomer with discussion of solution and interfacial reactions are also given in Appendix C. Composition and molecular weight characterization are discussed in Appendix D.

The characterization of HQ/BP PSF copolymers using thermal analysis, WAXS, and mechanical property testing will now be discussed. Thermal analysis and x-ray diffraction can specifically be used to determine if any of these systems show liquid crystalline character.

Thermal Analysis and Glass Transition Behavior

The nomenclature with different molecular weights of the HQ/BP PSF polymers that were synthesized in this investigation are given in Table 3. The molecular weights used in the discussion are those of the PSF oligomer and not the total polymer molecular weights.

The initial film sample investigated, denoted as HQ/BP PSF 1770, was cast from methylene chloride. The different molecular weight films in all cases were transparent with the exception of BP/PSF 3000 which was slightly turbid. DSC scans of the solvent cast 1770 material from ambient to higher temperatures shows a glass transition temperature at 208°C. All the DSC scans will be referred to as "second heating" unless otherwise noted. It was observed that there was no sign of any higher

TABLE 3 - Nomenclature of different molecular weights of the HQ/BP PSF, and BP/PSF polymers synthesized.

Polysulfone Oligomers(a)		IV (25°C)(b)	Added Biphenol(c) mole %/weight%
Mn	Bisphenols		
1690	HQ/BP PSF	--	5/0.55
1770	HQ/BP PSF	--	--
2210	HQ/BP PSF	0.70	
2210	HQ/BP PSF	--	100/5.20 (Added Hydroquinone)
2870	HQ/BP PSF	0.46	--
2870	HQ/BP PSF	--	10/0.35
2870	HQ/BP PSF	--	20/0.82
2870	HQ/BP PSF	--	30/0.98
2870	HQ/BP PSF		40/1.30
3840	HQ/BP PSF	--	--
5340	HQ/BP PSF	--	--
5340	HQ/BP PSF	0.87	10/0.35
5340	HQ/BP PSF	--	50/1.74
5340	HQ/BP PSF	--	75/2.61
6690	HQ/BP PSF	0.90	--
7260	HQ/BP PSF	1.07	--
3000	BP PSF	0.38 in NMP	--
3680	BP PSF	--	10/0.35
3680	BP PSF	--	20/0.82
3680	BP PSF	--	30/0.98

(a) 50/50 mole rates of hydroquinone and biphenol, unless otherwise noted.
(b) Measurements conducted in $CHCl_3$ unless otherwise noted.
(c) Added Biphenol unless otherwise noted.

order transition that might be attributed to any liquid crystallinity or melting behavior in this 1770 sample. It should be noted, however, that there is no excess biphenol in these samples and therefore this material may not be particularly prone to liquid crystalline formation. Some investigations were also carried out on HQ/BP PSF 1770 samples that were sheared at 250°C and observed between crossed polarizers in a hot stage system. While indeed birefringence colors were noted following shear induced orientation, again no distinct liquid crystalline textures could be identified.

The next sample that several investigations were carried out on was BP PSF 3000. In this sample it was expected that there maybe more chance for liquid crystalline formation due to the higher biphenol content (100 % BP). Interestingly, when these samples are cast from methylene chloride, there are signs of turbidity, and an initial DSC scan shows what appears to be melting behavior in the range of 240-270 C--see Fig. 34, curve 1. Rescans of the same material do not show any strong signs of crystallinity but the glass transition temperature now becomes more apparent and appears in the 220°C range with sometimes a very small endothermic "peak" being denoted in the range of 247 or slightly above--see curve 2 in Fig. 34. A third melting or reheating of the same sample shows a somewhat similar behavior as given in curve 3 in Fig. 34 thereby demonstrating the reproducibility of the thermal analysis results. If the same cast material is annealed for a period of time in the range of 230°C for ten minutes, sign is still present of some melting behavior in the 250°C region. If, however, virgin cast material is first annealed for ten minutes at 260°C, second or further heatings

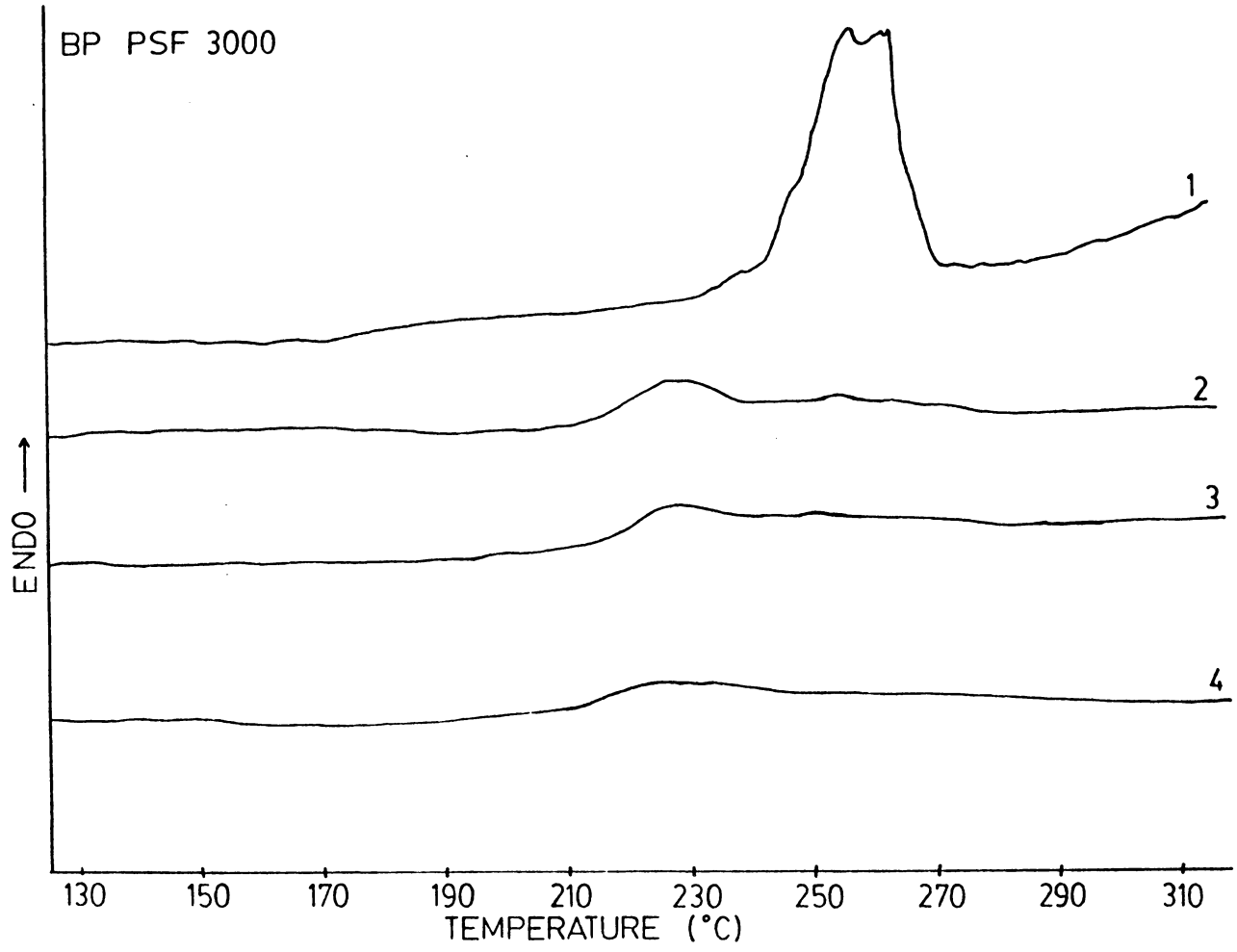

Fig. 34 DSC scans of BP/PSF 3000 samples. Curve 1). First heating, Curve 2). same sample as the curve 1 which has been cooled down and heated up for the 2nd time, Curve 3). same sample as the curve 1 which has been cooled down again and heated up for the 3rd time, Curve 4). A different BP/PSF 3000 sample which has been annealed at 258°C for 10 min. This scan is for the sample which has been cooled down and heated up for the 2nd time.

show no sign of the presence of any melting behavior, thereby again further confirming that the virgin solution cast material melts out in the range of 250-260°C--see curve 4 in Fig. 34. Further confirmation of the speculations made based on the thermal analysis data are supported by WAXS patterns which will be discussed shortly.

Sample HQ/BP PSF 5340 with 10 mole % excess BP or sample HQ/BP PSF 1690 with 5 mole % excess BP showed no signs of turbidity for the solvent cast films from either methylene chloride or chloroform and furthermore showed no signs of melting behavior by thermal analysis. The glass transition temperature, while not particularly distinct, again fell in the range of 220°C as is illustrated by curve 1 in Fig. 35. One must note that the amount of extra BP added on a molar basis may be 75 % extra, but on a weight basis it is only 4 % extra. The excess content of BP made relatively little difference in terms of the general glass transition behavior as shown by curve 2 in Fig. 35, which provides the DSC scan on sample HQ/BP PSF 5340 with 50 mole % excess BP. Curve 3 in Fig. 35 shows that similar data occurs for the second heating of sample HQ/BP PSF 5340 plus 75 mole % excess BP. In this latter scan, it is clear that the glass transition temperature falls in the range of 210 C.

Table 4 shows the glass transition temperatures determined by DSC for various molecular weights of the HQ/BP PSF systems that were thermally pressed at 285°C. The results indicate that there is a very slight increase in Tg as one increases the PSF segment molecular weights of these systems. Adding extra BP or HQ to the HQ/BP PSF systems did not provide any definite general trend in the Tg behavior

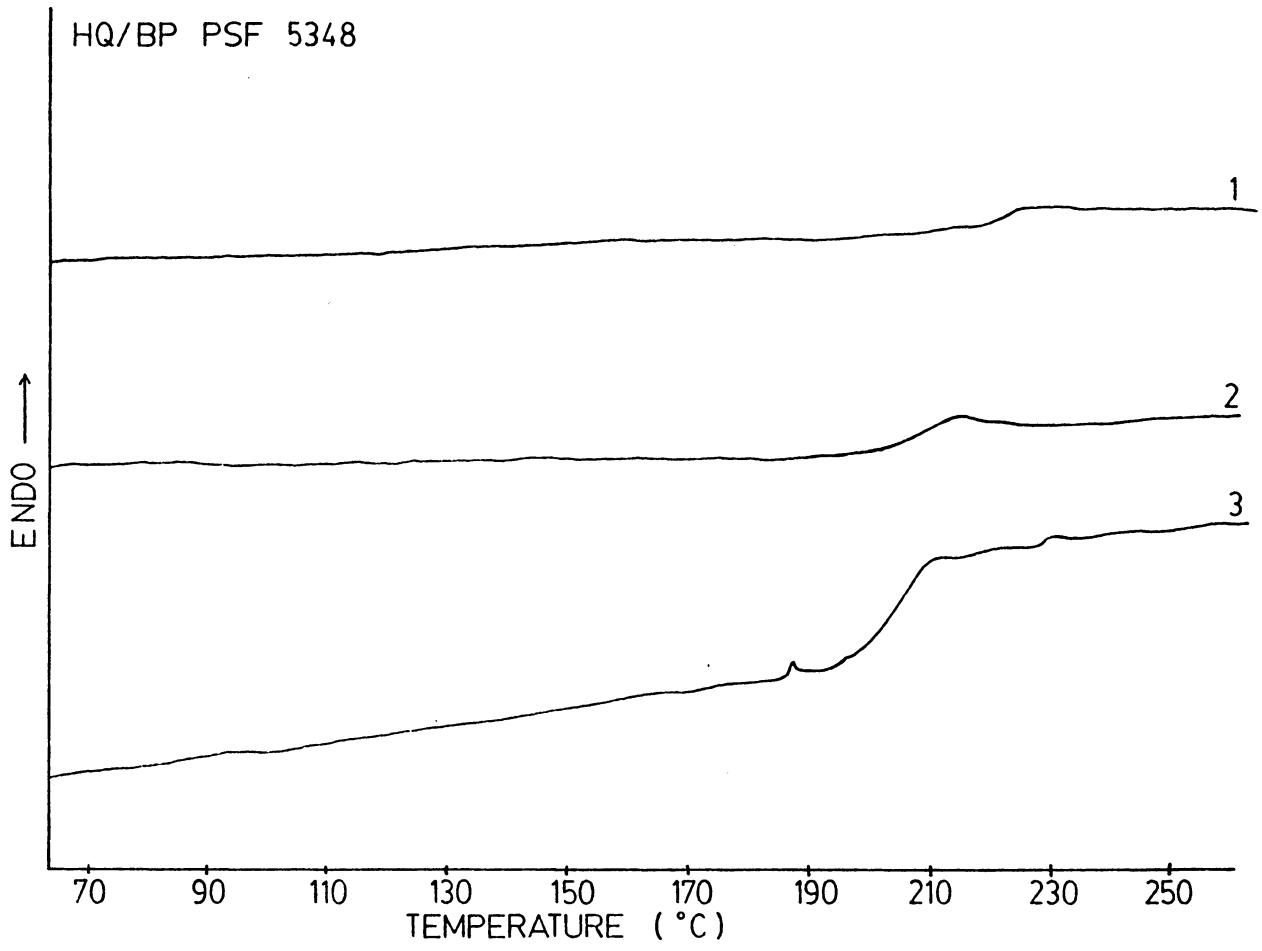

Fig. 35 DSC scans of samples which has been cooled down and heated up for the 2nd time.
Curve 1). HQ/BP PSF 5340 + 10 % extra BP
Curve 2). HQ/BP PSF 5340 + 50 % extra BP
Curve 3). HQ/BP PSF 5340 + 75 % extra BP

TABLE 4 - Glass transition temperatures determined by DSC for various segment molecular weights of HQ/BP PSF systems that were thermally pressed at 285°C.

Sample	Tg (°C)
HQ/BP PSF 2210	213
HQ/BP PSF 3840	217
HQ/BP PSF 5340	219
HQ/BP PSF 6690	218
HQ/BP PSF 7260	218

as is shown in Table 5. This is due to the fact that the extra BP or HQ in mole percentage is only a very slight increase in BP or HQ on a weight percent basis, as mentioned before. Therefore, excess BP or HQ do not alter the structure very much and do not produce any defined general trends in the Tg behavior. Also lowering segment molecular weight to 2210 lowered Tg to 197°C from 205°C for higher molecular weight samples. This indicate that there may be a minimum molecular weight for these samples for the Tg to be above 200°C.

Wide Angle X-ray Scattering (WAXS)

Wide angle x-ray photographs were utilized for purposes of denoting whether crystallinity was present in the virgin film material as well as those that had undergone various thermal treatments. In brief, the WAXS photograph shown in Fig. 36 A obtained from the methylene chloride cast films of BP PSF 3000 with no excess BP gave very distinct signs of crystallinity. Most other samples showed no sign of crystallinity, whether they were virgin or had undergone thermal annealing procedures. The solution cast films that did show signs of crystallinity are listed in Table 6. However, all the materials that showed crystallinity initially following casting apparently lost crystallinity upon heating above 260°C. Only a very low level of crystallinity could be recovered upon annealing as was denoted by wide angle x-ray scattering. As an example, after annealing the BP PSF 3000 sample at 230°C for 10 minutes, the sample still shows signs of crystallinity as shown in Fig. 36 B, but upon annealing at 258°C for 10 minutes, the crystallinity disappeared, as shown in Fig. 36 C.

TABLE 5 - Glass transition temperatures determined by DSC (2nd scan) for various segment molecular weights of HQ/BP PSF systems with extra BP or extra HQ, that were solvent cast in chloroform.

Sample	Tg (°C)
HQ/BP PSF 2870	212
HQ/BP PSF 2870 + 10% extra BP	200
HQ/BP PSF 2870 + 20% extra BP	213
HQ/BP PSF 2870 + 30% extra BP	208
HQ/BP PSF 2870 + 40% extra BP	202
HQ/BP PSF 2210	197
HQ/BP PSF 2210 + 100% extra HQ	196

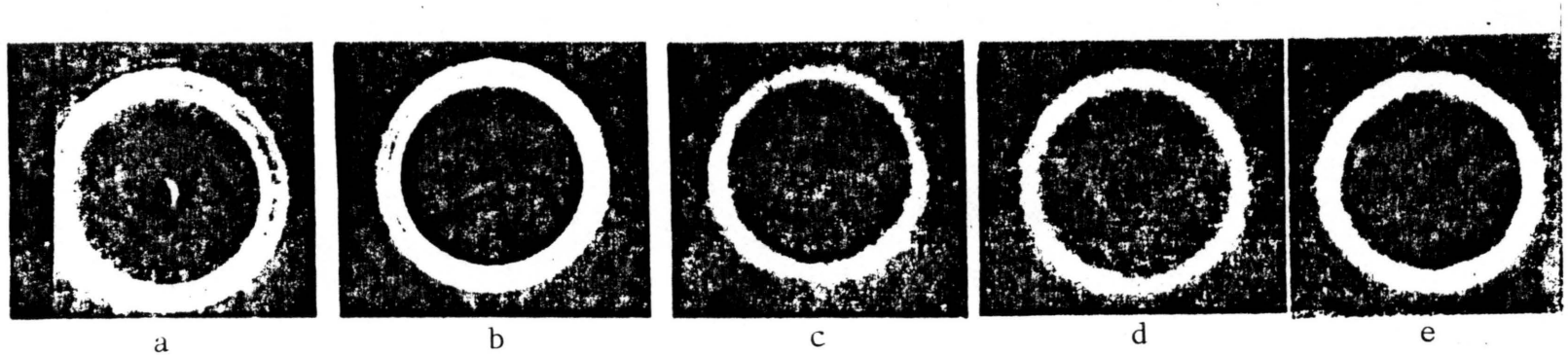

Fig. 36 WAXS patterns of samples with different conditions. (a-c), BP PSF 3000 samples with different thermal treatment, but cast in same methylene chloride. (d,e), HQ/BP PSF 1690 + 5 % extra BP samples cast in different solvents.
(a). Solvent cast film (No annealing)
(b). Annealed at 230°C for 10 min.
(c). Annealed at 258°C for 10 min.
(d). Solvent cast in methylene chloride
(e). Solvent cast in chloroform

TABLE 6 - Polymer samples which showed signs of solvent induced crystallinity by WAXS.

HQ/BP PSF 2870
HQ/BP PSF 2870 + 30% extra BP
HQ/BP PSF 2870 + 40% extra BP
BP PSF 3680 + 10% extra BP
BP PSF 3680 + 20% extra BP
BP PSF 3680 + 30% extra BP

In order to check if the choice of casting solvent influences crystallization on these systems, the HQ/BP PSF 1690 + 5 mole % BP sample was solvent cast from methylene chloride as well as chloroform. (These were the only two common solvents that were found that would dissolve this polymer) The WAXS patterns for both samples are shown in Fig. 36 D & E and indicate no sign of crystallinity, thereby indicating these materials could not be crystallized by either solvent. Then question could arise as to why some of the virgin samples showed crystallinity. The reason that some of the virgin samples showed crystallinity (from WAXS) could be due to the casting procedure for this polymer. All of the samples were cast according to the same procedure except that, depending on the amount of material available, a larger (9 cm) or small (5 cm) diameter Petri dish was used. There is a possible reason for the samples cast in the smaller Petri dish to show crystallinity. Smaller Petri dishes could have shortened the time required to completely evaporate the solvent from the polymer and therefore showed signs of crystallinity. In order to attempt to induce crystallinity into the HQ/BP PSF systems by thermal means, samples HQ/BP PSF 2210, 5340 and the latter 5340 with 50 mole % excess BP were annealed at 265°C for 30 minutes. Other samples of HQ/BP PSF 2210, 3840, 5340, 6690 and 7260, were thermally pressed at 285°C. The WAXS photographs for all these films show no crystallinity as given for samples of HQ/BP PSF 2210, 5340 and 7260 in Fig. 37. Again the WAXS results confirmed that crystallization could not be induced thermally on these systems. The reason some of these polymers were able to solvent crystallize (BP PSF sample with chloroform) and yet difficult to

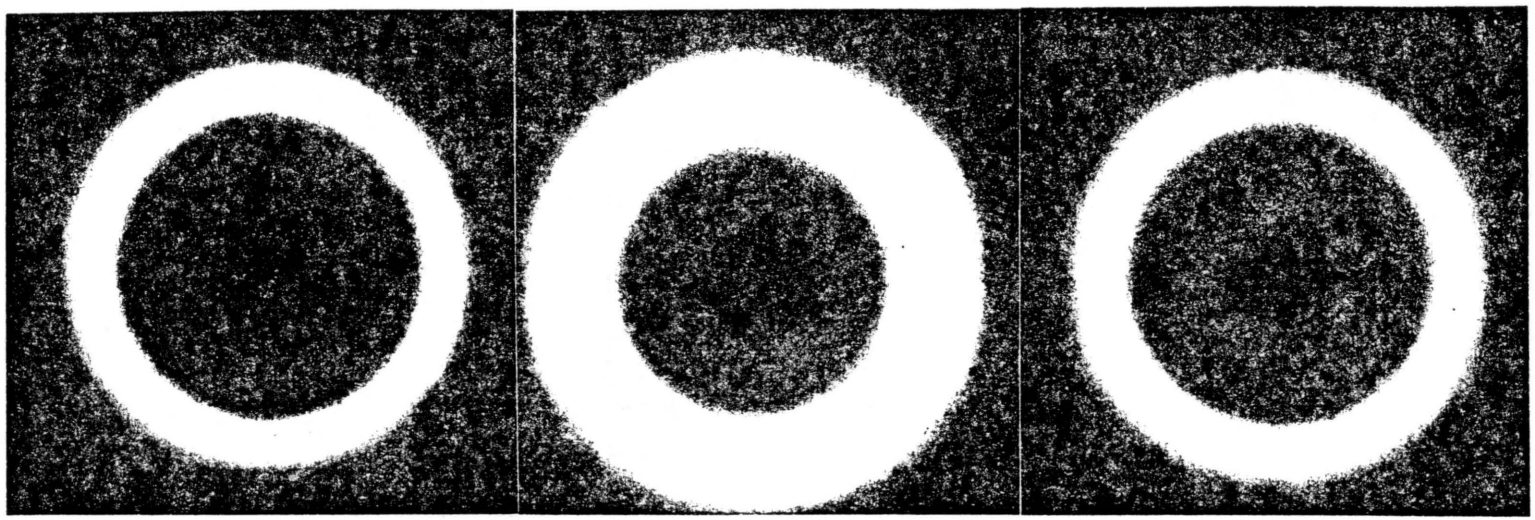

a b c

Fig. 37 WAXS patterns of samples thermally pressed at 285°C.
(a). HQ/BP PSF 2210
(b). HQ/BP PSF 5340
(c). HQ/BP PSF 7260

thermally crystallize, is because of the narrow window (Tm-Tg) of the sample.

In the simplest terms, the process of solvent induced crystallization may be considered as involving several steps. First, the solvent is imbibed in the polymer by diffusion. The solvent-polymer interaction causes enhanced mobility of the polymeric segments by disturbing the intersegmental forces. If the polymer solvent interaction is strong enough, then the polymer chains may be able to rearrange into a more thermodynamically lower energy state. As the polymer chains reduces to lower energy state, then the polymer chains drop out of the solution and reject the solution. The lower energy state is generally the crystal state if chain symmetry allows. (It is well known that for thermal-induced and for solvent-induced crystallization, stable crystallites may in turn develop into higher forms of ordered superstructure such as spherulites.) Thus, those solvents which are capable of strong interaction with a given polymer may be capable of inducing crystallization. Clearly, if the polymer-solvent interaction is favored as compared to the dispersion, polar, and hydrogen bonding forces holding the macromolecules together, solvent exposure may lead to complete dissolution. Typically, some dissolution in fact will occur at the interface between the pure solvent and sample surface due to a large concentration gradient.

In terms of a commonly measured quantity -- the glass transition temperature -- the foregoing may be restated as follows. The sorption of the solvent by the polymer has a plasticizing effect. This leads to a lowering of the glass transition temperature, Tg. As is well known,

crystallization occurs between the values of Tg and Tm. Solvents are also known to cause a depression in Tm, but generally the depression of Tm is considerably less than the depression of Tg.

The basic mechanism of solvent induced crystallization is very much the same as that of thermal-induced crystallization from the glassy state since both involve, as a necessary step, the inducement of segmental mobility. The former achieves the goal by use of chemical energy, and the latter does so by use of thermal energy. Specifically, in homogeneous nucleation, the nucleation density depends on the temperature in a manner that is somewhat predictable. It goes through a maximum as does the overall growth rate and growth rate of individual units. As supercooling increases, i.e., Tm-Tc increases, where Tc is the crystallization temperature, the driving force for crystallization through necleation increases; therefore, G (crystal growth rate) will increase--see Fig. 38. It can also be shown that the nucleation density in homogeneous nucleation is low near Tm but begins to increase as the supercooling increases. However, as the supercooling becomes still larger, the viscosity is increasing so that the ability of a molecule to diffuse to a growing crystal face decreases, and thus G will decrease toward zero as the crystallization temperature approaches Tg. Thus, the nucleation rate will also pass through a maximum for the homogeneous process. For this reason, crystallization by homogeneous nucleation is said to be diffusion controlled at high supercooling and nucleation controlled at low supercooling. For heterogeneous nucleation, only the growth of the nucleated crystals is temperature dependent, becoming diffusion limited at high supercooling (low crystallization

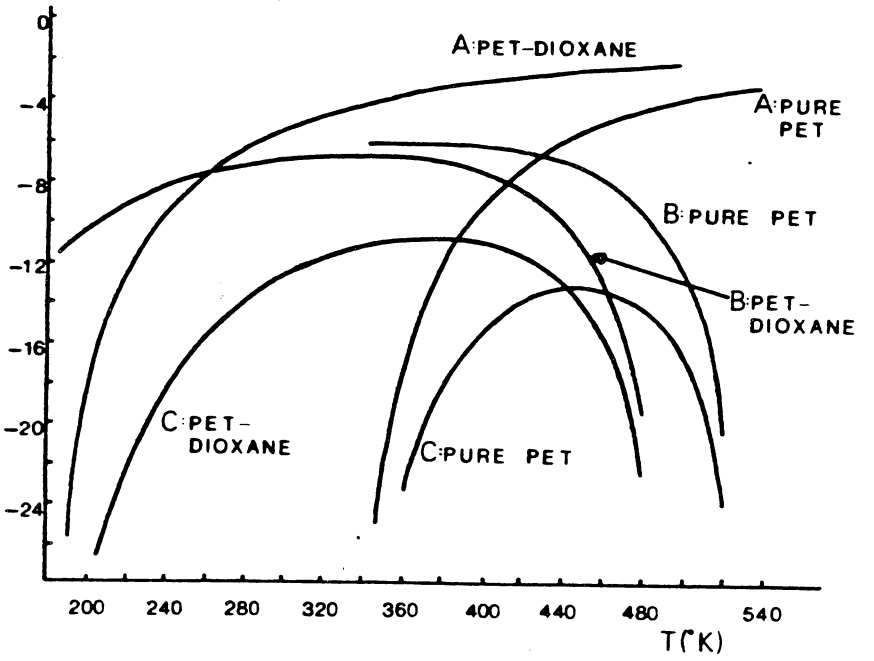

Fig. 38 Logarithmic plot of the transport term, nucleation term, and growth rate term versus temperature for the model PET-dioxane liquid-induced crystallization case and the pure PET thermal crystallization case. (71)

temperature). The difference between the homogeneous and heterogeneous nucleation is that homogeneous nucleation occurs in the absence of a second phase, spontaneously, by supercooling only. Heterogeneous nucleation is due to the presence of a second phase and occurs on the interphase of it. For more details on the kinetic theory of heterogeneous and homogeneous nucleation, references 69, 70 and 71 are useful. In summary, the narrower the window of crystallization, the lower the ease of crystallization for the HQ/BP PSF materials.

In order to attempt to induce crystallinity by strain, a sample film of HQ/BP PSF 2210 was elongated at an initial crosshead speed of 100 %/min in a high temperature chamber at 240°C. Corresponding WAXS results indicate no sign of crystallinity. Therefore, this particular material could not be strain induced crystallized by this method under these conditions. Sample availability has prevented further study on different molecular weight samples.

Excess biphenol was originally added to increase the likelihood of liquid crystalline behavior in these materials. The effect of adding extra BP to the HQ/BP PSF 5340 system does not induce crystallinity in the system as shown in the WAXS patterns of Figs. 39 A-C for 10, 50 and 75 mole % extra BP added to the HQ/BP PSF 5340 system. As mentioned before, the extra mole % BP added to the system does not show a real increase in extra weight percent BP. Generally, the inclusion of excess BP lowered Tg very little. Finally, the effect of increasing the oligomeric molecular weight does not seem to increase the level of crystallinity as shown in Fig. 40 A, B & C for the HQ/BP PSF 2870, 5340, 7260 materials, respectively. Therefore, from the WAXS

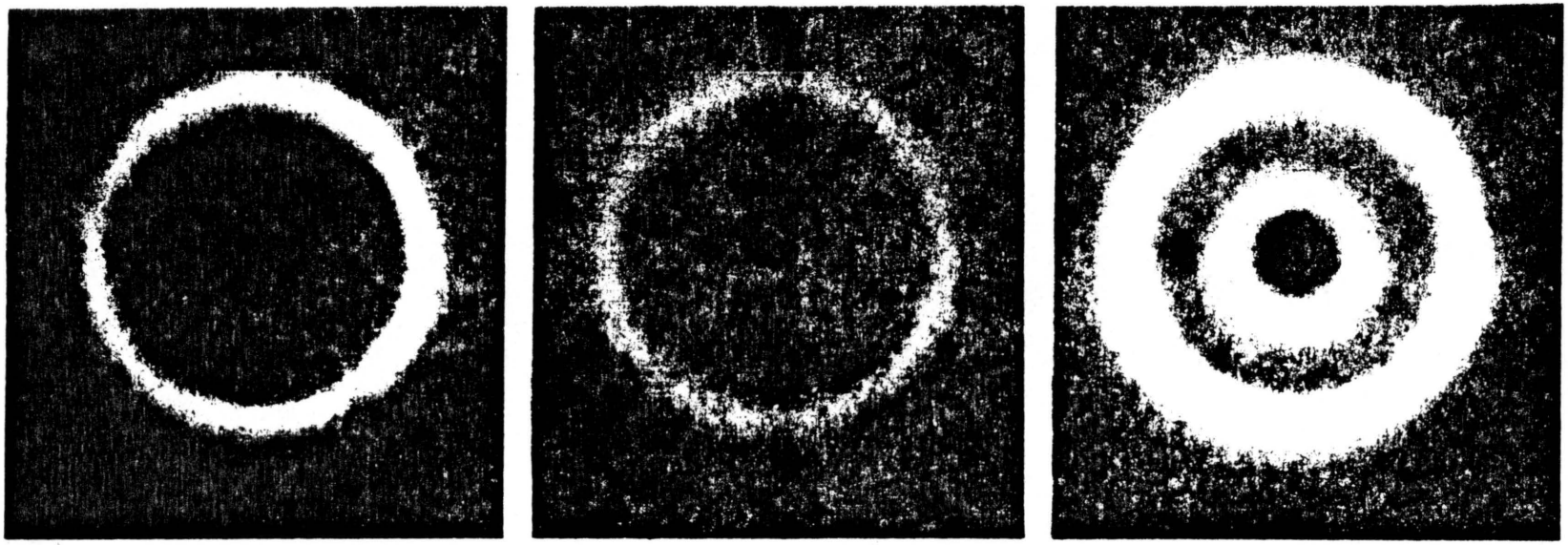

a b c

Fig. 39 WAXS patterns of HQ/BP PSF 5340 samples with extra biphenols (in mole %).
(a). HQ/BP PSF 5340 + 10% extra BP
(b). HQ/BP PSF 5340 + 50% extra BP
(c). HQ/BP PSF 5340 + 75% extra BP

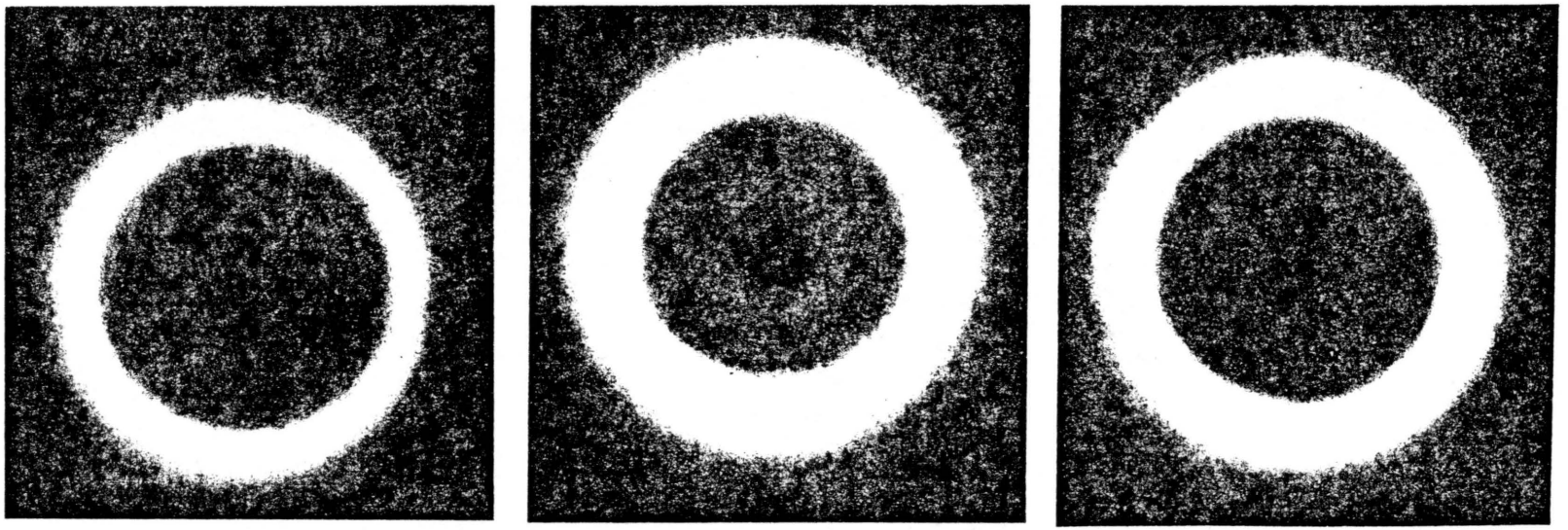

a b c

Fig. 40 WAXS patterns of samples with increasing oligomeric molecular weight.
(a). HQ/BP PSF 2870
(b). HQ/BP PSF 5340
(c). HQ/BP PSF 7260

results, it is concluded that most of the HQ/BP PSF systems of different molecular weights can not be crystallized by solvent, thermal, or strain induced crystallization methods. Exceptions have been noted and were discussed previously.

Static Mechanical Behavior

Figure 41 shows the values of Young's modulus determined at 240 C from the data of the stress-strain study on films that were either solvent cast from chloroform (23°C) or thermally pressed (285°C). It is clear from these data that the result of increasing the segment molecular weight increases the modulus. This is observed for both the solvent cast and thermally pressed films. Increasing segment molecular weight further increases the "rod like" structure in the segment which has high modulus along the backbone orientation direction. Solvent cast samples were generally higher in modulus than the corresponding thermally pressed samples. Solvent casting and compression molding can lead to different morphologies depending on polymer composition, solubility parameter of the solvent, and the kinetics of solvent evaporation. In this case, where the samples were cast with chloroform, the solvent cast sample's modulus was higher than that of the thermally pressed samples. Another reason for the solvent cast film's higher modulus may be due to the fact that there is plannar orientation in solvent casted films, but not in the thermally pressed films. In other polymeric systems and using different solvents, the thermally pressed films may have higher modulus than the solvent cast films (72). Also, by adding extra BP to the HQ/BP PSF 5348 system

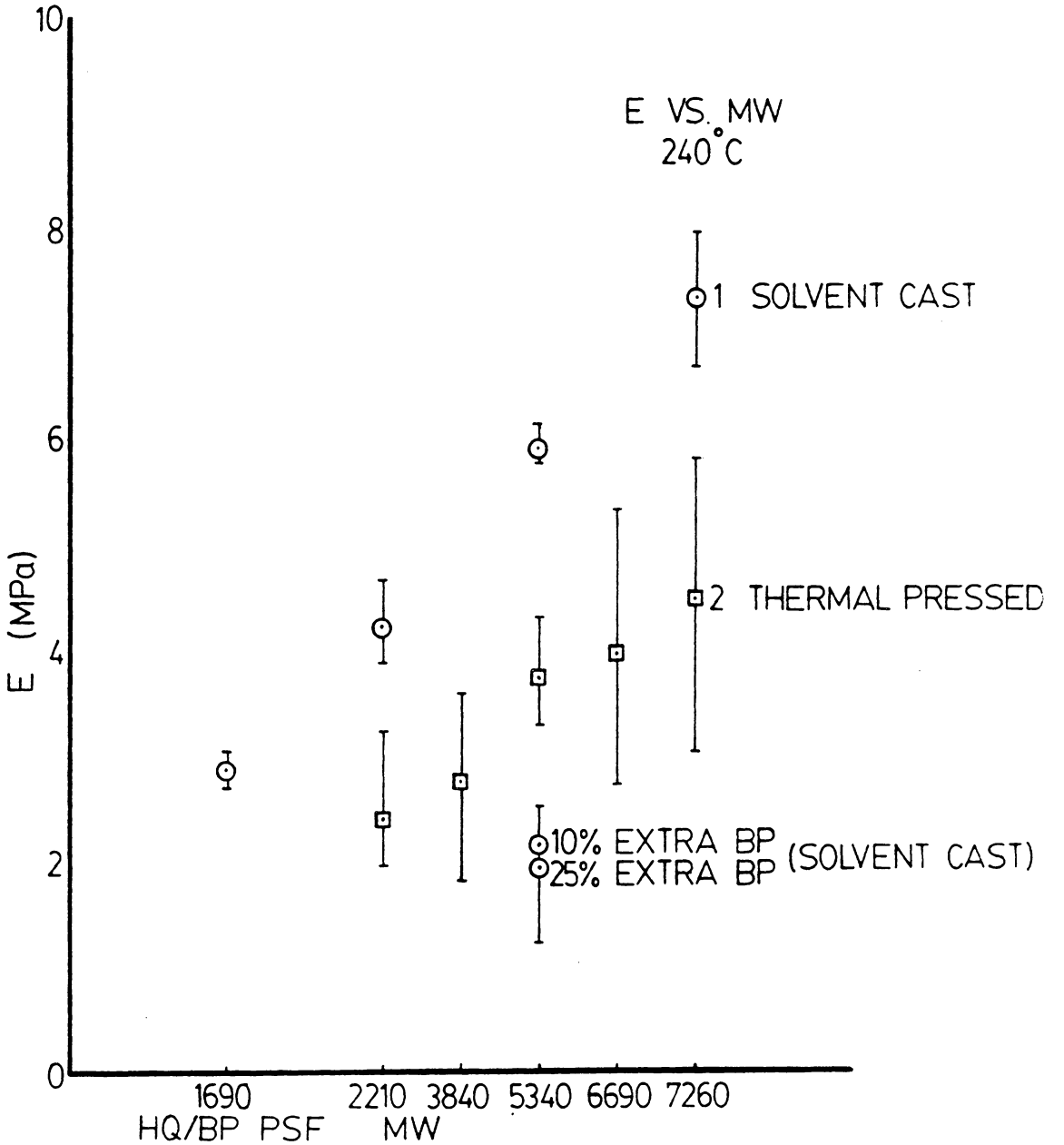

Fig. 41 Young's modulus of various segment molecular weights determined at 240°C.
plot 1). samples which have been cast in solvent
plot 2). samples which have been thermally pressed at 285°C.

even though it may not be much in weight percent, the modulus decreased when determined at 240°C. This incorporation of extra BP extends the rigid portion further, however due to the ether linkage in the biphenol moiety which lowers the Tg of the polymer. Therefore, when the modulus is determined at the same 240°C with lower Tg material, the modulus determined is lower than the modulus for the sample without excess BP. The stress-strain behavior for the HQ/BP PSF system determined at 240°C is shown in Fig. 42.

Figure 43 shows the values of Young's modulus determined at ambient temperature from the stress-strain study on films that were solvent cast from chloroform. As the molecular weight is increased, the modulus is increased also. This can be explained by the same argument as was the modulus determined at 240°C, that is the increasing oligomeric molecular weight further increases the rod like structure in the segment which would have its highest modulus along the backbone direction. However, adding extra BP to the HQ/BP PSF 2870 sample increases the modulus. In this point, it differs from the modulus determined at 240°C which showed a decrease in modulus with excess BP which was attributed to the lowering of the Tg of the material. However, it is possible this ether linkage in the biphenol moiety may simply lengthen the back bone chain at ambient temperature. Stress-strain curves determined at ambient temperature are shown in Fig. 44 for various molecular weights.

Dynamic Mechanical Behavior

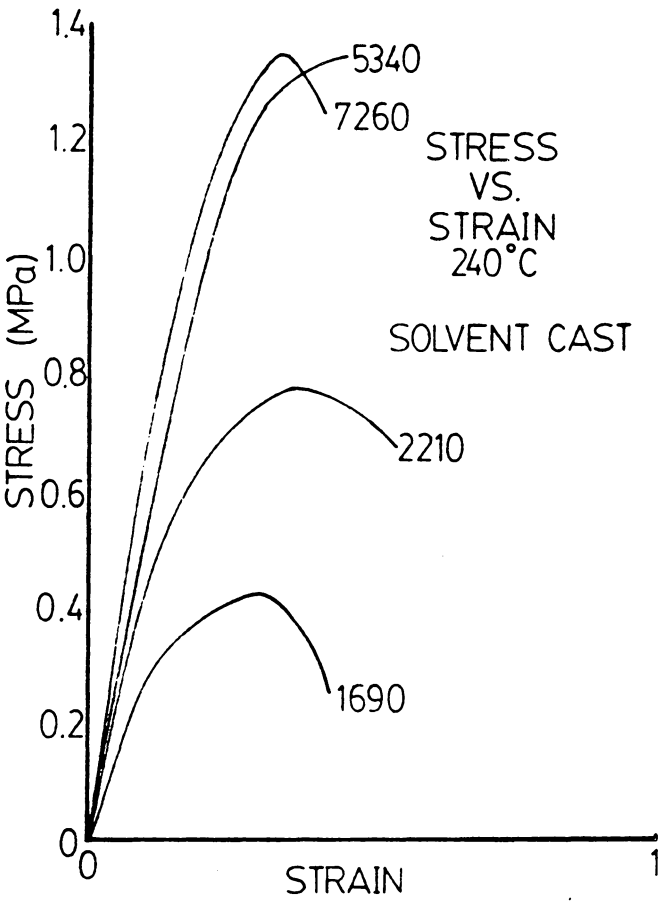

Fig. 42 Stress-strain curves of solvent cast films of various segment molecular weights determined at 240°C.

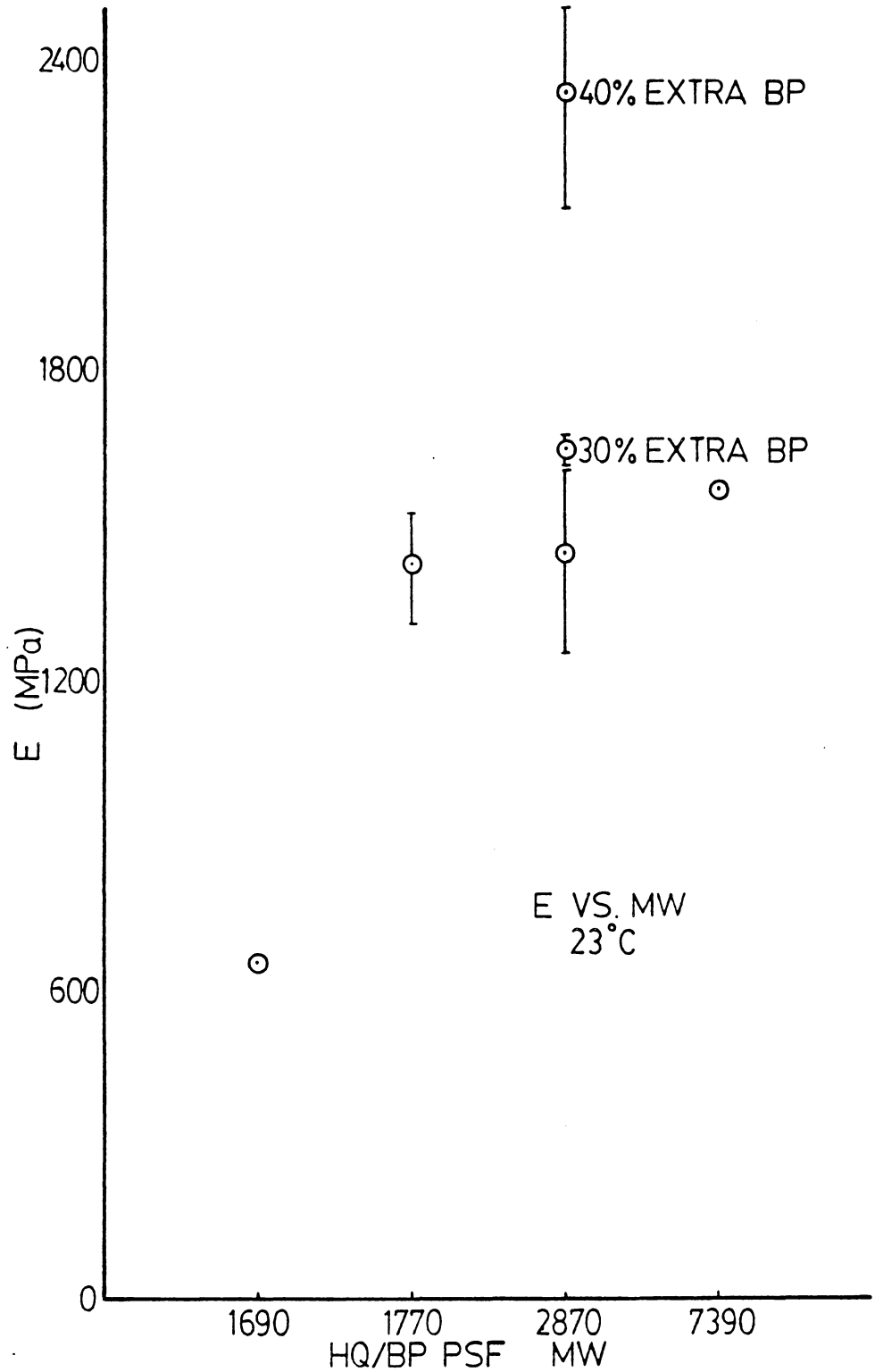

Fig. 43 Young's modulus of solvent cast films of various segment molecular weights determined at ambient temperature.

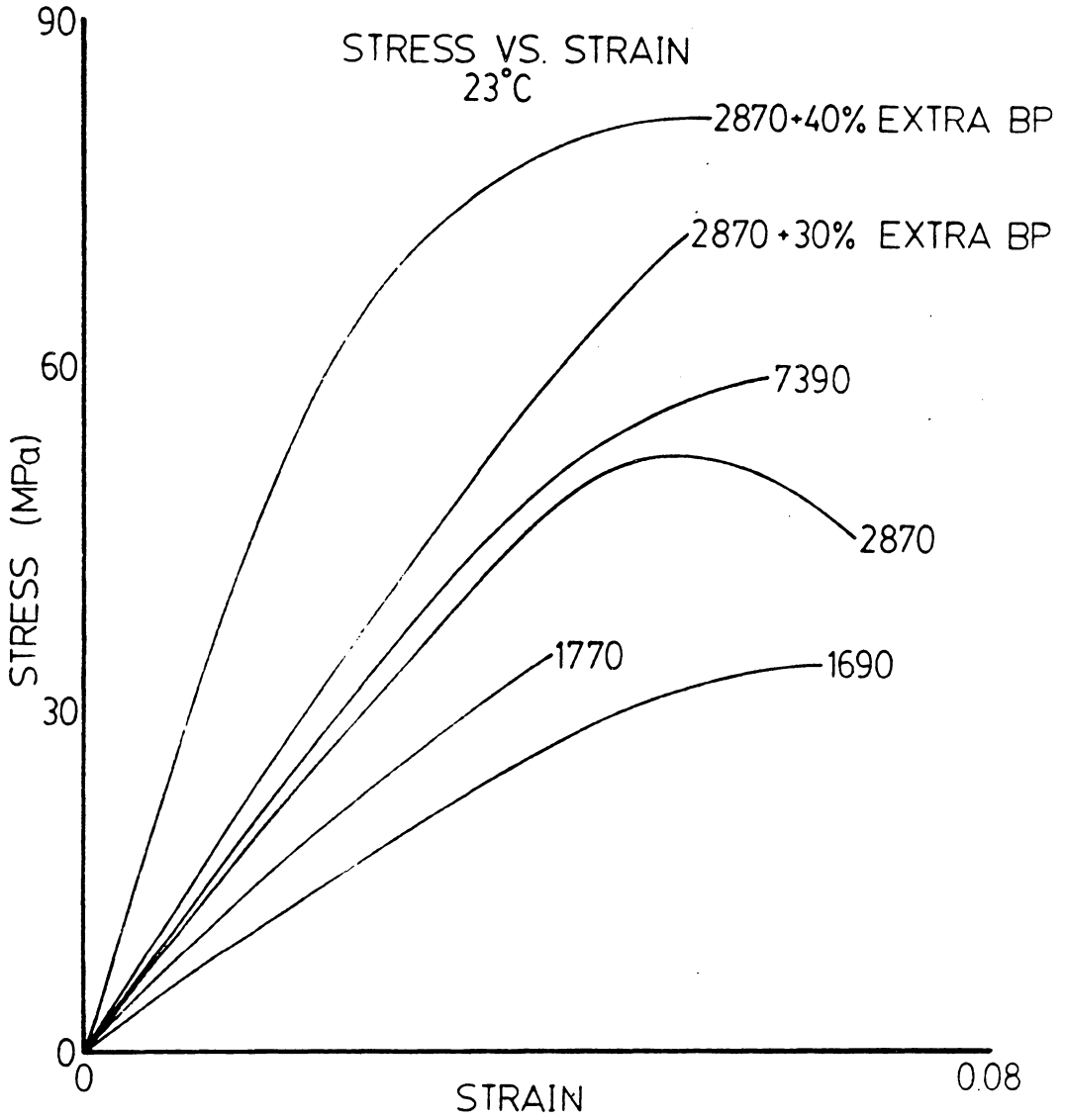

Fig. 44 Stress-strain curves of solvent cast films of various segment molecular weights determined at ambient temperature.

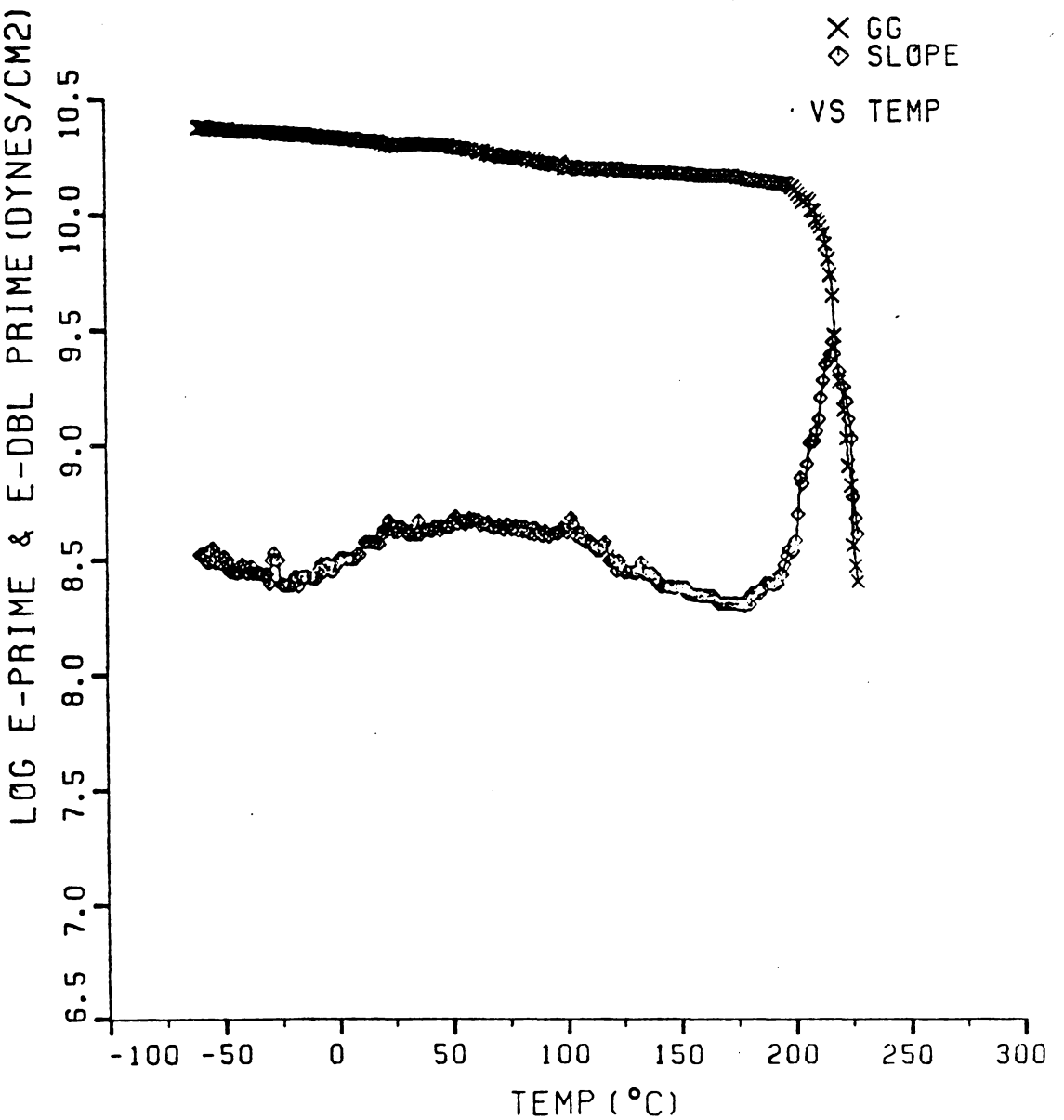

Fig. 45 Dynamic mechanical measurements of HQ/BP PSF 2870 polymer showing log E-prime and E-double prime.

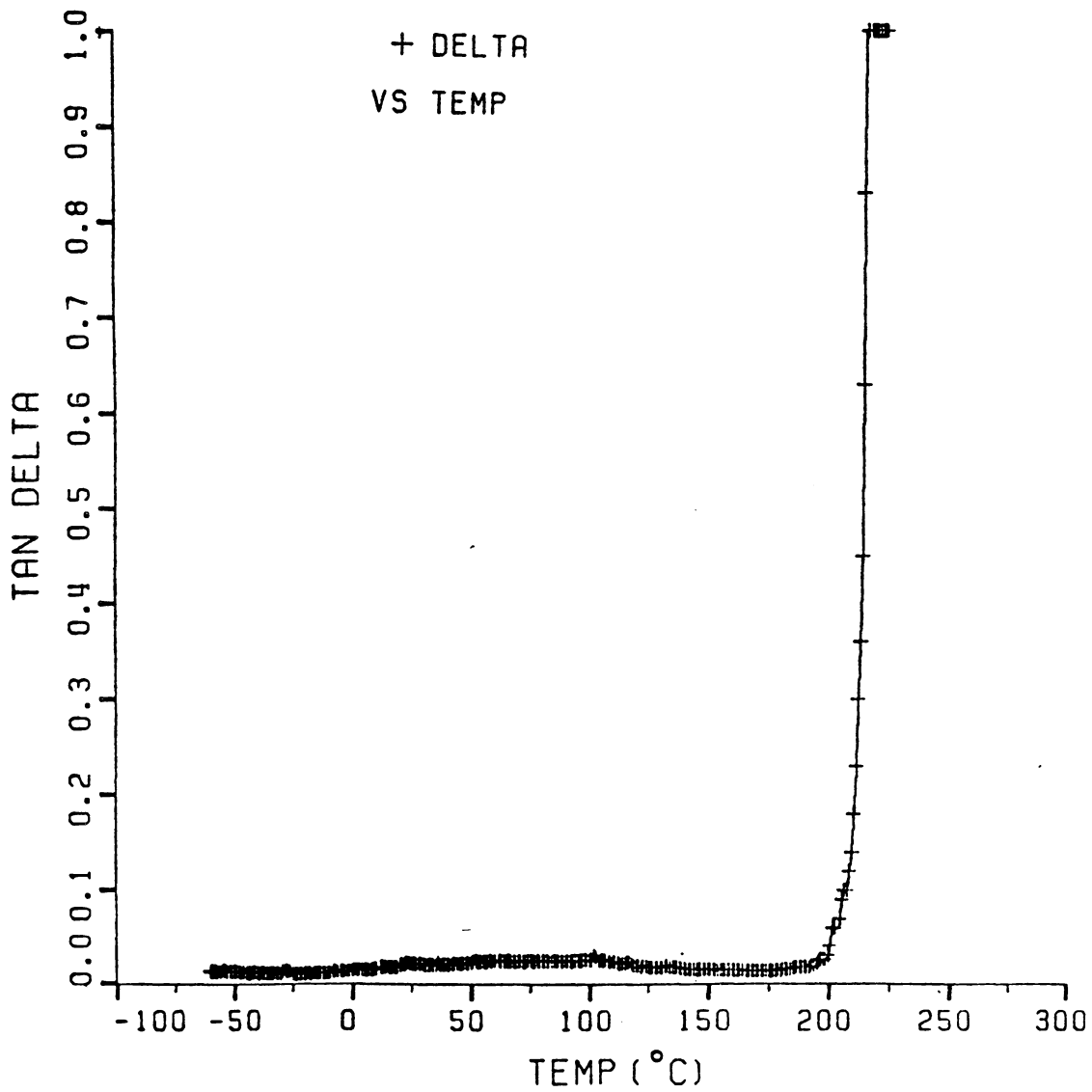

Fig. 46 Influence of temperature on tan δ for the HQ/BP PSF 2870 polymer.

High-temperature dynamic mechanical measurements made on the Rheovibron for HQ/BP PSF 2870 copolymer system are shown in Fig. 45. The glass transition temperature obtained from this study (210°C) was consistent with the earlier DSC results. Figure 46 shows the influence of temperature on tan δ for the HQ/BP PSF 2870 copolymer system. Low temperature mechanical properties of the copolymers showed a broad β-peak occuring at around 25°C. Good impact strength enhancements have been postulated to this β-transition, although this does not exclusively determine the toughness of such polymer (73,74). Dynamic mechanical measurements made for the HQ/BP PSF 7260 copolymer system were essentially similar to the HQ/BP PSF 2870 copolymer.

CONCLUSIONS

The purpose of this investigation was to gain some general knowledge of the thermal, mechanical and structure properties of the HQ/BP PSF polymer system, in particular to look for signs of liquid crystalline behavior. From this investigation, the following highlights may be denoted.

1. High molecular weight polymer of HQ/BP PSF can be synthesized by first preparing hydroxyl terminated polysulfone oligomer. Once the poly sulfone oligomers are synthesized they could be copolymerized to form terephthaloyl chloride extended arylene ether sulfone.

2. In general, most of the HQ/BP PSF polymer systems could not be crystallized by methylene chloride or chloroform solvents. Some exceptions were noted. Also, thermal or strain induced crystallization was not possible under the conditions utilized. All BP PSF systems of different oligomeric molecular weights showed crystallinity when solvent cast from chloroform. However, signs of crystallinity disappeared upon heating the sample to 258°C for 10 minutes. Liquid crystallinity was not observed on all HQ/BP PSF, and BP PSF systems studied.

3. Young's modulus as determined from the stress-strain measurements at 230°C was found to increase with increasing oligomeric molecular weight for both solvent cast and thermally pressed films. Also the Young's modulus determined at ambient temperature increased with increasing segment molecular weight for solvent cast films. Comparable study for the thermal pressed sample was not carried out.

This behavior was speculated by noting that increasing oligomeric molecular weight increases the chain length in the segment which has high modulus along the backbone orientation direction.

4. Young's moduli for the chloroform solvent cast films were higher than those for the thermal pressed films. This may be due to differences in morphology between the solvent and thermally pressed films and by the plannar orientation induced during the solvent casting precedure.

5. When the modulus was determined at 240°C for the samples with extra BP, the modulus decreased with excess BP. However, when the modulus was determined at ambient temperature, the modulus increased with excess BP. This is due to the lowering of Tg as one incorporates more of ether linkage in the biphenol moiety. Therefore, when the modulus is determined at the same 240°C with a lower Tg material, the modulus determined is lower than the modulus for the sample without excess BP. However, at ambient temperature the ether linkage in the biphenol moiety contributes to the modulus increase by lengthening the backbone chain.

RECOMMENDATIONS FOR FUTURE STUDIES

1. HQ/BP PSF plus extra 4 % wt. BP to the system did not show any signs of liquid crystallinity. However, future studies should be carried out with more wt. % extra BP to the HQ/BP PSF system.

2. High temperature dynamic mechanical measurement is recommended to allow a comparison of static mechanical testing at ambient temperature and 230 °C as a function of excess BP. Lower temperature dynamic mechanical measurements are also recommended to study the high impact strength of this material by studying the low temperature peak.

3. In order to further confirm the melting temperature of BP PSF 3000 polymer, which was 260°C, further crystallization study on BP PSF 3000 sample and other molecular weight BP PSF polymer samples is recommended.

4. The HQ/BP PSF polymer systems did not show any signs of liquid crystallinity and since these HQ/BP PSF systems were expected to show liquid crystallinity, structural study is recommended for reasons of no liquid crystallinity.

APPENDIX A

Procedures For The Synthesis Of HQ/BP PSF Copolymers.

Appendix A and the following appendices are referenced from the University report (Proposal No. 84-1460-03) prepared by J.E. McGrath and G.L. Wilkes.

Into an argon purged flask dichlorodiphenylsulfone (DCDPS) is added, followed by biphenol and hydroquinone. To these solids, NMP and toluene are added, and the temperature is raised to 150°C. As the mixture is slowly heated and stirred, a clear amber solution results. Potassium carbonate is then added to this solution which is maintained at 150°C. In these reactions the potassium carbonate serves as the base to form the phenolates of the biphenol and hydroquinone moieties. These phenolates can then attack the dichlorodiphenyl sulfone (DCDPS) at the activated chlorine sites in a nucleophilic step growth reaction. The temperature is maintained at 150°C for 3 hours. During this time, the refluxing toluene azeotropes nearly removes all the water from the system, including the water produced by the formation of the phenolate anions. After about 3 hours, the temperature is raised to 180-185°C and reaction is allowed to proceed for an additional 14-15 hours. After reaction, the temperature is lowered to between 120 and 140°C. The entire mixture is filtered through a coarse glass frit filter to remove the insoluble salts such as potassium chloride and potassium carbonate. Acetic acid is then added to the cooled solution to neutralize the phenolate end groups. The hydroxyl terminated poly(arylene ether

sulfone) is then obtained by adding small portions of the solution from a separatory funnel into a 10-fold excess of methanol in a Waring laboratory blender. The powdery oligomer is then washed with water and recollected by suction filtration and dried in a vacuum oven at 100 C for 12-15 hours.

Once the poly(arylene ether sulfone) oligomers are synthesized they may be copolymerized to form terephthaloyl chloride extended arylene ether sulfone-aryl ether by the solution process which will be discussed in Appendix C or by the interfacial process as now discussed.

In the interfacial process, both the hydroxyl terminated oligomer and the terephthaloyl chloride are dissolved in the organic phase. Sodium hydroxide or potassium carbonate dissolved in the water phase serves as the acid acceptor. Also, in an effort to add more "liquid crystalline" character to the above mentioned systems by incorporating additional biphenol, only the interfacial process is used. The general interfacial process is described below.

About 3 gm of hydroxyl terminated polysulfone oligomer is placed in the blender along with 20 ml of the methylene chloride. An aqueous sodium hydroxide solution is then added and this forms two layers in the blender. Also the terephthaloyl chloride is added to the blender. The blender is vigorously stirred for 20 minutes and 10 ml more of methylene chloride is added to replace any of the solvent which has evaporated and also for purposes of diluting the now viscous mixture. The solution is then placed in a separatory funnel. Small portions of the solution are added to a 10-fold excess of methanol in a stirring

blender to precipitate the polymer. The fibrous polymer can then be washed, vacuum filtered and dried under vacuum at 100°C for 15-20 hours. When adding additional biphenol to the hydroquinone/biphenol polysulfone system, the blender is charged with the hydroxyl terminated poly(arylene ether sulfone) oligomer and 20 ml of methylene chloride. In a separate Ehrlenmeyer flask, biphenol, sodium hydroxide solution and a phase transfer catalyst (PTC) tetraethyl ammonium chloride are dissolved in water. This solution is slowly poured into the blender to form two phases. The terephthaloyl chloride dissolved in 10 ml of methylene chloride is then added to the blender slowly, and the mixture is vigorously stirred for 20 minutes. After being stirred, the viscous white mixture can be transferred into a separatory funnel. A 10-fold excess of methanol is placed in a blender and small portions of the polymer solution are added from the funnel. The precipitant is collected, washed, and dried as before.

APPENDIX B

Description Of Potentiometric Titration And Ubbelohde Viscometer

(a). Potentiometric Titration For Molecular Weight Determination

The equipment involves, a pH meter (orion 601A) with glass and calomel electrodes (Thomas No. 4092-f15 and 2090 B-15 respectively), several 40 mm titration vessels, a 2 ml Gilmont microburet (Thomas No. 1996-B55), stirring bar (4 mm, 10 mm) purified DMAC and 1% solution of tetraethyl ammonium hydroxide in distilled water.

The procedure for this method is as follows. A sample of hydroxyl terminated polysulfone is first accurately weighed into a titration flask and dissolved in 20 ml DMAC with stirring, while dry, carbon dioxide free nitrogen is passed over the solution. After complete dissolution of the polymer, the electrodes are immersed in the solution and the buret lowered such that the tip just pierces the surface. After recording the initial volume and cell potential, 0.05 ml portions of the titrant are added. The titration is continued until the cell potential dropped steadily with each addition of titrant.

In order to calculate the molecular weight, the equation below can be used.

$$M=2(W)/(V)(C)$$

where: W=weight of sample in grams

C=concentration of titrant in moles per liter

V=volume of the titrant which is determined using a second

derivative plot of volume of titrants vs. the corresponding millivolt reading.

(b). Ubbelohde Viscometer for Viscosity Determination

The theory of dilute solution viscometry has been presented elsewhere (75) and will not be considered here. The intrinsic viscosity of the oligomers, homo, random and block copolymers can be determined in methylene chloride, THF or O-chlorophenol at 25°C or 30°C depending on the nature of the polymers. A typical experimental procedure is given below.

The equipment utilized was, one semi-micro dilution viscometer (Cannon Instrument Co.), a thermostatted water bath, nitrogen tank and polymer solution (20 gm/liter).

The procedure for this method involves two moles of the solvent that are added to the viscometer and allowed to equilibrate in the thermostatted water bath for at least ten minutes. Using nitrogen pressure, the solvent is forced up the viscometer tube until the meniscus rises above the upper viscometer mark. The solvent is then allowed to drain under gravity past the marks. The time elapsed to pass the two marks is noted to the nearest 0.1 second. At least three readings within 0.2 % are taken and the average value noted as the solvent flow time, T. Next, 2 ml of the prepared sample is added to the solvent in the viscometer such that the new concentration is approximately 10 g/liter. After equilibrating to temperature, the solution is then forced through the viscometer and its flow time determined. The same procedure is employed for at least three other concentrations prepared by continuously diluting the initial solution.

Calculations are as follows. The relative viscosity is taken as the ratio of solution flow time to solvent flow time ($\eta=t/t_o$). The reduced viscosity ($\eta_{sp}=(\eta-1)/C$) and the inherent viscosity ($\eta_{inh}=\ln \eta/C$), are calculated for each solution and plotted against concentration. Extrapolation of either of these curves to zero concentration provides the intrinsic viscosity (η). Comparison of the values of (η) for a series of similar oligomers provides an approximate estimate of their relative molecular weights.

APPENDIX C

Oligomer Synthesis And Characterization

(a). Oligomer Synthesis.

In order to form a HQ/BP PSF polymer, one must first prepare a hydroxyl terminated polysulfone oligomer. In order to make sure that the oligomer is hydroxyl terminated, the stoichiometry of the oligomer forming reaction requires a calculated excess of hydroquinone and/or biphenol. This excess amount of biphenol ensures that the oligomer chains will be hydroxyl terminated. The terminal hydroxyl groups also provide a good method to determine the number average molecular weight of the oligomer through a potentiometric titration procedure. Fourier transform infrared spectroscopy (FT-IR) provides an easy method to further characterize the oligomer. FT-IR shows that the oligomers are hydroxyl terminated and also display the characteristic sulfone peaks. Gel permeation chromatography data demonstrates that the oligomers formed are of high polydispersity and low molecular weight. The polydispersity is to be expected since the reaction is a step-growth or condensation type reaction. Large elution volumes (relative to elution volumes for the copolymers) suggest that the oligomers are of low molecular weight. Thus, it would seem that this oligomer synthesis method leads to well defined hydroxyl functional oligomers. The reaction is fast, easy and provides good yields. This method has also the advantage of being modified so as to produce oligomers which contains varying amounts of hydroquinone and biphenol in their backbone.

(b). Oligomer Characterization.

The yields obtained for various oligomers produced ranged from 61 to 99 %. To determine the actual number average molecular weights (Mn) of the oligomers, a potentiometric titration has been used.

A Nicolet MX-1 Fourier Transform Infrared Spectrophotometer was utilized to study the formation of the hydroxyl terminated poly(arylene ether sulfones). Specifically, the FT-IR shows that for all the oligomers, a hydroxyl stretching band is present indicating phenolic end groups as expected. Comparing the hydroxyl stretch intensity of a low Mn value oligomer with that of a high Mn value oligomer (see Figs. 47-48), one sees that the intensity of the hydroxyl peak decreases as the Mn values increase. This decrease is of course predicted since the concentration of end groups compared with the overall degree of polymerization decreases with an increasing Mn value. The FT-IR spectra also show the characteristic sulfone peaks which are to be expected in these oligomers.

An Ubbelohde (number 50) viscometer was used to determine the intrinsic viscosities of these oligomers. These intrinsic values can later be compared with the values obtained from the copolymers formed from them. A comparison of the values should then provide some indication of the molecular weight increase on "chain extension".

Gel permeation chromatography (GPC) performed on a Waters 244 instrument also provides useful information on the polysulfone oligomers. The GPC traces in Figs. 49 and 50 indicate a broad molecular weight distribution. The broad distribution is expected from the nature

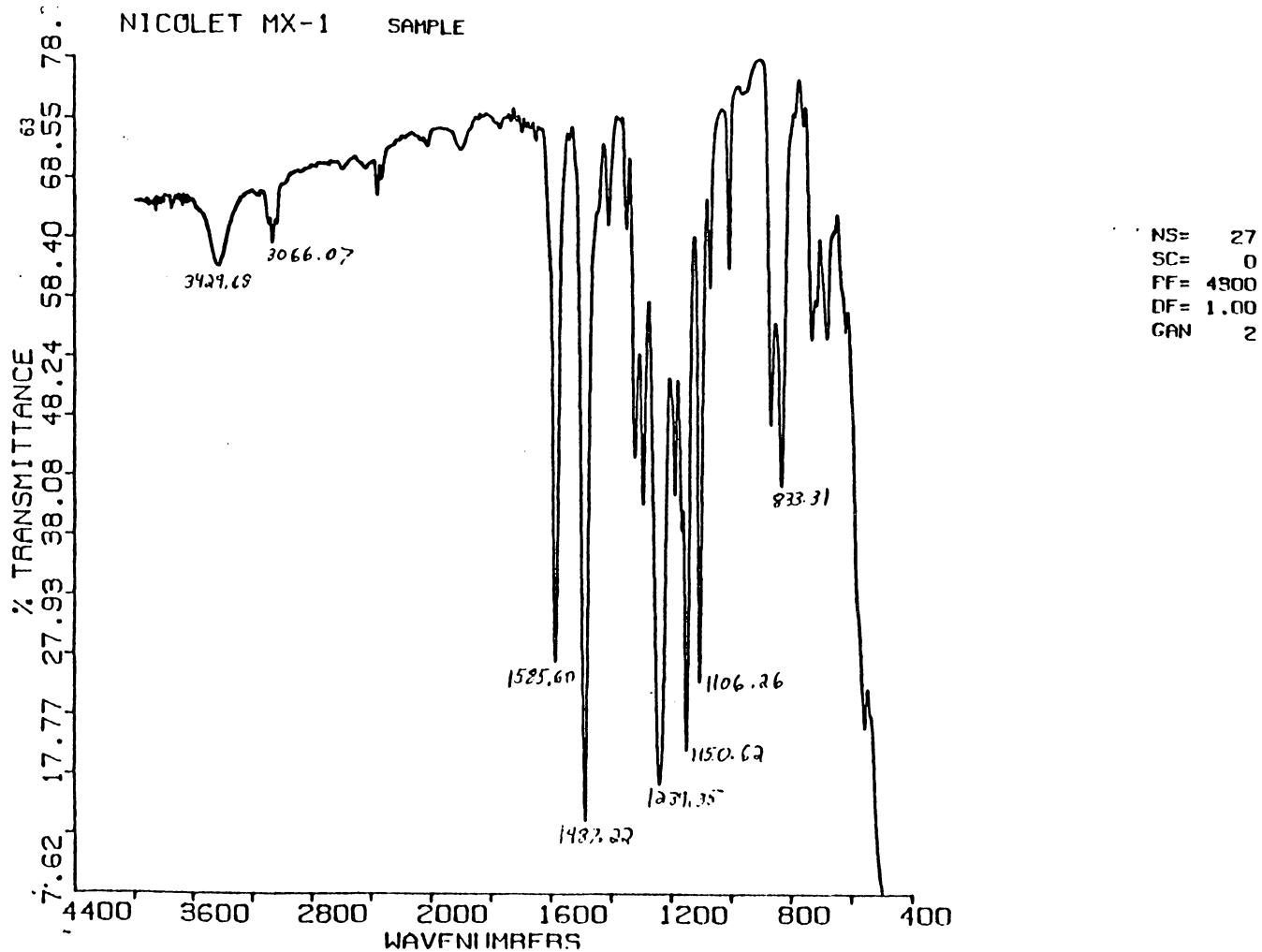

Fig. 47. FTIR of HQ/BP PSF 2210 OH terminated sample.

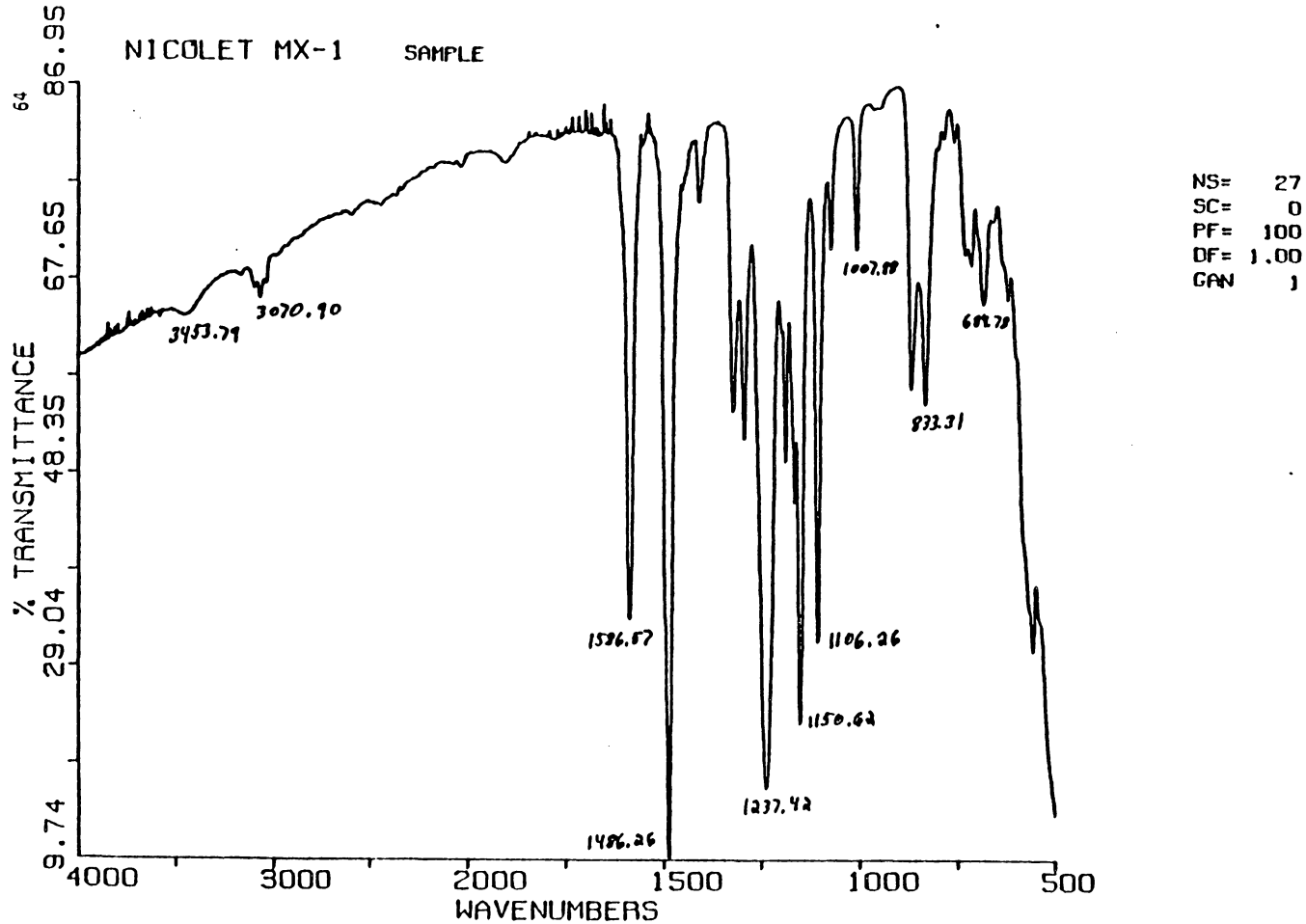

Fig. 48. FTIR of HQ/BP PSF 5340 OH terminated sample.

Fig. 49. Gel Permeation Chromatography trace of 1700 MW HQ/BP PSF oligomer sample.

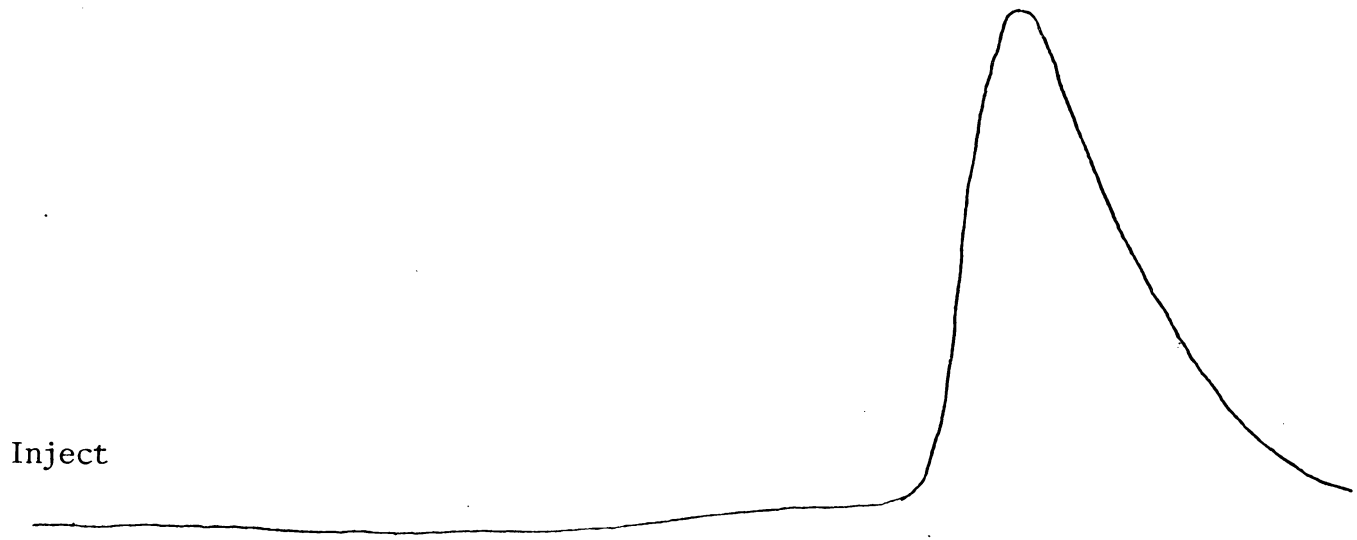

Fig. 50. Gel Permeation Chromatography trace of 5340 MW HQ/BP PSF oligomer sample

of the step growth reaction. These traces can also be used to compare with the corresponding copolymer traces as a relative indication of molecular weight increase.

(c). Copolymerization

Once the hydroxyl terminated poly(arylene ether sulfone) oligomers are synthesized and their number average molecular weights known, it is then possible that they be "extended" to form segmented copolymers. The extension reaction utilized is also a step-growth reaction between an acid chloride and the oligomer hydroxyl end groups. This reaction is known to be rapid and the aryl ester linkages formed are relatively stable. The by-product in both the solution and interfacial reactions is hydrogen chloride. However, it is effectively removed by a base or an acid acceptor. Removing the hydrogen chloride also directs the reaction further toward the polymer product. In addition to the simple acid chloride extended copolymers which can be prepared from these techniques, segmented poly(arylene ether sulfone)-biphenol terephthalate systems may also be prepared. These segmented systems result from the fact that the terephthaloyl chloride can react not only with the hydroxyl end groups of the polysulfone oligomers but also with any biphenol which has been added to the system. The only stipulation for these reactions is that there must be a 1 to 1 stoichiometry between the terephthaloyl chloride and the total number of hydroxyl end groups contributed by either the oligomer or added biphenol. Here some of the advantages and disadvantages of the solution and interfacial reactions that were used in copolymerization will be discussed below.

1. Solution Copolymerization.

The solution process is useful for forming the hydroquinone/biphenol polysulfone-terephthalate copolymers since the oligomers and copolymers remain soluble. However, the biphenol polysulfone oligomers are either only slightly soluble or insoluble. Therefore, the insolubility of many of the biphenol polysulfones and premature precipitation of several of the poly(arylene ether sulfone)-biphenol terephthalate segmented copolymers could pose problems. Another limitation is that methylene chloride and chloroform were the only solvents which were successfully used. Attempting to use NMP, tetrachloroethane and dimethyl acetamide solvents were not successful. In order to solve some of the problems associated with the solution process, the technique of interfacial process (which was discussed in detail in Appendix A section) was developed.

2. Interfacial Copolymerization.

In the interfacial reaction it was possible to add extra biphenol to extend the polymers. The added biphenol was dissolved in the aqueous phase in this technique, whereas in the solution technique it was dissolved in an organic solvent. Using this approach it was possible to add at least 75 mole % biphenol to 5350 Mn HQ/BP PSF and terephthaloyl chloride. The reason the interfacial process works better than the solution process for this particular reaction is believed to be that the growing polymer chains can still react in a swollen state interfacially. In the solution process, the growing chains precipitate after adding just a few of the biphenol units. Contamination of the polymers by phase transfer catalyst and potassium carbonate salts seem to be the major

drawback to this technique. Extensive washing of the polymer is necessary to possibly decrease or eliminate this problem.

APPENDIX D

Composition And Molecular Weight Characterization.

By the very nature of the monomers and oligomers used in the synthesis of the poly(arylene ether sulfone)-aryl ester copolymers, the exact chain structure of the copolymer is known. For example, it is known that the polysulfone oligomers are hydroxyl terminated and do not react with themselves. Thus, the hydroxyl terminated polysulfone oligomer may only react with a unit of terephthaloyl chloride. Therefore, the structure of the polymer is that of perfectly alternating copolymer of the type (AB)n. A Nicolet MX-1 Fourier Transform Infrared Spectrophotometer was utilized to obtain qualitative information on the copolymers. It has been shown by FT-IR that the copolymers formed contain the sulfone linked to the terephthaloyl chloride through ester linkages. However, the structure of the poly(arylene ether sulfone)-biphenol terephthalate terpolymers is somewhat different. In these polymers the biphenol or hydroxyl terminated polysulfone oligomer can react with the terephthaloyl chloride giving a random placement of the biphenol and polysulfone oligomers.

The molecular weights of the polymers formed can be compared on a relative scale. From the evidence presented by GPC and intrinsic viscosity data, the molecular weights are greater than those of the starting oligomers. The films cast from these copolymers are tough and ductile, which also indicate a relatively high molecular weight.

REFERENCES

1. A. Keller, *Ultra-High Modulus Polymers*, A. Ciferri and I.M. Ward, Ed., Applied Science Publishers, London (1979).

2. I.M. Ward, Polym. Sci. USSR, 21, 2819-2835 (1980).

3. W.B. Black, Ann. Rev. Mater. Sci. 10, 311-362 (1980).

4. K. Fujino, Y. Ogawa, and H. Kawai, J. Appl. Polymer Sci., 8, 2147-61 (1964).

5. M.J. Inoue, Polymer Sci., Part A, 1, 3427-38 (1963).

6. J.H. Wendorf, *Liquid Crystalline Order in Polymers*, A Blumstein, Ed., Academic Press, New York (1978).

7. W.J. Jackson and H.F. Kuhfuss, J. Polym. Sci., Polym. Chem. Ed., 14, 1043 (1976).

8. J. Economy, B.E. Nowak, and S.G. Cottis, Am. Chem. Soc., Polym. Preprints, 2, 1 (1970)

9. P. Meurisse, C. Noel, L. Monnerid, B. Fayolle, Br. Polym. J., Vol. 13, 55 (1981).

10. G.W. Calundann, U.S. Patent 4,161,470 (1980).

11. P.F. Bruins, ed., *Plasticizer Technology*, Reinhold, New York (1965).

12. L.A. Utracki, Polym. Eng. Sci., 23, 11, 602 (1983)

13. C.D. Han, Y.W. Kim and S.J. Chen, J. Appl. Polym. Sci., 19, 2381 (1975).

14. B.T. Hayes, Chem. Eng. Prog., 65, 10, 50 (1969).

15. P.V. Papero, E. Kabu, and L. Roldan, Textile Reserch J., 10, 823 (1967).

16. A.P. Plochocki, Polym. Eng. Sci., 23, 11, 618 (1983).

17. J.M. Starita, Trans. Soc. Rheol., 16, 339 (1972).

18. C.D. Han, Y.W. Kim, Trans. Soc. Rheol., 19:2, 245 (1975).

19. S. Newman and S. Strella, J. Appl. Polym. Sci., 9, 2297 (1965).

20. B.W. Bender, J. Appl. Polym. Sci., 9, 2887 (1965).

21. P.J. Flory, *Principles of Polymer Chemistry*, Cornell Univ. Press, Ithaca, New York (1953).

22. C.D. Han, T.C. Yu, and K.U. Kim, J. Appl. Polym. Sci., 15, 1149 (1971).

23. D'Orazio, Polym. Eng. Sci., 23, 9, 489 (1983).

24. T. Kunori and P.H. Geil, J. Macromol. Sci. Phys., B 18, 93 (1980).

25. M.R. Kamal, M.A. Sahto, and L.A. Utracki, Polym. Eng. Sci., 22, 1127 (1982).

26. M.R. Kamal, M.A. Sahto, and L.A. Utracki, Polym. Eng. Sci., 23, 637 (1983).

27. D.G. Baird and G.L. Wilkes, Polym. Eng. Sci., 23, 11, 632 (1983).

28. E.G. Joseph, PhD. dissertation, Dept. of Chem. Eng., Va. Tech, Blacksburg (1983).

29. F.C. Frank, A. Keller, and M.R. Mackley, Polymer, 12, 467 (1971).

30. A. Keller, Polymer, 19, 617 (1978).

31. A. Keller, J. Polym. Sci., Polym. Symp., 58, 395 (1977).

32. D.W. Van Krevelen, Chimia, 32, 8, 279 (1978).

33. A.J. Pennings, A.Awijnenburg, and R. Lageveen, Kolloid-Z.Z. Polymere, 251, 500 (1973).

34. A.J. Pennings, C. Schouteten, and A.M. Kiel, J. Polym. Sci., c38, 167 (1972).

35. A.J. Pennings, J. Polym. Sci., Part C, 59, 55 (1977).

36. P. Smith, P.J. Lemstra, and H.C. Booij, J. Polym. Sci., Phys. Ed., 19, 877 (1981).

37. A. Keller and M.R. Mackley, Pure Appl. Chem., 39, 195 (1974).

38. D.T. Grubb, A. Keller, and T. A. Odell, J. Mater. Sci., 10, 1510 (1975).

39. D.C. Prevorsek, *Polymer Liquid Crystals*, A. Ciferri, W.R. Krigbaum, and R.B. Meyer Ed., Academic Press, New York (1982).

40. E.S. Clark and L.S. Scott, Polymer Preprints 15, 153 (1974).

41. G. Capaccio and I.M. Ward, Polymer, 15, 233 (1974).

42. G. Capaccio, A.G. Gibson and I.M. Ward, *Ultra-High Modulus Polymers*, A. Ciferri and I.M. Ward Eds., Applied Science Publishers, London (1979).

43. W.C. Sheehan and T.B. Cole, J. Appl. Polym. Sci., 8, 2359 (1964).

44. A.E. Zacharides, W.T. Mead, and R.S. Porter, *Ultra-High Modulus Polymers*, A. Ciferri and I.M. Ward Eds., Applied Science Publishers, London (1979).

45. A.E. Zachariades, D.S. Grinwold, and R.S. Porter, Polym. Eng. Sci., 19, 6 (1979).

46. P.A. Egelstaff, *An Introduction to the Liquid State*, Academic Press, New York (1967).

47. A. deVris, *Liquid Crystals*, Saeva ed., Marcel Dekker (1979).

48. P.G. deGennes, The Physics of Liquid Crystals, Oxford Univ. Press, London (1975).

49. J. Preston, Die Angewandte Makromolekulare Chemie 109/110, 1-19 (1982).

50. A. Ciferri, W.R. Krigbaum, and R.B. Meyer Eds., *Polymer Liquid Crystals*, Academic Press, New York (1982).

51. A. Blumstein, Ed., *Liquid Crystalline Order in Polymers*, Academic Press, New York (1978).

52. P.J. Flory and G. Ronca, Mol. Cryst. Liq. Cryst. 54, 289 and 311 (1979).

53. W.J. Jackson, Br. Polym. J. 12, 154 (1980).

54. F.L. Hamb, U.S. Patent 3,772,405 (1973).

55. F.E. McFarlane, V.A. Necely, and T.G. Davis, Contemporary Topids in Polymer Science, 2, 109-138, Plenum Publishing Corp., New York (1977).

56. C. Aguilera and H. Ringsdorf, Polymer Bulletin, 12, 93-98, (1984).

57. B.W. Jo, J.I. Jin, and R.W. Lenz, Makromol. Chem., Rapid

Commun., 3, 23-27 (1982).

58. R.W. Lenz and J.I. Jin, Macromolecules, 14, 1405 (1981).

59. Y. Ide and Z. Ophir, Polym. Eng. Sci., 23, 5, 261 (1983).

60. Z. Ophir and Y. Ide, Polym. Eng. Sci., 23, 14, 792 (1983).

61. G.W. Calundann, U.S. Patent 4,184,996 (1980)

62. C.M. Chu and G.L. Wilkes, J. Macromol. Sci-Phys., B10(4), 551-578 (1974).

63. L.E. Alexander, *X-Ray Diffraction Methods in Polymer Science*, Wiley and Sons, New York (1969).

64. R.S. Stein and G.L. Wilkes, *Structure and Properties of Oriented Polymers*, I.M. Ward Ed., Wiley and Sons, New York (1975).

65. R.J. Samuels, *Structured Polymer Properties*, Wiley and Sons, New york (1974).

66. I.M. Ward, *Mechanical Properties of High Polymers*, Wiley and Sons, New York (1983).

67. E.A. Turi, *Thermal Characterization of Polymeric Materials*, Academic Press (1981).

68. A.P. Gray, Thermochimica Acta, 1, 563 (1970).

69. B. Wunderlich, *Macromolecular Physics-Vol.2-Crystal Nucleation Growth, Annealing*, Academic Press, New York (1976).

70. L. Mandelkern, *Crystallization of Polymers*, McGraw Hill, New York (1964).

71. P.J. Makarewicz and G.L. Wilkes, J. Polym. Sci., Polym. Phys. Ed., 16, 1559 (1978).

72. L.M. Robeson, A. Noshay, M. Matzner, and C.N. Merriam, Angew. Makromol. Chem., 29/30, 47 (1973).

73. D.C. Watts and E.P. Perry, Polymer, 19, 288 (1978).

74. Y. Aoki and J.O. Brittain, J. Polym. Sci., Polym. Phys. Ed., 14, 1297 (1976).

75. F. Billmeyer, *Textbook of Polymer Science*, Interscience (1971).

The vita has been removed from the scanned document

Studies of Blends Containing Liquid Crystalline Polymers with PET and Related Investigations of Hydroquinone/Biphenol Polysulfone Systems

by

Chan Uk Ko

(ABSTRACT)

The investigation of structure-property behavior of extruded cast films prepared from blends of thermotropic liquid crystalline copolyesters with polyethylene terephthalate (PET). Data were obtained which showed not only the temperature dependence of the moduli and stress-strain behavior but also the orientation effects that must be prevalent in order to explain the differences between the moduli measured parallel and perpendicular to the extrusion direction. Only at high liquid crystal polymer (LCP) compositions is the modulus particularly increased. The modulus enhancement with lower LCP content and utilization of process variables are discussed. Specifically, the extruder gear pump speed did not enhance Young's modulus at the same LCP content as extensively as did the effect of extruder screw speed. Also a study to synthesize and characterize new segmented copolymers that could produce unusual film properties are discussed. The approach involved the synthesis of high Tg (220 C) isotropic poly (aryl ether sulfone) oligomers of varying segment molecular weights. The thermal and mechanical studies of the copolymers have been carried out to probe the potential of these copolymers for signs of liquid crystalline character and to note their ability to thermally crystallize as

well as to crystallize by solvent or strain inducement. Along these lines, thermal analysis, polarizing hot-stage microscopy, wide angle x-ray scattering and mechanical testing were utilized in this investigation.